US ARMY CORPS
OF ENGINEERS
New England District

Contract No. DACW33-01-D-0004
Delivery Order No. 02
April 2004

Final Report

ANALYSIS OF DREDGED MATERIAL TRANSPORT POTENTIAL AT TWO DISPOSAL ALTERNATIVES IN RHODE ISLAND REGION

RHODE ISLAND REGION LONG-TERM DREDGED MATERIAL DISPOSAL SITE EVALUATION PROJECT

FINAL

Analysis of Dredged Material Transport Potential at Two Disposal Alternatives in Rhode Island Region

Rhode Island Region
Long-Term Dredged Material Disposal Site Evaluation Project

Contract Number DACW33-01-D-0004
Delivery Order No. 02

to

U.S. Army Corps of Engineers
North Atlantic Division
New England District
696 Virginia Road
Concord, MA 01742-2751

By:

Battelle
397 Washington Street
Duxbury, MA 02332
(781) 934-0571

April 2004

TABLE OF CONTENTS

1.0 INTRODUCTION....1
2.0 WIND ANALYSIS....2
3.0 WAVE ANALYSIS....5
4.0 HISTORICAL CURRENT ANALYSIS....7
5.0 DISPOSAL PLUME MODELING (STFATE)....12
5.1 STFATE Model Description....13
5.2 Model Input Requirements....14
5.3 Application of STFATE to Site W and Site E....15
5.4 Results....1 8
5.4.1 Site W....18
5.4.2 Site E....20
6.0 ZSF-WIDE SEDIMENT TRANSPORT MODEL (Grant-Madsen)....21
6.1 Method for Determining Bottom Sediment Motion....22
6.2 Development of Wave and Current Fields for Sediment Transport Model....25
6.2.1 Wave Field....25
6.2.2 Current Field....27
6.3 Sediment Transport Model....28
6.4 Sediment Model Results....29
7.0 COHESIVE SEDIMENT TRANSPORT MODELING OVER MOUNDS (LTFATE)...33
7.1 LTFATE Model Description....34
7.2 Application of LTFATE to the Alternative Sites....34
7.3 Results....4 2
7.3.1 Site W....42
7.3.2 Site E....46
8.0 REFERENCES....51

Appendix A: STFATE Model Simulation Results

LIST OF TABLES

Table 1. Model-Predicted Wave Heights and Periods at Sites W and E for Storms of Various Frequencies of Occurrence....6
Table 2. Tidal Ellipse Parameters for Near-bottom, Middle, and Surface Currents Measured in Site W, April-May 2002....10
Table 3. STFATE Model Input Parameter Requirements. 15
Table 4. STFATE Model Grid Parameters....15
Table 5. STFATE Model Disposal Operation Parameters....16
Table 6. Dredged Material Properties Used in STFATE Model Simulations....17
Table 6. LC_{50} Elutriate Results from Representative Area Harbors....18
Table 8. STFATE Model Parameters and Dilution Results for the Site W....20

Table 9. STFATE Model Parameters and Dilution Results for the Site E. 21
Table 10. Wave Model Validation Statistics for 1998.....27
Table 11. Storms Modeled with LTFATE Including Historical Storm Events Impacting Rhode Island Sound and Simulated Storms. 35
Table 12. Cohesive Sediments Erosion Potential Parameter from flume measurements made on Portland Disposal Site sediments.....42
Table 13. Model Predicted Erosion and Deposition over Site W for Four Storm Scenarios. 43
Table 14. Model Predicted Erosion and Deposition over Site E for Four Storm Scenarios.....47

LIST OF FIGURES

Figure 1. Alternative Ocean Dredged Material Disposal Sites W and E.....1
Figure 2. Wind Speed Exceeding 30 Knots (1985-1993) Recorded at the Buzzards Bay Tower C-MAN Station (41.40°N 71.03°W).....3
Figure 3. Average Wind Speed and Direction (by Season) Recorded at the Buzzards Bay Tower C-MAN Station (41.40°N 71.03°W).....4
Figure 4. Significant Wave Height and Dominant Wave Period (1990 to 1992) Recorded at the Buzzards Bay Tower C-MAN Station (41.40°N 71.03°W).....6
Figure 5. Maximum Ebb and Flood Tide Currents (Knots) Throughout Block Island Sound.....8
Figure 6. Current Speed and Direction (Tide Removed) Recorded at a Station in Site W in Rhode Island Sound (September 1999).....9
Figure 7. Surface and Bottom Tidal Ellipses at Site W.....11
Figure 8. Near-Bottom Turbidity, Near-Bottom Current, and Wave Height Measured at Site 69B in May and June of 2002.....12
Figure 9. Schematic Depicting Shear Stress on the Sea Bed.....22
Figure 10. Wind Model Grid. 26
Figure 11. ADCIRC Tidal Model Computational Domain. 28
Figure 12. Predicted Sediment Erodability Parameter for 0.5-mm Grain Size for Typical Peak Tide and 1 Percent Frequency of Occurrence Wave Conditions.....29
Figure 13. Predicted Sediment Erodability Parameter for 1.0-mm Grain Size for Typical Peak Tide and 1 Percent Frequency of Occurrence Wave Conditions.....30
Figure 14. Predicted Sediment Erodability Parameter for 2.0-mm Grain Size for Typical Peak Tide and 1 Percent Frequency of Occurrence Wave Conditions.....31
Figure 15. Predicted Relationship Between Depth and Sediment Erodability Parameter for 0.5-mm Grain Size, Typical Peak Tide, and 1 Percent Frequency of Occurrence Wave Conditions.....32
Figure 16. Predicted Relationship Between Depth and Sediment Erodability Parameter for 1.0-mm Grain Size, Typical Peak Tide, and 1 Percent Frequency of Occurrence Wave Conditions.....32
Figure 17. Predicted Relationship Between Depth and Sediment Erodability Parameter for 2.0-mm Grain Size, Typical Peak Tide, and 1 Percent Frequency of Occurrence Wave Conditions.....33
Figure 18. Storm 370 (1936) Time Series of Significant Wave Height, Wave Period, Sea Surface Elevation, Current Speed and Direction for Site W.....36

Figure 19. Storm 712 (1972 Hurricane Agnes) Time Series of Significant Wave Height, Wave Period, Sea Surface Elevation, Current Speed and Direction for Site W.....37
Figure 20. Storm 748 (1976 Hurricane Belle) Time Series of Significant Wave Height, Wave Period, Sea Surface Elevation, Current Speed and Direction for Site W.....38
Figure 21. Storm H1.7 Time Series of Significant Wave Height, Wave Period, Sea Surface Elevation, Current Speed and Direction for Site W.....39
Figure 22. Storm H2.5 Time Series of Significant Wave Height, Wave Period, Sea Surface Elevation, Current Speed and Direction for Site W.....40
Figure 23. Bathymetry of Site W Showing Configuration of Proposed Dredged Material Mounds. 41
Figure 24. Change in Bathymetry at the Site W Predicted for 5.4 ft Peak Wave Height Storm Simulation.....43
Figure 25. Change in Bathymetry at the Site W Predicted for 7.1 ft Peak Wave Height Storm Simulation.....44
Figure 26. Change in Bathymetry at the Site W Predicted for 13.7 ft Peak Wave Height Storm Simulation, Hurricane Belle.....45
Figure 27. Change in Bathymetry at the Site W Predicted for 14.9 ft Peak Wave Height Storm Simulation, Hurricane Agnes with no disposal mounds present.....45
Figure 28. Change in Bathymetry at the Site E Predicted for 5.8 ft Peak Wave Height Storm Simulation.....46
Figure 29. Change in Bathymetry at the Site E Predicted for 7.6 ft Peak Wave Height Storm Simulation.....47
Figure 30. Change in Bathymetry at the Site E Predicted for 14.7 ft Peak Wave Height Storm Simulation, Hurricane Belle.....48
Figure 31. Change in Bathymetry at the Site E Predicted for 16.0 ft Peak Wave Height Storm Simulation, Hurricane Agnes with no disposal mounds present.....49

1.0 INTRODUCTION

While most dredged material released into a designated disposal site will be deposited on the seafloor where it will remain, some may be transported away from the point of release. This can happen in two ways: fine dredged sediment may be carried by local currents while still in the water column immediately after disposal, or they may be deposited on the sea floor and then later resuspended into the water column by occasional high waves and/or strong currents. A modeling effort was undertaken for the Rhode Island Region Long-term Dredged Material Disposal Site Evaluation Project to help determine the conditions which may lead to the transport of dredged material away from the proposed disposal site alternatives (Site W and Site E), as well as the extent of such transport. Site W and Site E are located in Rhode Island Sound (Figure 1). This report describes the methods and results of that modeling effort.

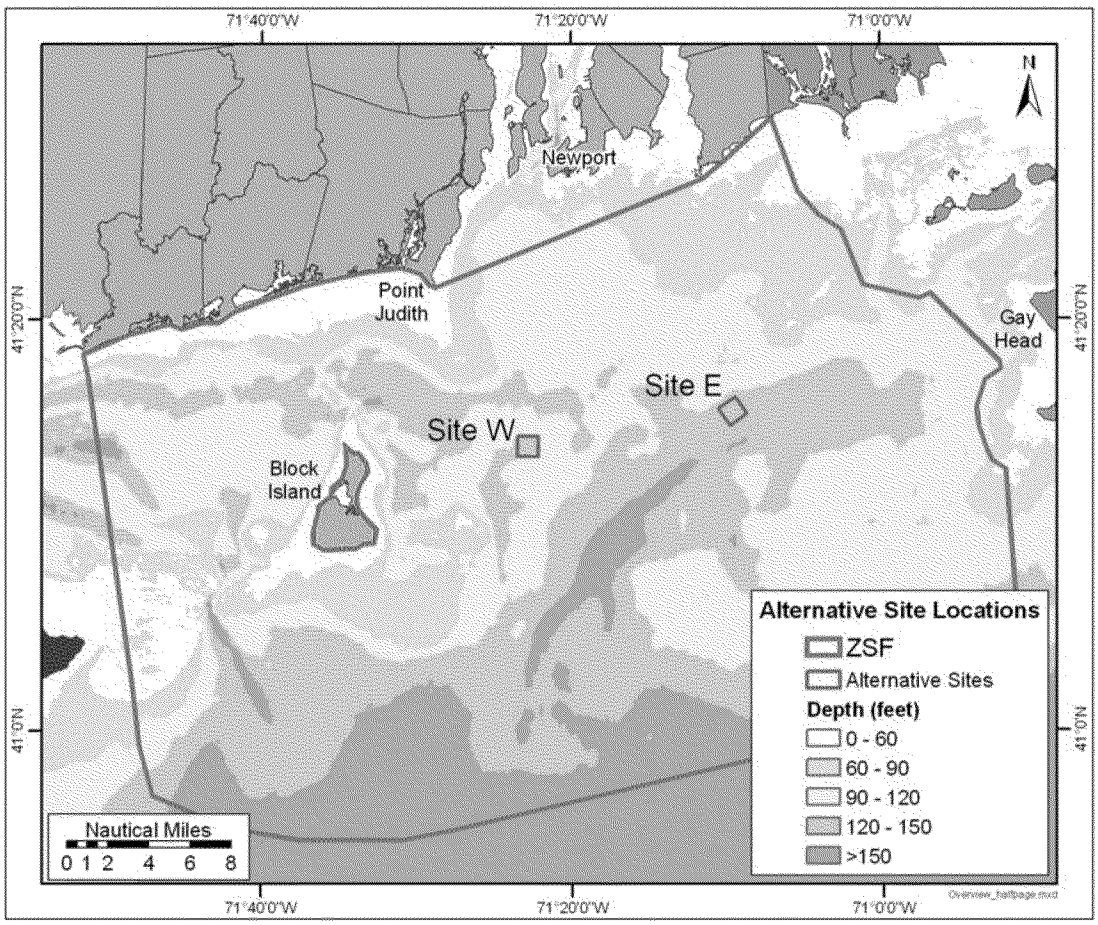

Figure 1. Alternative Ocean Dredged Material Disposal Sites W and E.

The transport, dispersion, and eventual fate of dredged material released into the marine environment depend upon both the physical characteristics of the dredge material and the structure and dynamics of the water column. Ocean currents directly affect the transport and dispersion of dredge material. Waves can resuspend bottom sediments and dredge material

particles previously deposited on the seafloor. The density structure of the receiving water, relative to the density of the released dredged material, influences the length of time the dredged material remains in the water column. Before transport modeling was undertaken, an analysis of wind, waves, and currents was completed to provide the necessary characterization of the Zone of Siting Feasibility (ZSF) and the proposed alternative sites.

2.0 WIND ANALYSIS

Winds in the area of Rhode Island Sound are an important influence on the ZSF environment, as they generate surface waves, affect water column mixing, and affect currents in the area. Meteorological data and climatological statistics used to evaluate conditions in Rhode Island Sound and Block Island Sound were obtained from the National Oceanic and Atmospheric Administration (NOAA) (http://www.ndbc.noaa.gov/). The coastal maritime weather of the ZSF (including Rhode Island Sound and Block Island Sound) is characterized by a climate of extremes, typical of the northeast United States, with hot summers and cold, stormy winters. In summer, the predominant winds blow from the southwest and are usually light, except for occasional tropical storms and hurricanes, which are normally experienced in this area during August, September, or October. In winter, the predominant winds blow from the northwest.

Wind observations recorded by the National Weather Service show that during the winter, wind speeds average 16 to 17 knots over the open water. This can be twice the wind speed found on the coast. The results is that seas of 10 feet or greater occur 5 percent to 7 percent of the time. Storms also have a transient effect on water column currents both through the effect of the winds they generate and the effect of the large scale barometric pressure gradients present in the storms. While the average current flow over the continental shelf is toward the southwest at about 5 centimeters per second (cm/s) near the surface, energetic wind-driven events, primarily during the winter months, can significantly alter the mean flow pattern increasing the mean current (non-tidal) to as high as 40 cm/s (Mayer *et al.*, 1979).

The National Data Buoy Center (NDBC) of NOAA maintains offshore meteorological buoys and platforms throughout the coastal and offshore waters of the United States. The NDBC has maintained a meteorology and wave station on the Buzzards Bay Tower (outside the entrance to Buzzards Bay at 41.40°N 71.03°W) since 1985. Data from the station are presented for the period July 1985 through December 1993 in Figure 2 and Figure 3. Figure 2 shows the frequency with which winds greater than 30 knots occur during each month of the year. Wind speeds exceed 30 knots more than 5 percent of the time in November, December, and January, with the peak in December when wind speeds exceed 30 knots 7.6% of the time. Figure 3 presents four charts, one for each season of the year, in which the frequency of occurrence of winds at different speeds and directions are presented. During winter, the predominant wind direction is out of the northwest, but winds from the southwest and northeast (nor'easters) are not uncommon. During March and April, winds are more southerly but can still be strong; March winds exceed 30 knots over 4 percent of the time. The summer charts in Figure 3 show that during the summer months, winds from the southwest predominate.

No studies have been conducted at either alternative site to directly measure meteorological conditions; however, the climatology for the region is well understood. The marine climate across the open waters of the ZSF, and indeed across the open water of all of southern New England, is very consistent, as seen in the long-term record of meteorological parameters for the region. Given the broad-scale nature of storms, winds, rainfall, and cloud cover, the climatology at each alternative site can be assumed to be similar to that described for the open waters of the ZSF in general.

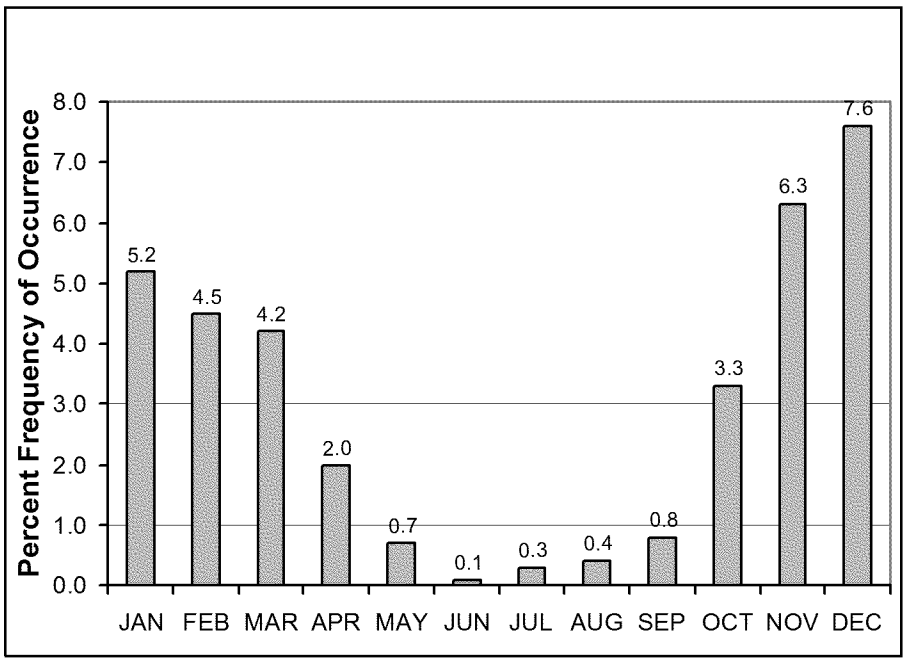

Source: NDBC
Note: Wind measured at 81 ft above mean sea level.

Figure 2. Wind Speed Exceeding 30 Knots (1985-1993) Recorded at the Buzzards Bay Tower C-MAN Station (41.40°N 71.03°W).

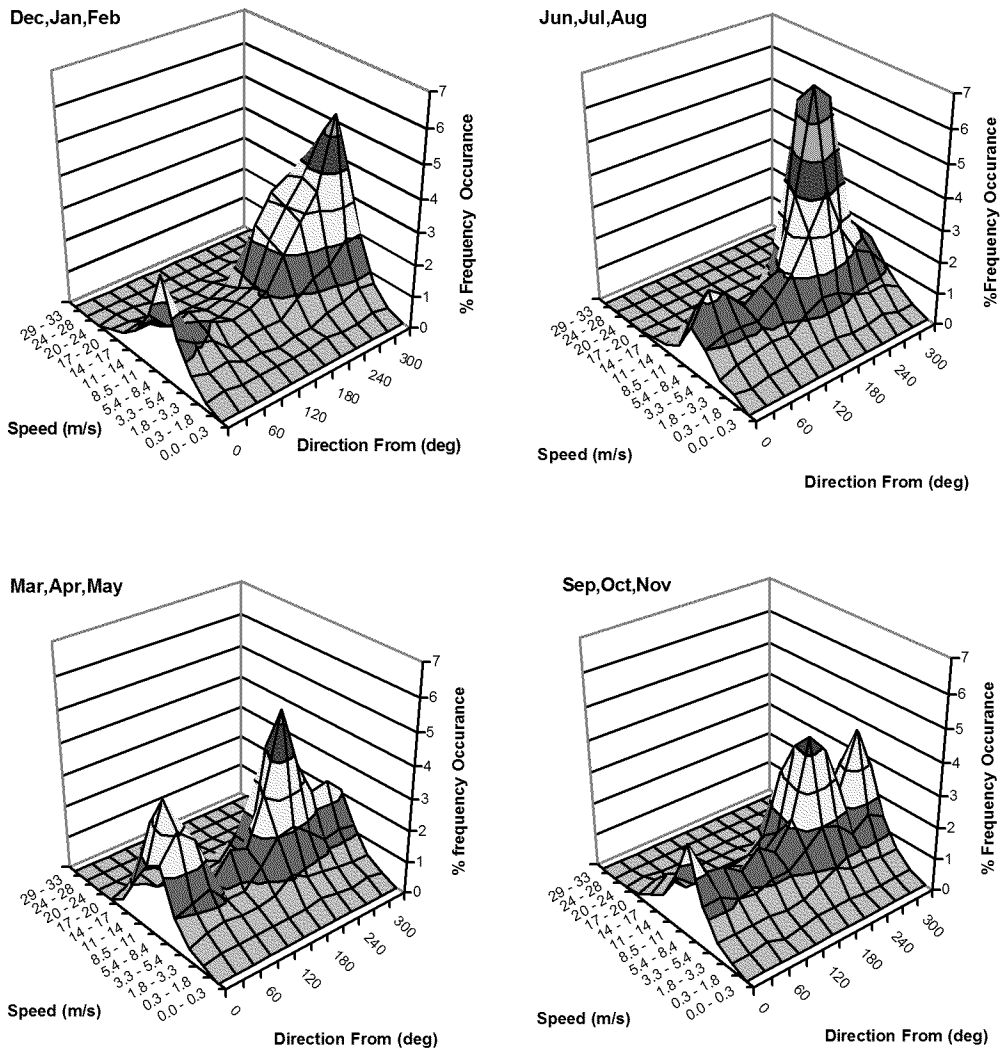

Source: NDBC Data (1985 – 1993)
Note: Wind measured at 81 ft above mean sea level. Contours represent percent frequency of occurrence of wind speed (m/s) and direction (from).

Figure 3. Average Wind Speed and Direction (by Season) Recorded at the Buzzards Bay Tower C-MAN Station (41.40°N 71.03°W).

3.0 WAVEANALYSIS

The ZSF is subject to waves that are generated locally by local winds and that propagate into the area from distant storms. In winter, average wind speeds in the ZSF of 16 to 17 knots are common, and gales (> 34 knots) occur up to 5 percent of the time. Waves that result from winds over the region depend on both wind speed and direction, since the fetch is limited to the north. The frequency of occurrences of certain wave heights and periods (measured by the NDBC at the meteorological station on the Buzzards Bay Tower during the period 1990 to 1992) are presented in Figure 4. A long-term record of waves in the region is not available; however, the available data are consistent with a 10-year wave model hindcast presented in Section 6 below. The most common occurrence of high waves is in March and November-December, when wave heights exceeded 6.5 feet more than 10 percent of the time. The 1990-1992 data showed that the average monthly wave heights are lower during January and February, when winds are strong but predominantly out of the northwest, than during the early spring, when predominant winds are somewhat weaker but southerly. Wave heights exceeded 10 ft more than 5 percent of the time in March. Long period swells (wave periods that exceeded 11 seconds [sec]) result from either severe local storms or storms offshore in the North Atlantic Ocean and occur most often in the spring and fall. Waves that exceeded 10-ft heights and 11-sec periods occur 5 percent of the time in March and 1 percent to 2 percent of the time in November-December and represent a very stormy wave climate capable of substantial reworking of sediments on the seafloor.

No wave measurements are available at or near Site W or Site E (Figure 1). The sites can be expected to experience a wave climate similar to that described previously for the ZSF in general; however, the fetch varies somewhat between the two sites which will result in some variation in wave climatology from the general area. The exposure of Site W to winds and waves from the southwest is partly blocked by the presence of Block Island and its surrounding bathymetry. The exposure of Site E to winds and waves from the east-southeast is partly blocked by the presence of Martha's Vineyard. (The fetch from the north is of little interest because the primary concern is for the large ocean swell and large storm-generated waves that propagate into the area from the south). To determine the effect of fetch at Site W and Site E, the results of the 10-year wave model hindcast presented in Section 6 were examined. Table 1 presents model-predicted wave heights and periods at Sites W and E for storms occurring at different frequencies (predictions are based on climatology data). A storm with a 5% frequency of occurrence can be expected to occur in the ZSF several times a year, while a storm with a 0.2-percent frequency of occurrence can be expected to occur only once in several years. These model results indicate that Site W will experience wave heights that are slightly lower and wave periods that are slightly shorter than those experienced at Site E under the same storm conditions. These wave heights are consistent with observations measured by the NDBC at the meteorological station on the Buzzards Bay Tower during the period 1990 to 1992.

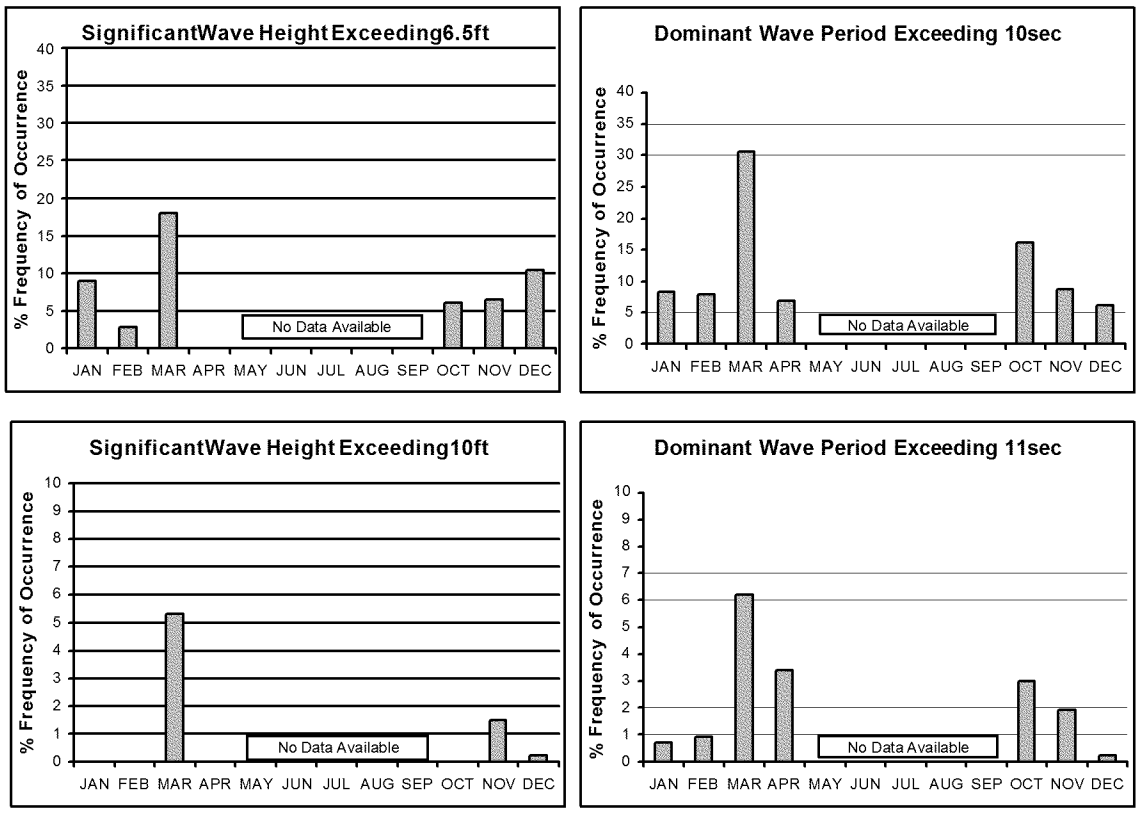

Source: NDBC.
Note: The left two charts represent frequency of occurrence of significant wave heights (percent of all waves that exceed 6.5 and 10 ft height). The right two charts represent frequency of occurrence of the dominant wave period (percent of all wave periods that exceed 10 and 11 seconds) during each month of the year.

Figure 4. Significant Wave Height and Dominant Wave Period (1990 to 1992) Recorded at the Buzzards Bay Tower C-MAN Station (41.40°N 71.03°W).

Table 1. Model-Predicted Wave Heights and Periods at Sites W and E for Storms of Various Frequencies of Occurrence.

Storm Frequency of Occurrence	Site E		Site W	
	Estimated Wave Height (ft)	Estimated Wave Period (sec)	Estimated Wave Height (ft)	Estimated Wave Period (sec)
5 %	9.5	7.2	8.9	6.6
1%	14.4	9.4	13.4	9.0
0.2 %	16.1	14.2	15.1	14.2

4.0 HISTORICAL CURRENT ANALYSIS

Circulation in Rhode Island and Block Island Sounds largely results from three influences, each working on different time scales: (1) a weak mean current, or mean drift, to the southwest (on the order of 5 cm/s); (2) occasional storm wind-driven currents, stronger in winter, with a time scale of 5 to 7 days (on the order of 25 cm/s); and, (3) 12-hour tidal currents (ranging from 20 cm/s to 250 cm/s, depending on the location). These different processes produce the regional current structure, which is dominated by tides close to shore, but with more variability due to storm-driven currents in the deeper open waters.

Tides are dominated by a semi-diurnal lunar tidal component. Maximum surface tidal current speeds approach 250 cm/s in the Race, a narrow channel on the eastern end of Long Island Sound that connects Long Island Sound to Block Island Sound (Figure 5). These are some of the highest tidal currents on the east coast of the United States. The tidal flows decrease eastward from the Race, to about 125 cm/s in Block Island Channel and about 70 cm/s between Block Island and Point Judith. Ebb currents are generally stronger than flood currents in Block Island Sound. Maximum surface tidal currents throughout Rhode Island Sound are less than 50 cm/s, usually ranging between 25 and 50 cm/s.

Block Island Sound exhibits characteristics of an estuary, with weak mean eastward surface flow and weak westward bottom flow. This represents the drift of surface waters out of, and bottom water into, Long Island Sound, which is driven by the estuarine circulation of Long Island Sound. The residual eastward flow at the surface, out of Long Island Sound into Block Island Sound, has been measured at 6 cm/s. Riley (1948) and Hicks (1959) observed southwesterly drift along the coast in Rhode Island Sound, which enters Block Island Sound and passes out to the Atlantic Ocean through Block Island Channel. Beardsley and Boicourt (1981) showed that the mean current flows were southwestward along depth contours at an average rate of 6 to 8 cm/s at a series of stations south of the ZSF. The mean southwest drift of continental shelf water contributes to the exchange of water between Rhode Island Sound and the Atlantic Ocean. However, the mean southwest drift is small relative to the tidal current at any given point. The magnitude of currents generated by wind events occasionally rivals the tidal current in the central portion of Block Island Sound and again contributes to the net flow of water into and out of Block Island Sound.

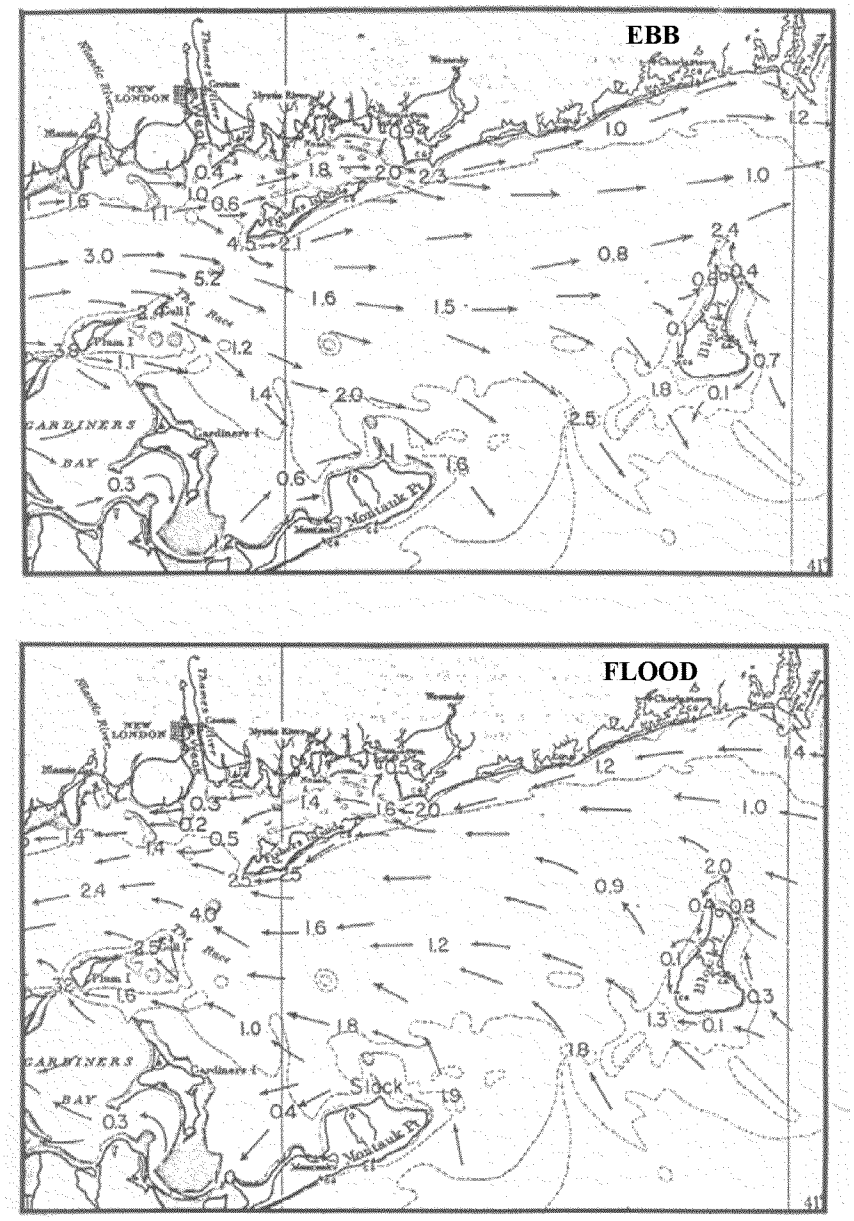

Source: NOAA Tidal Current Chart.

Figure 5. Maximum Ebb and Flood Tide Currents (Knots) Throughout Block Island Sound.

Rhode Island Sound and the outer portion of the ZSF experience much weaker tidal currents than Block Island Sound, with surface tides generally between 25 and 50 cm/s. The long-term mean (or net) southwest drift can also be seen here. Superimposed on the regular ebb and flood motions of the tides and the weak southwest mean drift are fluctuations in current speed and direction caused by storm systems. Wind-driven flows can be most important to the sediment transport climate, as the majority of sediment transport occurs during large storms when wind stress is highest and wave heights are their largest. Beardsley and Boicourt (1981) documented

that the mean southwestward circulation on the continental shelf throughout the New York Bight is dramatically altered by weather events. Southwestward flow is greatly enhanced by winter storms, when winds are from the northeast. Beardsley and Boicourt (1981) showed that strong winter storms could produce along-coast currents from 20 to 50 cm/s in the mid-shelf region. This is consistent with short-term current measurements made at three stations in Rhode Island Sound in September 1999 during hurricane Floyd. Non-tidal current velocities recorded at Site W reached 20 to 30 cm/s during the passage of hurricane Floyd, with the strongest surface currents directed offshore and the strongest bottom currents directed onshore (Figure 6). Hurricane Floyd's winds were strong but of short duration. Longer wind stress events, such as nor'easters, tend to generate even stronger flows.

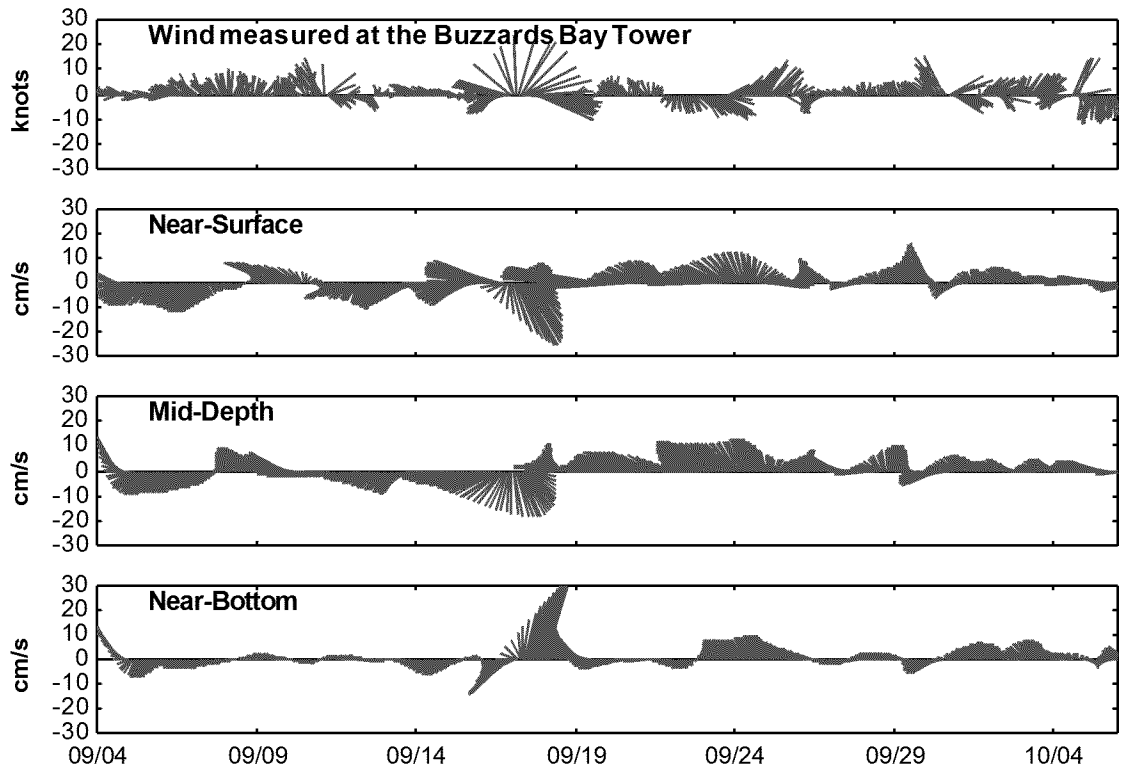

Note: The figure presents hourly observations of wind and current as a series of sticks whose length represent speed and whose direction represent the direction of the flow, with upward being north.
Source: Corps, 2004

Figure 6. Current Speed and Direction (Tide Removed) Recorded at a Station in Site W in Rhode Island Sound (September 1999).

Sites E and W are located in the open waters of the ZSF, where the factors that drive water column currents, including the tide, winds, storms, and water column stratification, are generally consistent across the ZSF. The direction of tidal currents, however, varies somewhat throughout the ZSF due to the influences of Long Island Sound and Buzzards Bay/Vineyard Sound. No long-term current measurements are available from within Site E or from the vicinity of Site E. A short-term current meter was deployed at a location several miles east of Site E in the spring of 1995 (Paul, 2003). The information from that deployment is limited but shows the tidal currents

are between 10 to 20 cm/s and are directed north or northeast and south or southwest. Currents observed during the 45-day deployment period reached as great as approximately 45 cm/s but appear to exceed 25 cm/s only about 5 percent to 10 percent of the time, which is consistent with previously described tidal current observations for the ZSF in general.

Long-term current measurements are not available from within Site W or from the vicinity of Site W. Short-term measurements, however, are available from a 1-month current meter deployment in the fall of 1999 (Corps, 2001a) and a 2-month deployment in April and May 2002 (Corps, 2003) and can provide anecdotal evidence of the local conditions. Tidal ellipse parameters for surface, middle, and near-bottom currents based on 2002 data (Corps, 2004) are presented in Table 2. The dominant tidal flow directions were northwest and southeast, with the narrow ellipses indicating little flow perpendicular to the dominant flow direction (Figure 7). The amplitude of the tidal velocity decreased with depth. The surface tidal amplitude was 11.8 cm/s, and the near-bottom amplitude was approximately 7.9 cm/s. Based on these data, only 40 percent to 60 percent of the current variance during the 2-month late spring deployment period was due to the tide. The remainder was caused primarily by wind stress and atmospheric pressure gradients associated with storms.

Table 2. Tidal Ellipse Parameters for Near-bottom, Middle, and Surface Currents Measured in Site W, April-May 2002.

Layer	Major Amplitude (cm/s)	Minor Amplitude (cm/s)	Inclination (deg)	Phase (deg)	% Vx Tidal Variance	% Vy Tidal Variance
Surface	11.8	1.6	111	31	13.7	41.6
Middle	10.9	0.8	104	27	11.2	62.9
Near-Bottom	7.9	2.0	120	10	33.4	61.9

Source: Corps, 2004

Near-surface currents recorded at Site W reached as high as 50 cm/s flowing toward the southwest. Currents this strong, however, were infrequent, with current speeds greater than 30 cm/s occurring only 3 percent of the time near-surface. Surface currents tend to be much stronger due to the effect of the wind stress on the surface layer. Throughout the rest of the water column, the maximum currents were only 30 cm/s and occurred only very infrequently. Velocities of 30 cm/s occurred only 2 percent of the time at mid-depth and 0.1 percent of the time near-bottom. Currents greater than 20 cm/s occurred approximately 9 percent of the time at mid-depth and 1 percent of the time near-bottom. The mean current for the station was 2.5 cm/s directed toward the southwest at mid-depth and 1.7 cm/s toward the southwest near-bottom.

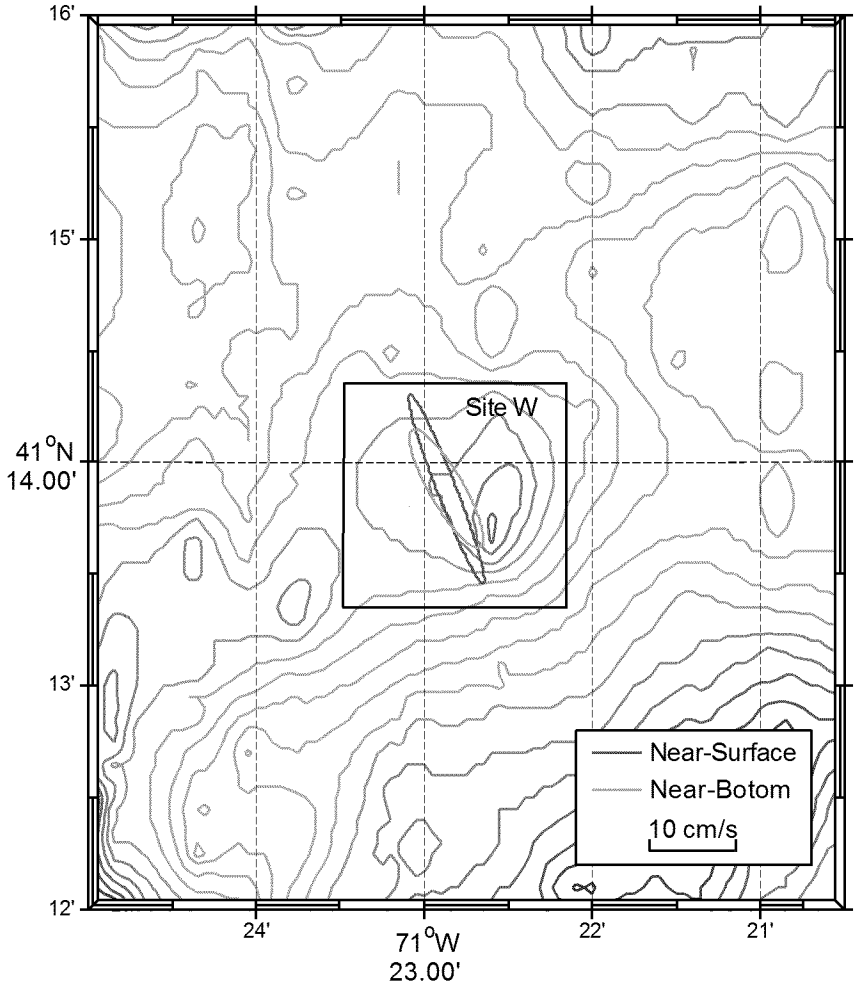

Figure 7. Surface and Bottom Tidal Ellipses at Site W.

Current meter and turbidity data from a 2-month measurement period in 2002 at Site 69B (unpublished data) provides some evidence that the alternative sites experience resuspension of local sediment several times each year. During the May–June 2002 measurement period, the background turbidity at Site 69B was observed to be 2 to 3 Nephelometric Turbidity Units (NTU)1 (Figure 8). During storm events on May 15th and 17th, however, near-bottom turbidity was recorded at 2 to 6 times above background levels. The peaks in turbidity corresponded to periods of large waves (wave heights between 2.0 and 2.5 m), but did not correspond to an increase in near-bottom currents. The wind speeds and wave heights observed during the two storms were not particularly high for the area with wind speeds reaching about 30 knots on May 15th and about 25 knots on the 17th. Historic records of wind speeds at Buzzards Bay Tower (see Section 2) indicate that wind speeds of 30 knots or more occur about two percent of the time

[1] As a point of reference, in the United States the allowable standard for turbidity in drinking water is 1 NTU.

during April. In contrast, wind speeds of greater than 30 knots occur 7.6 percent of the time in December. By extrapolation, higher and more frequent turbidity peaks can thus be expected during the winter months. Note that small increases above background turbidity were observed in the 2002 measurement record, which correspond to wave heights as small as 1.5 m to 1.7 m. These data suggest that there are particles that are resuspended frequently. These likely are fine particles (probably surface floc from the upper 1 to 2 mm of sediment) that are typically present on sediment surfaces (Figure 8).

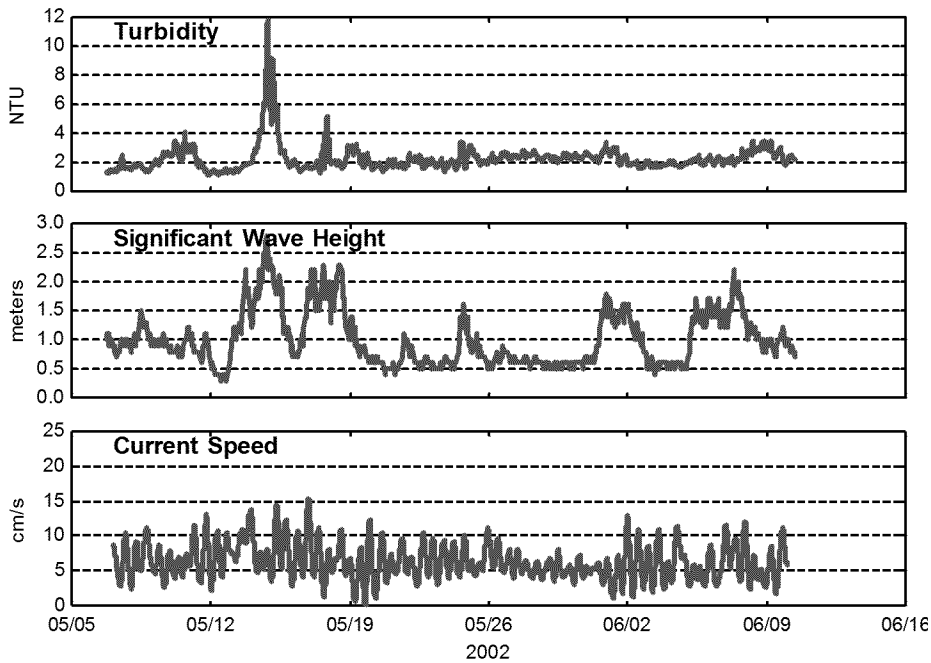

Source: Corps, 2004

Figure 8. Near-Bottom Turbidity, Near-Bottom Current, and Wave Height Measured at Site 69B in May and June of 2002.

5.0 DISPOSAL PLUME MODELING (STFATE)

While the bulk of dredged material released into the water column will settle to the bottom in the first few minutes after release, low concentrations of fine particles may persist in suspension for several hours, during which time they may be moved by the currents and diffused. For example, Rhodes (1994) suggests that between 0 and 6 percent of the dredged material (dry mass) can remain suspended in the water column as a turbid plume to be transported away from the disposal point (extrapolating from measurements at the Rockland disposal site [SAIC, 1988]). This is consistent with estimates by Tavolaro (1984) and Dragos and Lewis (1993) based on disposal events at the New York Mud Dump Site in the New York Bight and with laboratory experiments (Adams, personal communication).

5.1 STFATE Model Description

The Corps of Engineers' Short Term Fate (STFATE) dredged material disposal model was applied at each of the two alternative sites to predict disposal plume behavior. STFATE was developed to model disposal plume behavior including physical mixing, transport, settling and contaminant dilution in and around a disposal site during the first few hours after the release of dredged material. It is based on the work of Brandsma and Divorky (1976) and Koh and Chang (1973). STFATE models the behavior of the plume as a dense liquid (since the concentration of discharged dredged material in the plume is usually low), applying conservation of mass, momentum, buoyancy, and particle fall velocities. The results can be used to establish conditions in the discharge permit for management and monitoring of disposal in accordance with Corps regulations.

During release of a volume of dredged material into the water column, the behavior of the plume is separated in three phases: 1) convective descent, during which the plume settles under the influence of gravity; 2) dynamic collapse, occurring when the descending plume impacts the bottom or reaches a neutrally buoyant position in the water column and diffuses horizontally due to its own momentum; and 3) passive diffusion, beginning when transport and diffusion of the plume are caused more by the ambient oceanographic conditions (currents and turbulence) than by the dynamics of the plume body. This analysis is somewhat idealized, but it contains all the important hydrodynamic elements of the physical process and is based on the work of Scorer, 1957; Woodward, 1959; Csanady, 1973; Brandsma and Divoky, 1976; Tsai and Proni, 1985; Ecker and Downing, 1987; Kraus, 1991. See Figure 9.

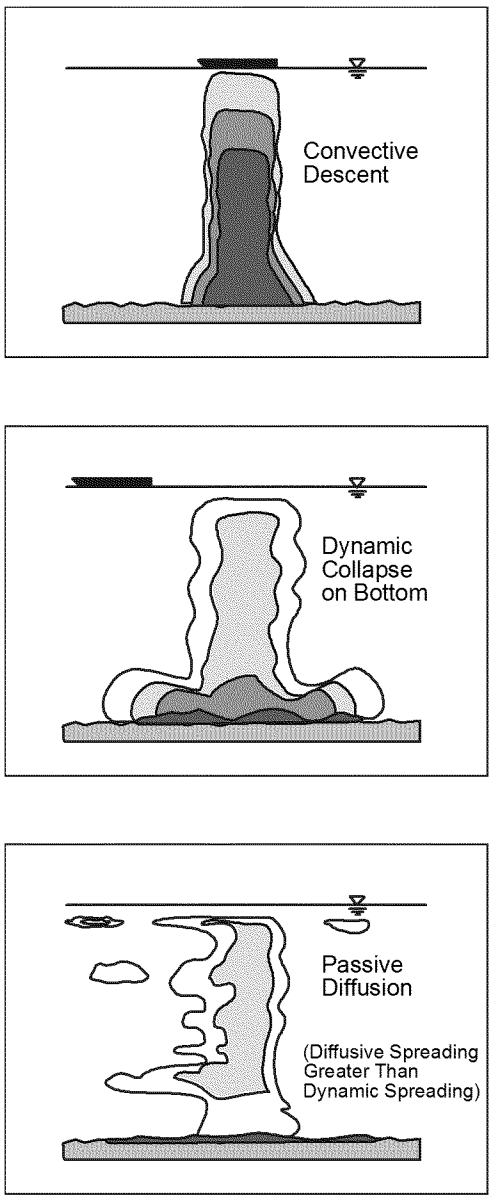

Figure 9. Illustration of Idealized Dredged Material Plume Behavior.

During the convective descent phase, the dredged-material plume maintains its identity as a single plume by the formation of a vortex ring structure. This analysis (Brandsma and Divoky, 1976) was based upon the work of Scorer (1957) and Woodward (1959) whose work treated a buoyant plume composed entirely of fluid. The study showed that once released, the plume will descend due to its initial momentum and its negative buoyancy. During its descent, it experiences drag from the ambient fluid that it is displacing. The plume grows as the receiving water is entrained into it and the concentration of the plume is greatly reduced due to the

entrainment and turbulence. The convective descent phase will typically last only a few seconds in shallow water.

If the plume immediately impacts the bottom, the dynamic collapse phase consists of the impact and collapse of the cloud as momentum spreads it horizontally. In shallow water, dredged materials have sufficient momentum to travel hundreds of meters laterally after impact with the bottom. If, while mixing with the receiving water, the plume's density approaches the local density, the plume may reach the depth of neutral buoyancy before hitting the bottom. This is more likely to occur under conditions of a stratified water column. In this case, the dynamic collapse phase is somewhat different. The plume's downward vertical momentum will tend to make it overshoot the neutral buoyant depth. The plume will then tend to return to the depth of neutral buoyancy. The result will be decaying vertical oscillations about the depth of neutral buoyancy. These oscillations increase the turbulence and increase the speed with which the plume tends to collapse vertically and spread out horizontally as it seeks hydrostatic equilibrium. Studies have shown that dredged material plumes released in shallow water (less than 25 m) usually experienced dynamic collapse by impacting the bottom as their initial momentum is too great to be overcome the plume buoyancy.

The final phase is the period of passive diffusion which occurs when transport and diffusion of the plume are caused more by the ambient oceanographic conditions (currents and turbulence) than by the momentum of the plume itself. Passive diffusion is the long-term dispersion and transport of the plume in which the cloud is passively carried by the local currents while undergoing gaussian diffusion. It operates on time scales of hours to days.

STFATE models the physical processes of the three phases described. The model simulates the descent and dynamic collapse of the plume and estimates from that the footprint of material that lands on the bottom and the amount and size distribution of the material that remains suspended in the water column after the collapse. Then, using ambient currents, it tracks the movement of the remaining suspended particles during the passive diffusion phase, modeling their slow fall to the seafloor due to gravity, the counterbalancing effect of turbulence which tends to keep them suspended, and the horizontal diffusion of the plume.

5.2 Model Input Requirements

Input data required by the model have been grouped into three categories: (1) description of the disposal operation, (2) description of the ambient oceanographic conditions at the disposal site, and (3) description of the dredged-material. The model input parameter requirements are shown in Table 3. In addition, the model uses default coefficients that parameterize poorly quantified physical processes including entrainment, settling, and dissipation, which may be modified if desired.

It should be noted that the authors of this model have indicated that limitations of the model include the model sensitivity to assumed model coefficients including the turbulent entrainment coefficient, the drag coefficient, and the vertical diffusion. The model also assumes that a dredged material plume will behave as a dense liquid; this simplification is reasonable only if the dredged material is composed primarily of fine-grained solids.

Table 3. STFATE Model Input Parameter Requirements.

Disposal Operations
Volume of dredged-material in barge
Barge course & speed
Barge length & width
Post disposal draft of barge
Disposal Site
Water depth
Water column density profile
Water Column Velocity Profile
Dredged-Material
Bulk density
Bulk contaminant concentration
Moisture content
Number of solid fractions
Solid-fraction volumetric concentration
Solid-fraction specific gravity
Solid-fraction deposited void ratio
Solid-fraction settling velocity
Solid-fraction cohesiveness

5.3 Application of STFATE to Site W and Site E

The STFATE model simulations were performed for each of the two alternative disposal sites on grids encompassing the disposal site and surrounding area (Table 4). For Site E, the grid was rotated counter-clockwise 35° to align it with the boundaries of the site. The model is not sensitive to small variations in depth due to the natural bathymetry, so the water depths were set to a uniform depth of the approximate mean depth of the site. A stratified density profile representing typical summer conditions was determined from historical data (Williams, 1969; Corps, 2003) and used for all model runs (surface layer salinity of 32 ppt, 19°C and bottom layer 32.5 ppt, 8°C) representing the most conservative case. It was also assumed that water from the dredging site would be fresher (less saline) than water at the disposal site. The disposal operation parameters, including volume of dredged material and barge dimensions, were based on information from typical dredge barges previously used by the Corps (Table 5). Estimates of the current velocities were determined from the analysis of current meter data described previously (Section 4.0). Time variant currents are not modeled by STFATE.

Table 4. STFATE Model Grid Parameters.

	Site W	**Site E**
Num Z Grid Points	40	40
Num X Grid Points	40	40
Z Grid Spacing (ft)	177	177
X Grid Spacing (ft)	177	177
Depth (ft)	118	125

Table 5. STFATE Model Disposal Operation Parameters.

	Site W	Site E
Disposal Operation Type	Split Hull Barge	Split Hull Barge
Disposal Location	Geographic center of site	Geographic center of site
Length of Disposal Bin (ft)	160	160
Width of Disposal Bin (ft)	42	42
Pre-Disposal Draft (ft)	17	17
Post Disposal Draft (ft)	4	4
Time to Empty (sec)	20	20

Sediment samples collected for the recent harbor dredging projects in the Providence River, RI, New Haven, Norwalk, and Guilford, CT were used to establish grain size and contaminant toxicity parameters (Corps, 2001b; 2001c; 2001d; 2001e) and are considered representative of typical dredged sediments that might be disposed in the alternative sites. The average geotechnical composition of the sampled sediments was selected for use in the model and consisted of a mix of 10% fine sand, 76% silt, and 14% clay (dry weight). Field experience shows that the clamshell dredging operations typically used to dredge sediments in the region results in a significant portion of the cohesive sediment remaining as clumps within the barge and during disposal and have free water at the top of the barge. For that reason, mixes of 40% and 60% clumps and 10% and 30% free water, were used for all STFATE modeling runs (see Table 6). The percent sand, silt, and clay were adjusted to volumetric concentrations taking into account clumps and free water (Table 6). Model simulations were run until the plume leading edge crossed the site and began to exit the site. Running simulations longer would result in the simulated plume impacting the grid boundary which results in unpredictable model behavior. The model simulation durations are given in Table 6.

Biological tests can be used as one part of the suitability determination for open water disposal of dredged material. One biological test used to make this suitability determination uses the sensitivity of indicator organisms to elutriated contaminants. This is done by determining the dilution required for sediment samples to reach elutriate levels fatal to 50 percent of the indicator organisms (i.e., LC_{50}). A summary of results from representative area harbors is presented in Table 7. For the two more commonly used species, *Mysidopsis bahia* (mysid shrimp) and *Menidia beryllina* (silversides), the average of the two most toxic samples had LC_{50} values of 28% and 26%. The lower of these two values (26%) was selected as a worst case. To represent more typical values, the LC_{50} value corresponding to the 85th percentile of samples was also selected (LC_{50} = 38%). The "Green Book" Evaluation of Dredged Material Proposed for Ocean Disposal — Testing Manual (EPA and Corps, 1991), sets a dilution criterion of 1/100th of the elutriate LC_{50} concentration. This criterion is not expected to be exceeded after the period of initial mixing (4 hours after dumping) anywhere in the designated disposal site or at anytime outside the disposal site. The STFATE model was used to evaluate water quality by tracking the predicted plume dilution in the water column and comparing it to the water quality criteria of 1/100th of the elutriate LC_{50} (0.26 percent and 0.38 percent). STFATE model runs were performed that varied the percentage of clumps and water content of the sediment in the barges,

plus the strength of the currents. This provided a matrix of conditions against which to compare the alternative sites for water quality impacts (Table 6).

Table 6. Dredged Material Properties Used in STFATE Model Simulations.

Model Run	Current Velocity (cm/s)	Simulation Duration (sec)	Barge Volume (cy)	Clumps (% vol)	Free Water (% vol)	Moisture Content (% wt)	Vol Water (% of tot)	Vol Clumps (% of tot)	Vol Sand (% of tot)	Vol Silt (% of tot)	Vol Clay (% of tot)
Site W											
RIS-FW01	20	5400	3000	40%	10%	100%	70.62	13.06	1.63	12.40	2.29
RIS-FW02	20	6000	3000	60%	30%	100%	72.21	23.82	0.40	3.02	0.56
RIS-FW03	17	6000	3000	40%	10%	100%	70.62	13.06	1.63	12.40	2.29
RIS-FW04	17	6000	3000	60%	30%	100%	72.21	23.82	0.40	3.02	0.56
RIS-FW05	20	6000	5000	40%	10%	100%	70.62	13.06	1.63	12.40	2.29
RIS-FW06	20	6000	5000	60%	30%	100%	72.21	23.82	0.40	3.02	0.56
RIS-FW07	17	7200	5000	40%	10%	100%	70.62	13.06	1.63	12.40	2.29
RIS-FW08	17	7200	5000	60%	30%	100%	72.21	23.82	0.40	3.02	0.56
RIS-FW11	20	5400	3000	40%	10%	100%	70.62	13.06	1.63	12.40	2.29
RIS-FW12	20	6000	3000	60%	30%	100%	72.21	23.82	0.40	3.02	0.56
RIS-FW13	17	6000	3000	40%	10%	100%	70.62	13.06	1.63	12.40	2.29
RIS-FW14	17	6000	3000	60%	30%	100%	72.21	23.82	0.40	3.02	0.56
RIS-FW15	20	6000	5000	40%	10%	100%	70.62	13.06	1.63	12.40	2.29
RIS-FW16	20	6000	5000	60%	30%	100%	72.21	23.82	0.40	3.02	0.56
RIS-FW17	17	7200	5000	40%	10%	100%	70.62	13.06	1.63	12.40	2.29
RIS-FW18	17	7200	5000	60%	30%	100%	72.21	23.82	0.40	3.02	0.56
Site E											
RIS-FE01	20	5400	3000	40%	10%	100%	70.62	13.06	1.63	12.40	2.29
RIS-FE02	20	6000	3000	60%	30%	100%	72.21	23.82	0.40	3.02	0.56
RIS-FE03	17	6000	3000	40%	10%	100%	70.62	13.06	1.63	12.40	2.29
RIS-FE04	17	6000	3000	60%	30%	100%	72.21	23.82	0.40	3.02	0.56
RIS-FE05	20	6000	5000	40%	10%	100%	70.62	13.06	1.63	12.40	2.29
RIS-FE06	20	6000	5000	60%	30%	100%	72.21	23.82	0.40	3.02	0.56
RIS-FE07	17	7200	5000	40%	10%	100%	70.62	13.06	1.63	12.40	2.29
RIS-FE08	17	7200	5000	60%	30%	100%	72.21	23.82	0.40	3.02	0.56
RIS-FE11	20	5400	3000	40%	10%	100%	70.62	13.06	1.63	12.40	2.29
RIS-FE12	20	6000	3000	60%	30%	100%	72.21	23.82	0.40	3.02	0.56
RIS-FE13	17	6000	3000	40%	10%	100%	70.62	13.06	1.63	12.40	2.29
RIS-FE14	17	6000	3000	60%	30%	100%	72.21	23.82	0.40	3.02	0.56
RIS-FE15	20	6000	5000	40%	10%	100%	70.62	13.06	1.63	12.40	2.29
RIS-FE16	20	6000	5000	60%	30%	100%	72.21	23.82	0.40	3.02	0.56
RIS-FE17	17	7200	5000	40%	10%	100%	70.62	13.06	1.63	12.40	2.29
RIS-FE18	17	7200	5000	60%	30%	100%	72.21	23.82	0.40	3.02	0.56

Table 7. LC_{50} Elutriate Results from Representative Area Harbors.

	M. bahia	*M. menidia*	*A. punctulata*	*M. beryllina*	Notes
Providence River, 1994					
	23% 65% 42% 33%	18% 65% 18% 17%			96hr. Location and depth of samples unknown.
Providence River, 1997					
			26% 6% 21%		Composites. Location and depth of samples unknown. This represents a deferent endpoint.
New Haven, CT, 2001					
	100% 59% 100% 100% 66%			100% 30% 100% 72% 49%	Location and depth of samples unknown.
Norwalk, CT, 2000					
	97% 65% 79% 69% 100% 56% 74% 53% 100%			63% 66% 35% 22% 100% 70% 62% 59% 100%	Location and depth of samples unknown.
Guilford, CT, 2000					
	100% 100% 100%			74% 100% 70%	Location and depth of samples unknown.
Summary					
mean of all <	60%			56%	
lowest	23%			22%	
average of 2	28%			26%	
85th percentile	41%			38%	

5.4 Results

5.4.1 Site W

For Site W, the STFATE model calculations were performed on a 7,080 feet by 7,080 feet grid encompassing the disposal site and surrounding area with grid resolution of 177 feet N by 177 feet E. The water depth was set to a uniform depth of 118 feet. An analysis of current data was used to characterize current velocities for Site W (described previously). Tidal currents at the site are directed northwest and southeast with an average diurnal tidal flow of 12–13 cm/s near-surface. However, only 40% to 50% of the current variance measured during the 2-month late spring deployment period was due to the tide (Section 4). The remainder was caused by wind

stress and atmospheric pressure gradients associated with storms. Depth-averaged currents of 20 cm/s resulting from the influences of the wind and the tide, which are directed toward the northwest, were selected for the period of the simulation. This corresponds to a 10 percent frequency of occurrence (currents of 20 cm/s or less were measured 90 percent of the time). These conditions are consistent with release during peak flood tide with a storm-driven current running in the same direction. The current speed was adjusted downward slightly in a second set of simulations to account for the diminishing of the tidal current that will occur during the 2-3 hrs of plume advection.

STFATE predicts the spread of the material in the water column during settlement, the footprint of the material on the bottom, and the distribution in space and time of the residual plume of suspended solids and contaminants relative to background conditions. Model results for Site W are summarized in Table 8 and are presented in detail in Figures A-1 though A-48. For each model run, three figures are presented including 1) predicted change in dredged material plume concentration over time, 2) predicted maximum horizontal plume concentration, and 3) predicted distribution of the footprint of new material on the bottom. Model simulations showed that the vast majority of the released dredged material settled to the bottom in close proximity to the point of release. The current conditions chosen for the simulation were the most significant factor in determining the residual plume behavior. This might be expected given that a current of 20 cm/s will cross half the width of Site W in approximately 1.25 hrs. For all simulations, the release point was chosen as the center of the site. The results of the STFATE model predictions for dilution relative to the toxicity criterion (1/100th of the LC_{50}) showed that all dilutions were well within the limits after the four-hour initial mixing period (Table 8; Figures A-1 through A-48). However, the toxicity criterion was exceeded in two cases when the plume passed out of the site boundaries approximately 100 minutes after release (Figures A-13 though A-18). This represents the worst case of sediment contamination properties, large barge volume, and high current speed (Table 8). Model simulations were run only until the plume just crossed the site boundary and began to exit the site. Dilution curves suggest that dilution would return to permissible levels within 10 to 20 minutes after the plume crossed the site boundary. If a larger upcurrent distance from the release point to the site boundary were used, the dilution criterion would not have been exceeded. This kind of management strategy might be difficult to apply to Site W, however, since the tidal currents account for only 40 percent to 50 percent of the total current variance, making it difficult to predict actual currents at the site at any given time. Barge size was another significant factor, but the percent volume of clumps and percent volume of free water used in the simulations were not significant within the ranges simulated. The results suggested that dilution of contaminants below the proscribed 1/100th LC_{50} level could be achieved for projects involving highly contaminated sediments by adjusting the management approach either by 1) limiting barge size, 2) properly positioning the release point according to the ambient currents, or 3) expanding the site boundaries. Dredged materials with contaminant levels equal to the 85th percentile rank for the four harbors reviewed (LC_{50} = 38%) were not shown to exceed water quality criteria.

Table 8. STFATE Model Parameters and Dilution Results for the Site W.

1/100th of the LC_{50}	Barge Volume (CY)	Current Speed (cm/s)	Clumps (% vol)	Free Water (% vol)	Elutriate Criteria Model Exceedence (Cause)	Figure Number
0.26%	3,000	20	40%	10%	Not Exceeded	A-1, A-2, A-3
0.26%	3,000	20	60%	30%	Not Exceeded	A-4, A-5, A-6
0.26%	3,000	17	40%	10%	Not Exceeded	A-7, A-8, A-9
0.26%	3,000	17	60%	30%	Not Exceeded	A-10, A-11, A-12
0.26%	5,000	20	40%	10%	Exceeded Outside Boundary	A-13, A-14, A-15
0.26%	5,000	20	60%	30%	Exceeded Outside Boundary	A-16, A-17, A-18
0.26%	5,000	17	40%	10%	Not Exceeded	A-19, A-20, A-21
0.26%	5,000	17	60%	30%	Not Exceeded	A-22, A-23, A-24
0.38%	3,000	20	40%	10%	Not Exceeded	A-25, A-26, A-27
0.38%	3,000	20	60%	30%	Not Exceeded	A-28, A-29, A-30
0.38%	3,000	17	40%	10%	Not Exceeded	A-31, A-32, A-33
0.38%	3,000	17	60%	30%	Not Exceeded	A-34, A-35, A-36
0.38%	5,000	20	40%	10%	Not Exceeded	A-37, A-38, A-39
0.38%	5,000	20	60%	30%	Not Exceeded	A-40, A-41, A-42
0.38%	5,000	17	40%	10%	Not Exceeded	A-43, A-44, A-45
0.38%	5,000	17	60%	30%	Not Exceeded	A-46, A-47, A-48

5.4.2 Site E

For Site E, the STFATE model calculations were performed on a 7,080 ft by 7,080 ft grid rotated 35° counter-clockwise to align the grid with the site boundaries. The grid resolution was set to 177 ft by 177 ft. The water depth was set to a uniform depth of 125 feet. The analysis of current data used to characterize current velocities in Site E was described previously (Section 4). No current measurements are available from directly within Site E. A short-term current meter record was recorded at a location several miles east of the Site in the spring of 1995 (Walter Paul, personal communication). The information from that deployment is limited, but shows the tidal currents are between 10–20 cm/s and are directed north or northeast and south or southwest. Currents observed during the 45-day deployment period reached as great as approximately 45 cm/s, but exceeded 25 cm/s only about 10 percent of the time. Depth-averaged currents of 25 cm/s directed toward the northeast were selected for the period of the simulation as corresponding approximately to a 10 percent frequency of occurrence (currents of 25 cm/s or less measured 90 percent of the time). The current speed was adjusted downward slightly in a second set of simulation to account for the diminishing of the tidal current that will occur during the 2-3 hrs of plume advection.

Model results for Site E are summarized in Table 9 and are presented in detail in Figures A-49 through A-96. For each model run, three figures are presented including 1) predicted change in dredged material plume concentration over time, 2) predicted maximum horizontal plume concentration, and 3) predicted distribution of the footprint of new material on the bottom. As with Site W, Site E model simulations showed that the vast majority of the released dredged material settled to the bottom in close proximity to the point of release. The current conditions chosen for the simulation were the most significant factor in determining the plume behavior. For all simulations, the release point was chosen as the center of the site. The results of the STFATE model predictions for dilution relative to the toxicity criterion (1/100th of the LC50)

showed that all dilutions were within the limits after the four-hour initial mixing period (Table 9).

Table 9. STFATE Model Parameters and Dilution Results for the Site E.

1/100th of the LC_{50}	Barge Volume (CY)	Current Speed (cm/s)	Clumps (% vol)	Free Water (% vol)	Elutriate Criteria Model Exceedence (Cause)	Figure Numbers
0.26%	3,000	20	40%	10%	Exceeded Outside Boundary	A-49, A-50, A-51
0.26%	3,000	20	60%	30%	Exceeded Outside Boundary	A-52, A-53, A-54
0.26%	3,000	17	40%	10%	Not Exceeded	A-55, A-56, A-57
0.26%	3,000	17	60%	30%	Not Exceeded	A-58, A-59, A-60
0.26%	5,000	20	40%	10%	Exceeded Outside Boundary	A-61, A-62, A-63
0.26%	5,000	20	60%	30%	Exceeded Outside Boundary	A-64, A-65, A-66
0.26%	5,000	17	40%	10%	Exceeded Outside Boundary	A-67, A-68, A-69
0.26%	5,000	17	60%	30%	Exceeded Outside Boundary	A-70, A-71, A-72
0.38%	3,000	20	40%	10%	Not Exceeded	A-73, A-74, A-75
0.38%	3,000	20	60%	30%	Not Exceeded	A-76, A-77, A-78
0.38%	3,000	17	40%	10%	Not Exceeded	A-79, A-80, A-81
0.38%	3,000	17	60%	30%	Not Exceeded	A-82, A-83, A-84
0.38%	5,000	20	40%	10%	Exceeded Outside Boundary	A-85, A-86, A-87
0.38%	5,000	20	60%	30%	Exceeded Outside Boundary	A-88, A-89, A-90
0.38%	5,000	17	40%	10%	Not Exceeded	A-91, A-92, A-93
0.38%	5,000	17	60%	30%	Not Exceeded	A-94, A-95, A-96

However, the toxicity criterion was exceeded in 8 of 16 cases when the plume passed out of the site boundaries, approximately 1 to 1.5 hours after release. Dilution returned to permissible levels usually within 30 minutes after the plume crossed the site boundary. If a larger upcurrent distance from the release point to the site boundary were used, the dilution criterion would not have been exceeded. Barge size was another significant factor, but the percent volume of clumps and percent volume of free water used in the simulations were not significant within the ranges simulated. Dredged materials with contaminant levels equal to the 85th percentile rank for the four harbors reviewed (LC50 = 38 percent) resulted in fewer exceedences but still exceeded water quality criteria for the case of large barge volume and higher currents. The results suggested that dilution of contaminants below the proscribed 1/100th LC50 level for worst case projects could be achieved by adjusting the management approach either by 1) limiting barge size, 2) properly positioning the release point according to the ambient currents, or 3) expanding the site boundaries. However, management of contaminated material would be more difficult for Site E because of the slightly higher currents there.

6.0 ZSF-WIDE SEDIMENT TRANSPORT MODEL (GRANT-MADSEN)

A model of sediment transport was applied to the entire ZSF to determine erosion potential on a broad scale. This section presents a description of methods used to develop tidal current and wave fields, the sediment transport modeling methods and the model results.

6.1 Method for Determining Bottom Sediment Motion

To estimate the potential resuspension of sediments caused by a wave and current field, the bottom shear stress generated by the wave and current forces is determined. Shear stress is the frictional or "sliding" force that horizontal currents exert on the sea bed (Figure 10).

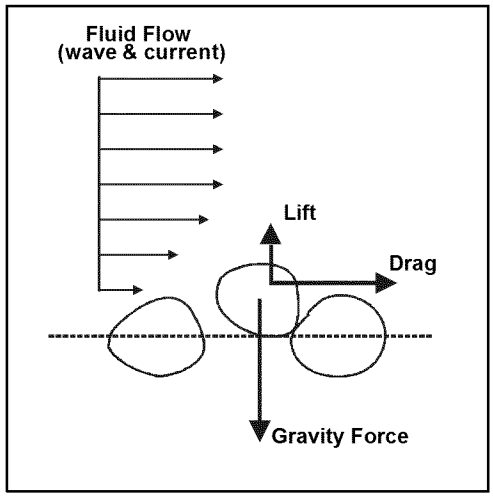

Figure 10. Schematic Depicting Shear Stress on the Sea Bed.

Resuspension is estimated by comparing shear stress exerted by the waves and currents to the critical shear stress that causes the initiation of sediment motion. Bottom shear stress is a function of the current velocity, wave height, wave period, water depth, and bottom roughness. Critical shear stress is estimated from size and density of the grains.

In Madsen and Grant (1986), the interaction of wave-induced currents (high frequency) and "background" currents with longer timescales (low frequency) is modeled. The result of Madsen and Grant (1986) is to provide a method for estimating the combined wave-current friction factor (f_{wc}) for sediments, which is necessary for the computing of non-cohesive sediment motion and sediment transport rates at a site on the sea bottom.

The Shields parameter is used as an indicator of incipient sediment motion, and is the ratio of the shear force τ acting on the bottom sediment, to the submerged weight of the grains. The Shields parameter is expressed as

$$\theta = \frac{\tau}{(s-1)\rho g d}$$

where s is the sediment specific gravity, ρ is the density of water, g is the gravitational constant and d is the diameter of the sediment grain. The shear stress is a function of the bottom friction factor f, and the magnitude of the fluid velocity U at the sediment bed, and is expressed as

$$\tau = \tfrac{1}{2} f \rho U^2$$

A critical value of the Shields parameter is determined using the Shields diagram (e.g., see Madsen, 1991), which defines the point of incipient sediment motion based on the boundary Reynolds number. For instantaneous values of the Shields parameter that are less than the critical value, no sediment motion will occur.

For conditions of ambient currents with superimposed wave currents, a combined wave-current friction factor f_{wc} must be determined. A method for computing f_{wc} is given by Madsen (1991), which is essentially an iterative method that modifies the bottom boundary layer based on the interaction with waves. Initially, in this method the wave friction factor f_{wc} for waves in the presence of currents is determined by using the equation

$$\frac{1}{4\sqrt{f_{wc}/C_\mu}} + \log\frac{1}{4\sqrt{f_{wc}/C_\mu}} = \log\frac{C_\mu u_b}{k_s \theta} - 0.17$$

where k_s is a characteristic bottom roughness, u_b is the magnitude of the velocity under the wave (in linear wave theory $u_b(t)=\sin[kx - \omega t]$), and the coefficient $C\mu$ is described as

$$C_\mu = \left(1 + 2\cos\theta_c \mu + \mu^2\right)^{1/2}$$

where

$$\mu = \left(\frac{u_{*c}}{u_{*wm}}\right)^2$$

and θ_c is the angle between the wave approach and the current direction, u_{*c} is the current shear velocity, u_{*wm} is the magnitude of the maximum wave shear velocity in the presence of currents (determined using linear wave theory assumptions). In this procedure, an initial guess for the value of μ must be made, because u_{*wm} is initially not known.

The final value of f_{wc} is computed using the equation:

$$f_{wc} = 2\left(\frac{u_{*c}}{u_r}\right)^2$$

where u_{*c} is the current shear velocity, and u_r is the magnitude of the measured current, measured at a particular height above bottom, z_r. The current shear velocity is determined by the equation

$$u_r = \frac{u_{*c}}{\kappa}\left(\ln\frac{z_r}{\delta_{cw}} + \frac{u_{*c}}{u_{*m}}\ln\frac{\delta_{cw}}{z_0}\right), \text{ for } z_r > \delta_{wc}$$

which is quadratic in u_{*c}, and

$$u_{*wm}^2 = \frac{1}{2} f_{wc} u_b^2,$$

$$u_{*m}^2 = C_\mu u_{*wm}^2,$$

$$\delta_{cw} = \frac{\kappa u_{*m}}{\omega},$$

where,

u_{*wm} = magnitude of the maximum wave shear velocity in the presence of currents,

f_{wc} = wave friction factor, for waves in the presence of currents,

u_{*m} = combined wave-current shear velocity,

δ_{cw} = wave bottom boundary layer thickness,

u_r = measured current velocity magnitude, at depth z_r,

u_{*c} = current shear velocity,

Dyer (1986) simplified this by stating that for sediment motion, the mobility factor, M / M_c must be greater than 1, where

$$M = \frac{\rho U_b^2}{(s-1)\rho g d}$$

is the wave-driven bottom shear stress, and U_b is the fluid velocity at the sediment bed, and

$$M_c = 0.46\pi\left(\frac{d_0}{d}\right)^{\frac{1}{2}}$$

is the critical shear stress needed to mobilize sediment, when d_0 is the wave orbital diameter, determined from linear wave theory, wave height and period.

6.2 Development of Wave and Current Fields for Sediment Transport Model

6.2.1 Wave Field

Wind fields, used to drive the wave model, were based on enhancements to the wind data generated by the National Centers for Environmental Prediction - National Center for Atmospheric Research NCEP-NCAR Reanalysis Project (http://www.cpc.ncep.noaa.gov).. A file of continuous daily wind fields was developed for the decade of the 1990's (1990-1999) over the North Atlantic. All available historical marine surface data (buoys, ships, coastal stations, scatterometer data) were adjusted to effective neutral 10-m winds. Any tropical cyclone effects within 240 nautical miles from the storm centers were assimilated into the wind fields after using a tropical cyclone boundary layer model with input from the NCAR hurricane database and reconnaissance data from the Tropical Prediction Center's Annual Data files (http://www.nhc.noaa.gov/). The historic data were then incorporated into the wind fields interactively so that extratropical and tropical systems were properly represented while incorporating surface data that were of sufficient quality and reasonableness. The time increment of the final wind fields was 6 hours. The wind fields were produced on a rectangular latitude/longitude grid with a resolution of 0.833 degrees in longitude and 0.625 degrees in latitude (Figure 11).

The wind data were validated using U.S. buoys and the Comprehensive Ocean-Atmosphere Data Set (COADS) data set (http://www.cdc.noaa.gov/). The COADS project is a cooperative effort between NOAA -- its NESDIS/National Climatic Data Center (NCDC) and its OAR/Climate Diagnostics Center (CDC) -- and NCAR. COADS provides a standard of comparison and gives meaning and context to the environmental measurements being collected daily around the globe. Global marine data observed between 1784 and 1997 (the currently available period-of-record), primarily from ships of opportunity, have been collected, edited, and summarized statistically for each month of each year of the period. These measurements of temperatures, humidity, winds, pressures, waves, and clouds have been applied to global and regional studies of oceanographic and atmospheric phenomena. Altimeter data were also used for back-validation.

Quantile-quantile and exceedence plot comparisons of wind speed showed excellent agreement between the hindcasted winds and the measurements at NOAA Buoy 44025 and 44028. Both buoys were used as sources of data during the wind field development process. Buoy 44025 is located about 20 miles south of Long Island. Buoy 44028, is located at the entrance to Buzzards Bay, Massachusetts, and provides a good measurement of marine winds in close proximity to the ZSF. The hindcasted winds compare well with the measurements over the range of wind speeds where data exist. At Buoy 44028, located closest to the study site, a best-fit line indicates a small overprediction of approximately 2.6 knots (1.3 m/s), or about 5% or less, at the maximum recorded winds speeds. Although storms are represented to a high degree of accuracy, a higher temporal resolution would be required to make the continuous daily wind field data set appropriate for storm hindcasting.

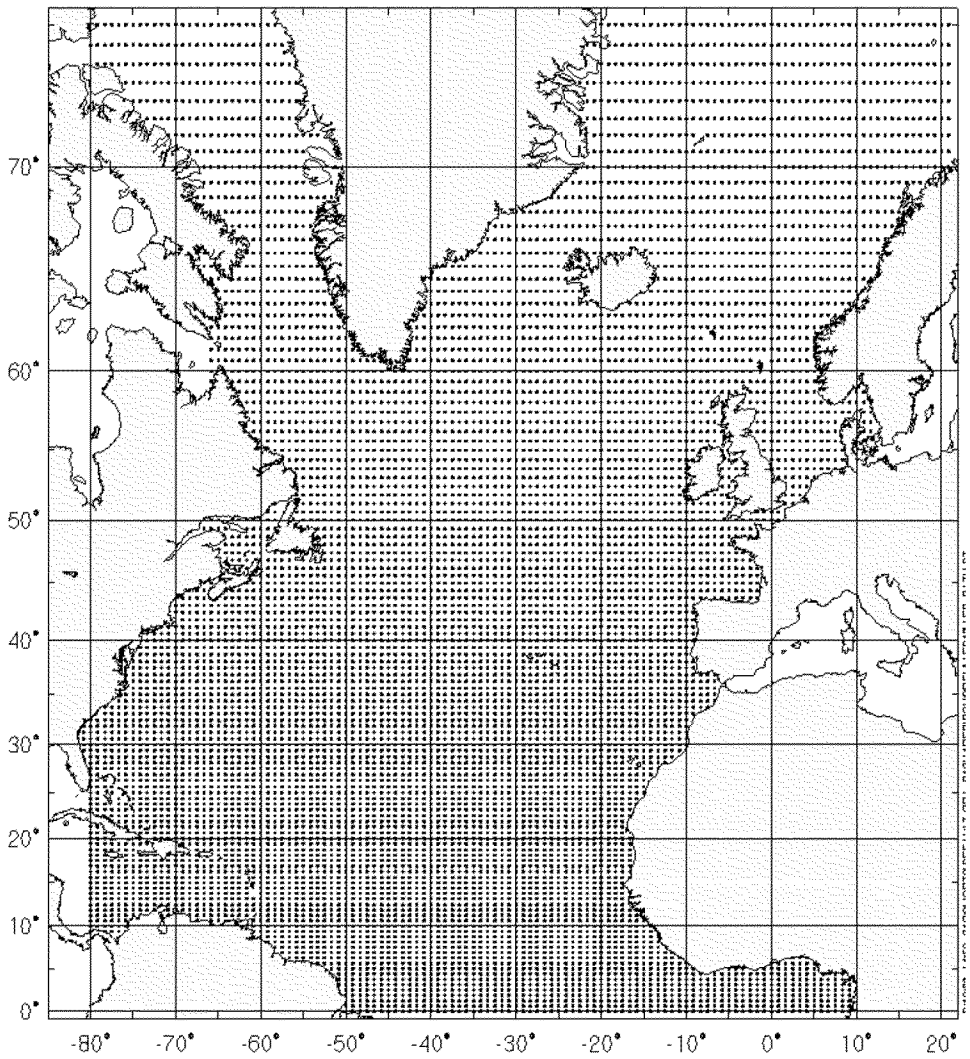

Figure 11. Wind Model Grid.

A directional spectral time-stepping wave model WAVAD (also known as WISWAVE) was applied to characterize long term wave climate by modeling ten-years of continuous waves during the 1990's. Bathymetric data implemented for the wave modeling were obtained from several sources. Open ocean bathymetry was obtained from NOAA nautical charts and bathymetry for Rhode Island Sound was used from a USGS database. Two levels of nesting were used to generate the wave data at a resolution appropriate for the Rhode Island Sound grid:

- A 0.25-degree (approximately 15 nautical mile) grid extending from 50 degrees to 80 degrees West longitude and from 20 to 45 degrees North latitude, to include ocean swell;

- A 0.04167-degree (approximately 2.5 nautical mile) grid extending from 71.9998W to 71.0415W and from 40.8750N to 41.5833N.

The 10-years of winds were hindcasted on a 6-hourly time increment that is meant to define the long-term wave distribution in the area of interest. The spatial coverage of the wind input grids is the same as the wind grids described earlier in this report.

Although there are no available wave data sets to validate the wave modeling locally at project sites, the wave data produced by the hindcast model were assessed at NOAA buoy 44025 for a one-year period and for a significant storm event. The 6-hourly wave conditions were averaged over the year 1998 as an indication of the long-term performance of the model (Table 10). The year 1998 was selected because the wave conditions included a wide range of wave heights including a large stormy period in February. The results indicate that over the year, the model reproduces the average zero moment wave height, Hmo, within 0.26 ft, the average peak spectral wave period, Tp, within 1.2 seconds and the average peak spectral wave direction within 5 degrees. These comparisons are considered acceptable for a long-term hindcast. The storm peak in early February is modeled to within 0.66 ft of the 18.4 ft peak wave height during the storm.

Table 10. Wave Model Validation Statistics for 1998.

	Hindcast	**Measured at Buoy 44025**
Mean Annual Hmo (ft)	3.8	4.0
MeanAnnual Tp (s)	6.05	7.25
Mean Annual Peak Wave Direction (degrees from North)	169.3	164.1

6.2.2 Current Field

Sediment resuspension will most likely occur during the time of peak flood tide. A tidal model was used to simulate a constituent-driven ocean tide. Modeling was performed with the finite element numerical Advanced Circulation (ADCIRC) model, described in Luettich, *et al.*, 1992.

Bathymetric data implemented for the ADCIRC water level modeling and the wave modeling were obtained from several sources. Open ocean bathymetry was obtained from NOAA. Bathymetry for Rhode Island Sound was developed using data from a USGS database. Model validation was performed by reviewing constituents and time history output for mean tidal conditions at Newport and Montauk. The model mesh coverage is illustrated in Figure 12.

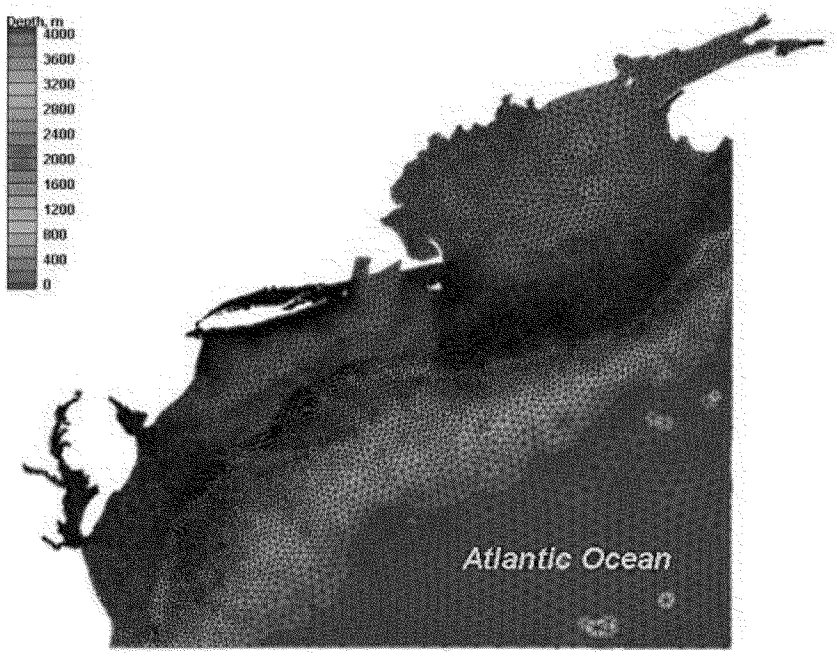

Figure 12. ADCIRC Tidal Model Computational Domain.

6.3 Sediment Transport Model

The outputs from the tidal current model and wave model were generated over a 2.5-minute grid extending from 71.9998W to 71.0415W and from 40.8750N to 41.5833N. The results from the tidal model consisted of a field of north- and east-directed components of current at peak flood tide. The flow patterns and magnitudes compared favorably to the NOS Tidal Current Charts (1971).

The results from the wave model were 6-hourly matrices of zero-moment wave height, peak spectral wave period and mean wave direction at the peak of the wave spectrum.

The output was analyzed at a 6-hour increment for the entire 10-year hindcast period. The wave data over the analysis region were tabulated to compute the percent exceedence at even increments of wave height. The wave-driven bottom horizontal orbital velocity was calculated at every grid point in the region and the percent exceedence was determined for even increments of this current speed. Bottom orbital velocity was calculated using linear wave theory, becoming zero when the water depth exceeds half the wave-length.

Sediment resuspension potential was calculated by the bottom shear stress and the size and density of the sediment particles. The bottom shear stress is a function of the current velocity, wave height, wave period, water depth, and bottom roughness. The bottom sediment size was assumed to be 1mm, which represents a finer but consolidated noncohesive material. The peak flood tide current speed was added to the wave-driven bottom orbital velocity, assuming that the directions of the two were coincident.

6.4 Sediment Model Results

The model of sediment transport was then applied to the ZSF for various grain sizes, tidal current, and wave conditions. The model predicted the distribution of sediment erodability (the ratio of the wave and current-induced bottom shear stress to the critical threshold shear stress). The predicted distribution of sediment erodability over the ZSF for the 1 percent frequency of occurrence wave conditions combined with the typical peak tidal currents for 0.5 mm, 1.0 mm, and 2.0 mm grain sizes is shown in Figures 13-15. The modeled wave conditions represent the waves expected during the strongest winter storm of a single year. Cohesive sediments, typical of harbor dredged material, are more resistant to erosion by hydrodynamic forces. To compensate, coarse grain sizes were chosen for use in the non-cohesive model to offset the effect. Lower sediment erodability values indicated that less energy was available for the erosion, resuspension, and transport of bottom sediments. Sediment erodability parameter values less than 1 indicated that wave and current energy were not sufficient to resuspend and transport even non-cohesive bottom sediments for the given storm conditions and indicated depositional areas. Sediment erodability parameter values greater than 1 but less than 3 indicated that wave and current energy may occasionally be sufficient to mobilize non-cohesive bottom sediments and indicated areas of some sediment sorting and reworking. Sediment mobility parameter values greater than 3 indicated high wave and current energy environments and areas of coarse-grained deposits and/or erosion or non-deposition.

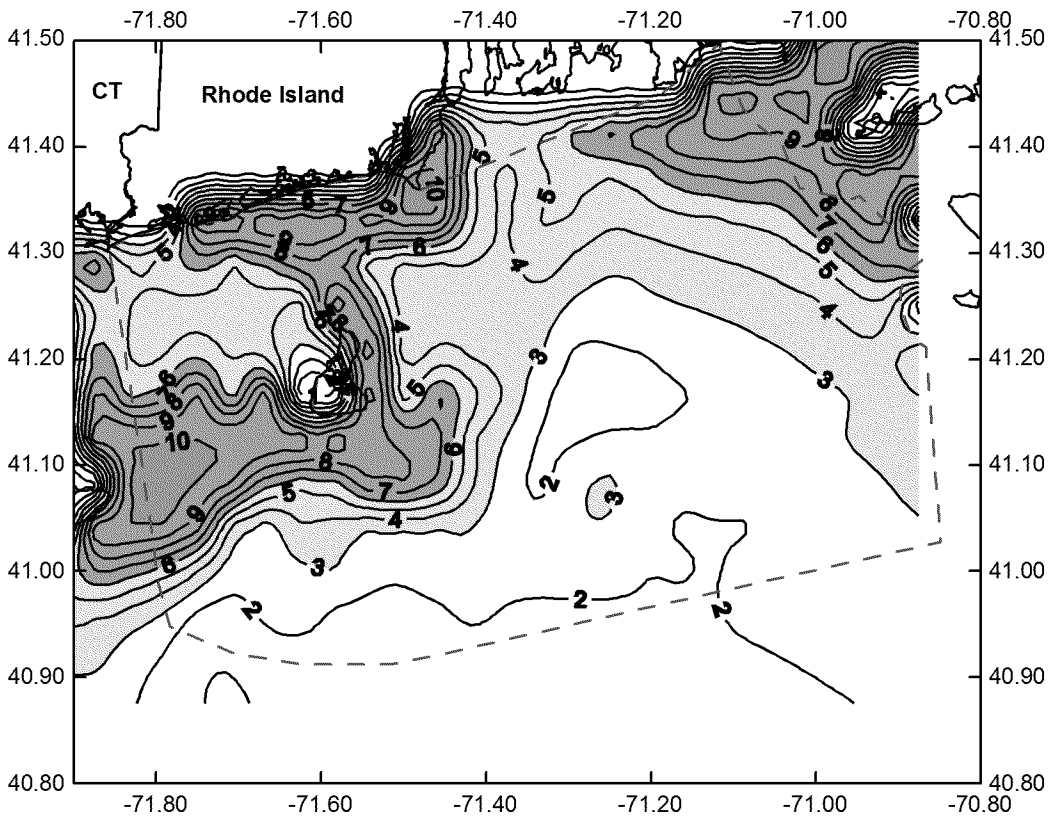

Figure 13. Predicted Sediment Erodability Parameter for 0.5-mm Grain Size for Typical Peak Tide and 1 Percent Frequency of Occurrence Wave Conditions.

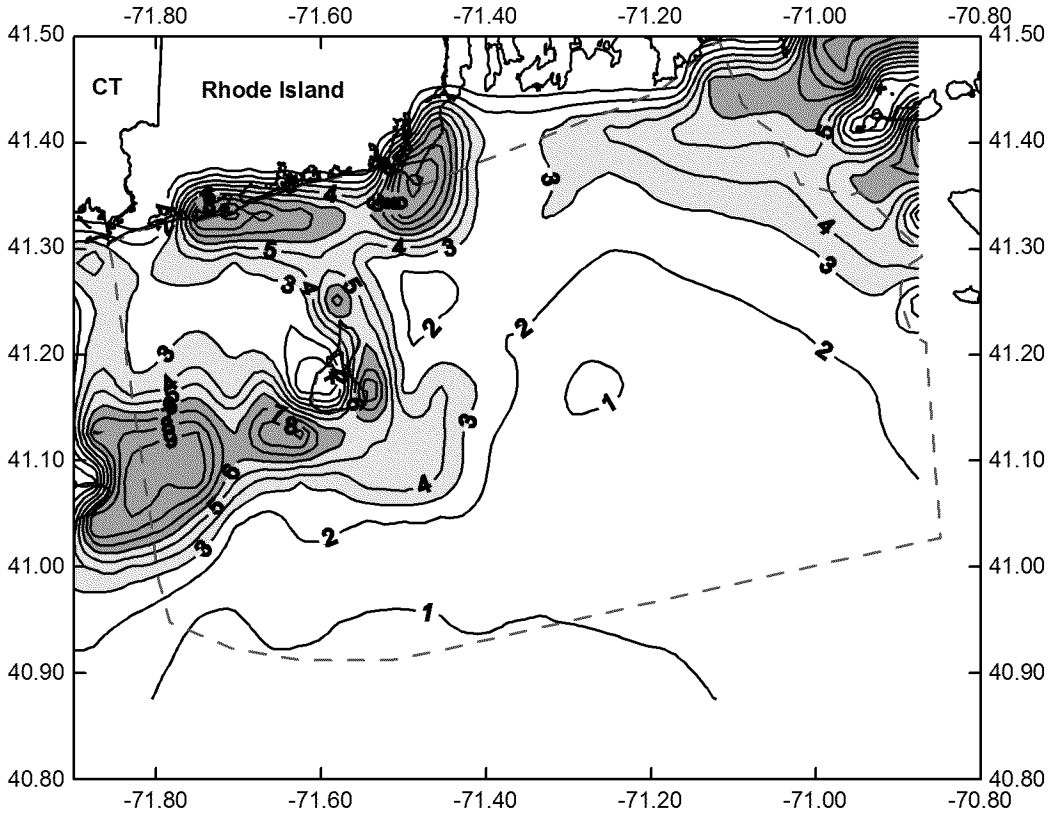

Figure 14. Predicted Sediment Erodability Parameter for 1.0-mm Grain Size for Typical Peak Tide and 1 Percent Frequency of Occurrence Wave Conditions.

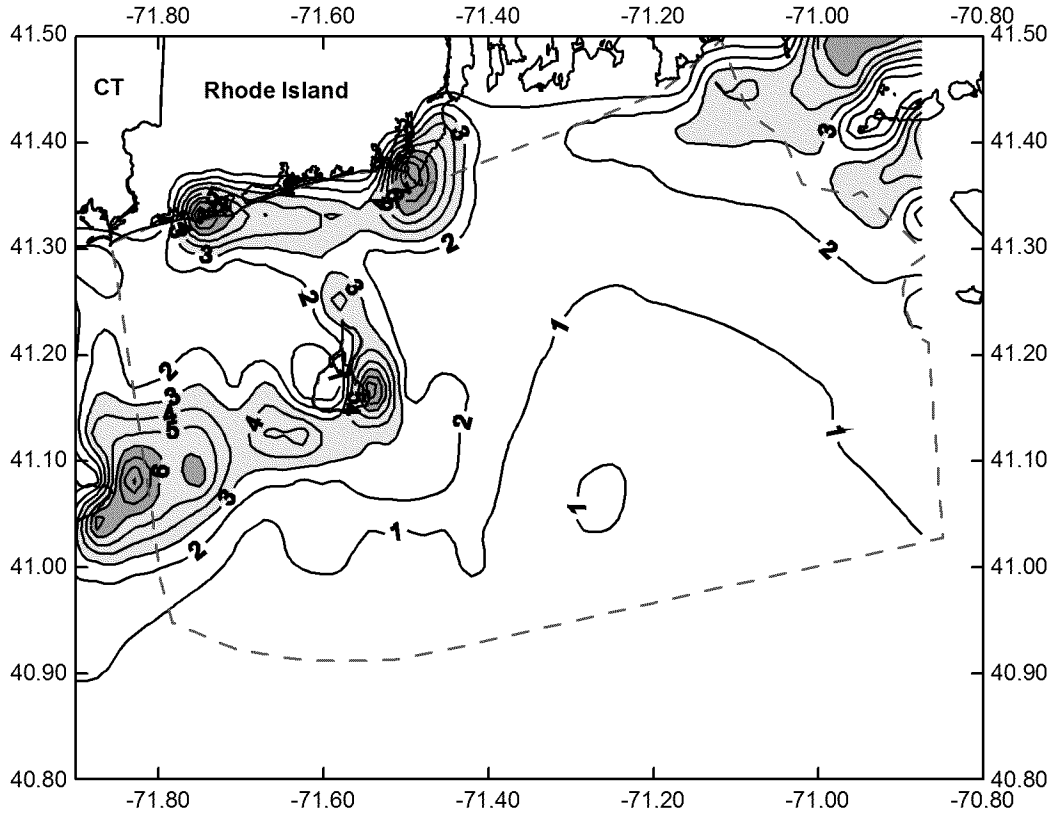

Figure 15. Predicted Sediment Erodability Parameter for 2.0-mm Grain Size for Typical Peak Tide and 1 Percent Frequency of Occurrence Wave Conditions.

Figures 13-15 show the modeled areas of deposition (erodability parameter less than 1) in deep water offshore and in the central bathymetric depression of the ZSF for grain sizes of >0.5 mm. The figures also show areas of infrequent reworking of bottom sediments (erodability parameter between 1 and 3) in the north-central portion of the ZSF and in central Block Island Sound for grain sizes >0.5 mm (although the effect of the tidal currents in Block Island Sound may be under estimated based on the modeling results). For the unsheltered area of the outer ZSF, the model predicted that sediments >0.5 mm were not expected to be resuspended at depths below 170 ft and would probably only occasionally be resuspended at depths below 105 ft. Inshore, it was more difficult to relate potential erodability to depth alone, because of the sheltering effect of Block Island and Martha's Vineyard on wave heights and the strong tidal currents between Block Island and Point Judith and Block Island and Montauk Point. The relationship between erodability parameter and depth is presented in Figure 16 through Figure 18 for different grain sizes.

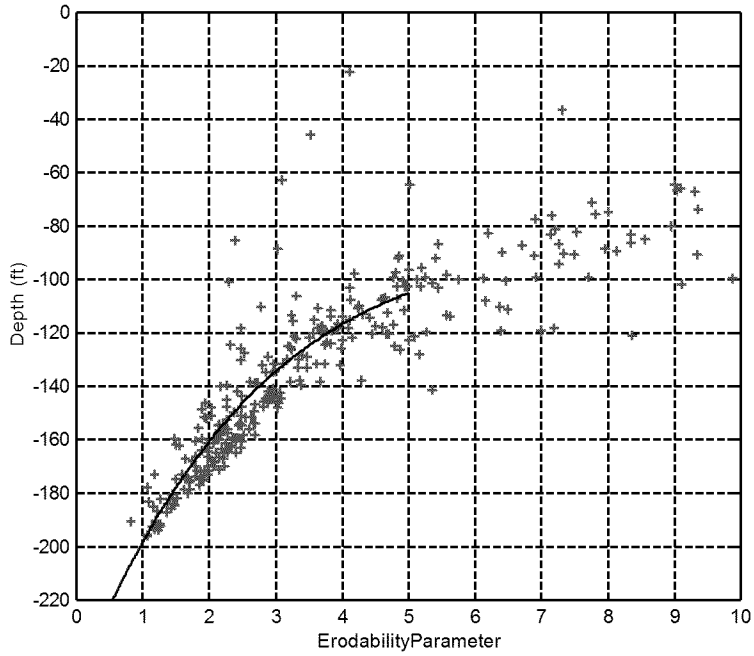

Figure 16. Predicted Relationship Between Depth and Sediment Erodability Parameter for 0.5-mm Grain Size, Typical Peak Tide, and 1 Percent Frequency of Occurrence Wave Conditions.

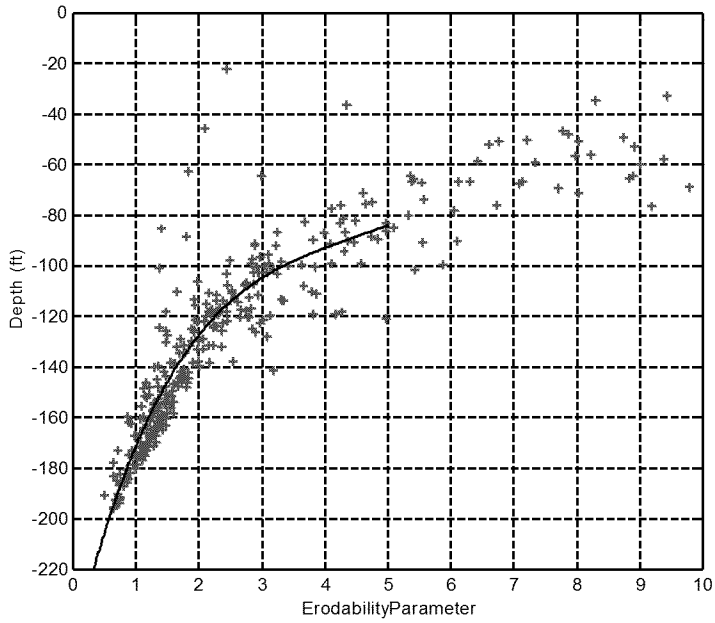

Figure 17. Predicted Relationship Between Depth and Sediment Erodability Parameter for 1.0-mm Grain Size, Typical Peak Tide, and 1 Percent Frequency of Occurrence Wave Conditions.

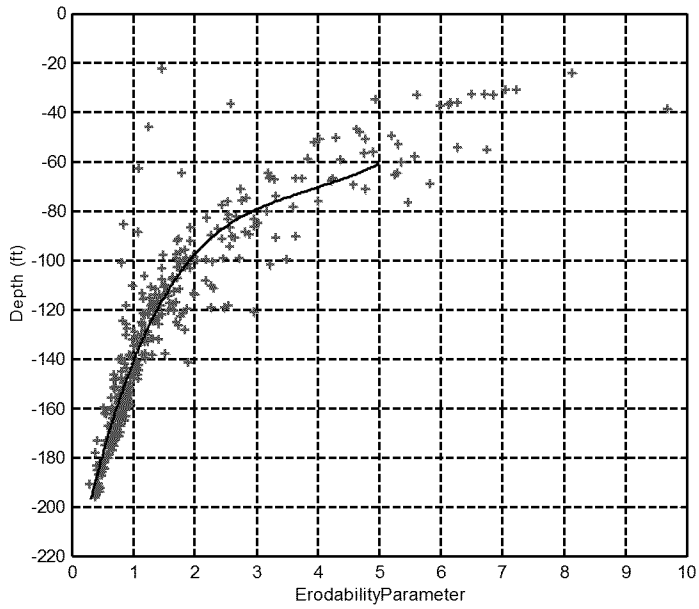

Figure 18. Predicted Relationship Between Depth and Sediment Erodability Parameter for 2.0-mm Grain Size, Typical Peak Tide, and 1 Percent Frequency of Occurrence Wave Conditions.

These results are consistent with observations of the surficial sediments of disposal mounds at Site 16, the historic disposal site. A mix of fine and coarse grains was observed below a depth of approximately 90 ft, but coarse grains were observed in depths shallower than 90 ft (Corps, 1979). This indicated that the fine grains had been winnowed out by the action of waves in depths shallower than 90 ft. The model results were also consistent with the results of another modeling study performed as part of the Providence River and Harbor Maintenance Dredging Project EIS (Gailani *et al.*, 2001), which examined the likelihood of erosion and transport of cohesive sediments proposed for placement at Site 69B, located at a depth of 128 ft. Gailani *et al.* concluded that a disposal mound placed at Site 69B would not be dispersive under any conditions other than the most severe (50-year return period) hurricane; their results, however, were based on an assumption of extremely cohesive sediments and should therefore be viewed as potentially underpredicting erosion.

7.0 COHESIVE SEDIMENT TRANSPORT MODELING OVER MOUNDS (LTFATE)

The disposal of dredged material at open ocean sites results in the deposition of non-native sediments in a 'footprint' or mound on the sea floor. Over time, as currents move over this mound, hydraulic forces act on the sediment particles in the form of shear and lift. The response of the particles to these forces is related to current speed, particle size, shape, density, and any friction or cohesion exerted by adjacent sediment grains. At some point, the fluid exerts sufficient force to cause the grains to move and the sediment will be eroded from the bottom and suspended (or resuspended) into the water column for transport. The Long-Term Fate

(LTFATE) sediment erosion and transport model (Scheffner *et al.*,1995; Scheffner 1996) was applied in an effort to derive estimates of sediment erosion and transport for cohesive, fine-grained sediments on a site specific basis.

7.1 LTFATE Model Description

LTFATE (Scheffner *et al.*, 1995; Scheffner 1996) was developed by the U.S. Army Corps of Engineers to model sand and fine-grained, cohesive silt and clay transport from dredged material placement sites. The inter-particle forces between fine-grained silt and clay sediments, unlike sand, are significant when estimating transport processes. Grain size distribution, mineralogy, bulk density, and organic content have been demonstrated to significantly affect erosion rates, such that sediments which are otherwise similar, but with different organic content, for example, may have orders of magnitude difference in their erosion rates (Lavelle, et al., 1984). In addition, the erosion rates tend to decrease with depth below the sediment/water interface even for sediments of consistent mineralogy and grain size distribution. Fine-grained silt and clay sediments will tend to become cohesive over time due to consolidation and biological reworking. The LTFATE model incorporates the effects of sediment cohesion, along with hydrodynamics, in its simulations of sediment transport. It also predicts changes in mound geometry as dredged material erosion and deposition cause bathymetry changes (i.e., mound evolution). Without extensive field measurements for model calibration and verification, the predictions of LTFATE should be considered estimates only. However, because the model represents physical processes consistently, their use provides a valid comparison between the alternative sites

LTFATE models hydrodynamics using linear wave theory and a combined wave and current bottom shear stress formulation similar to what was described previously for Grant-Madsen. The formulation can be seen in detail in WES, 1998. In addition, it incorporates a commonly used method of relating erosion to shear stress where erosion is a function of shear stress to some exponential power, $\in$, in g/cm^2 /sec:

$$\in = A_0 \left(\frac{\tau - \tau_{cr}}{\tau_r} \right)^m$$

where A_0 and m are site specific parameters which vary with depth (and are usually determined by laboratory or field experiments on the sediments of interest), τ is the shear stress due to currents and waves, τ_{cr} is the site specific critical shear stress below which no erosion occurs (assumed to vary with depth), and τ_r is a reference shear stress (set to a constant in dyne/cm^2). This equation was developed for moderate stresses. The model must be regarded as limited in this way since the storms modeled in this effort represent high shear stresses, but the physical processes are well represented by the model and much can be determined by using the moderate shear equations.

7.2 Application of LTFATE to the Alternative Sites

The LTFATE model was applied to each alternative site by using a series of simulations. For all simulations, the model assumed 8.8 million cubic yards (total estimated future disposal needs), deposited in 10 mounds distributed throughout each site. A data set of severe storms that passed near Rhode Island Sound from 1933 through 1985 (Gailani *et al.,* 2001) provided model input

for waves and currents. The data set included nine hurricanes and two extra-tropical storms. Gailani et al. used historical storm tracks, wind speed, and central pressure values to predict wave fields using a wave model and current time histories by combining tidal currents and modeled storm currents. LTFATE simulations were performed for five storms summarized in Table 11 and shown for Site W in Figure 19 through Figure 23.

Table 11. Storms Modeled with LTFATE Including Historical Storm Events Impacting Rhode Island Sound and Simulated Storms.

	Maximum Significant Wave Height (ft)		Peak Wave Period (sec)		Maximum Current Magnitude (cm/s)	Minimum Tidal Elevation (ft)	Maximum Tidal Elevation (ft)
Storm ID	**Site E**	**Site W**	**Site E**	**Site W**			
370 (1936)	23.3	21.7	11.6	11.0	20	-2.1	2.0
712 (1972 Hurricane Agnes)	16.0	14.9	9.5	9.0	25	-1.6	2.6
748 (1976 Hurricane Belle)	14.7	13.7	8.4	8.0	8	-1.4	1.7
H1.7	5.8	5.4	7.7	7.3	20	-2.1	2.0
H2.5	7.6	7.1	5.6	5.3	8	-1.4	1.7

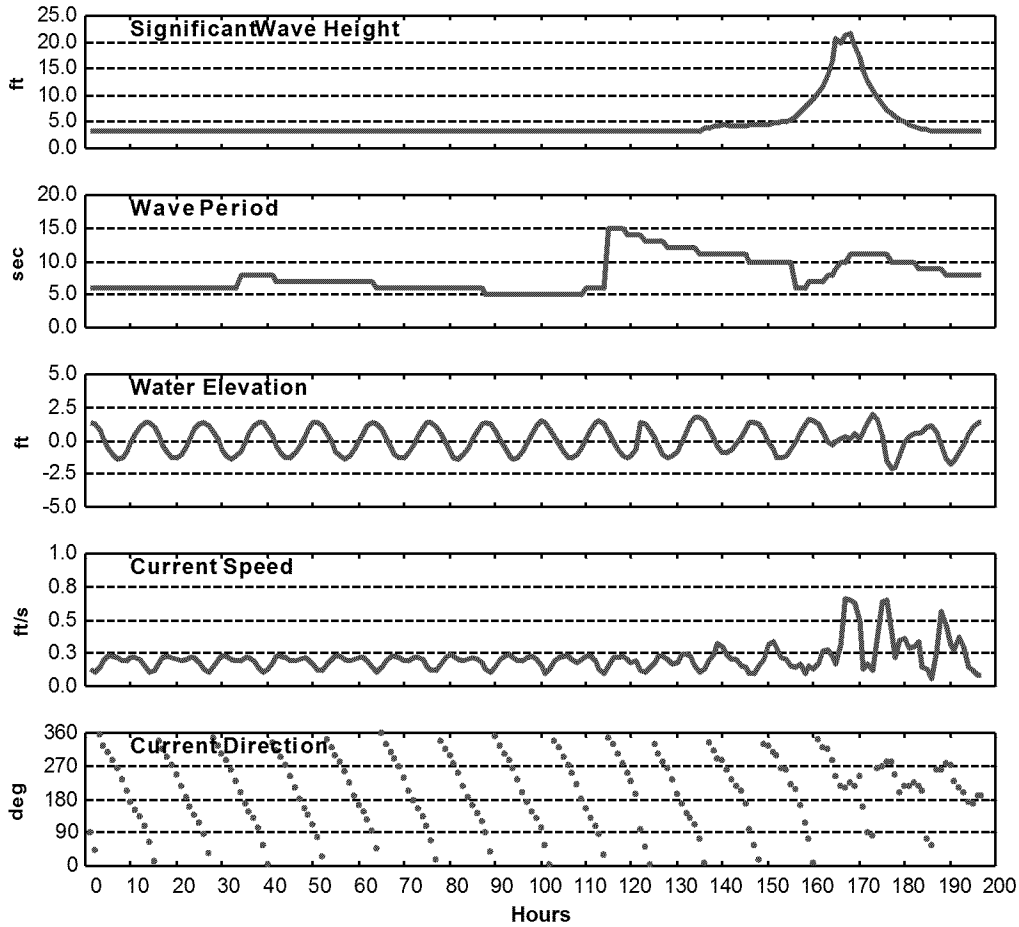

Figure 19. Storm 370 (1936) Time Series of Significant Wave Height, Wave Period, Sea Surface Elevation, Current Speed and Direction for Site W.

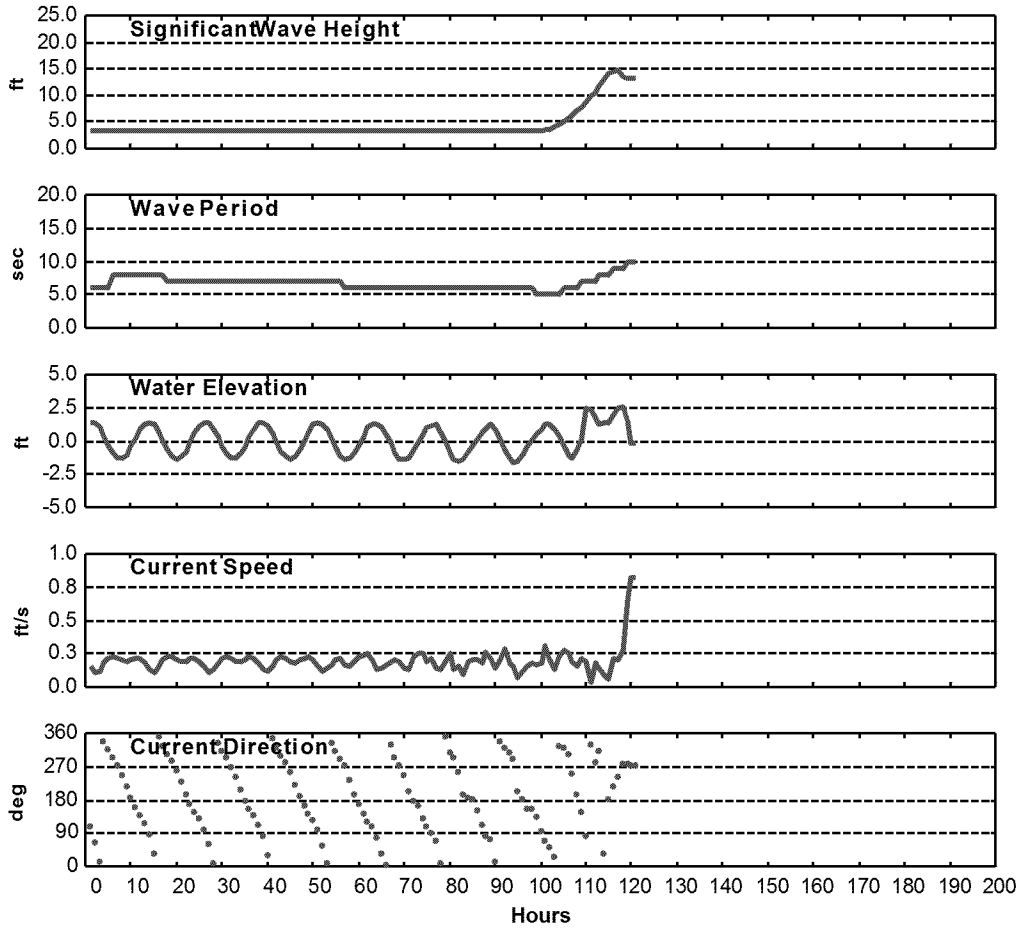

Figure 20. Storm 712 (1972 Hurricane Agnes) Time Series of Significant Wave Height, Wave Period, Sea Surface Elevation, Current Speed and Direction for Site W.

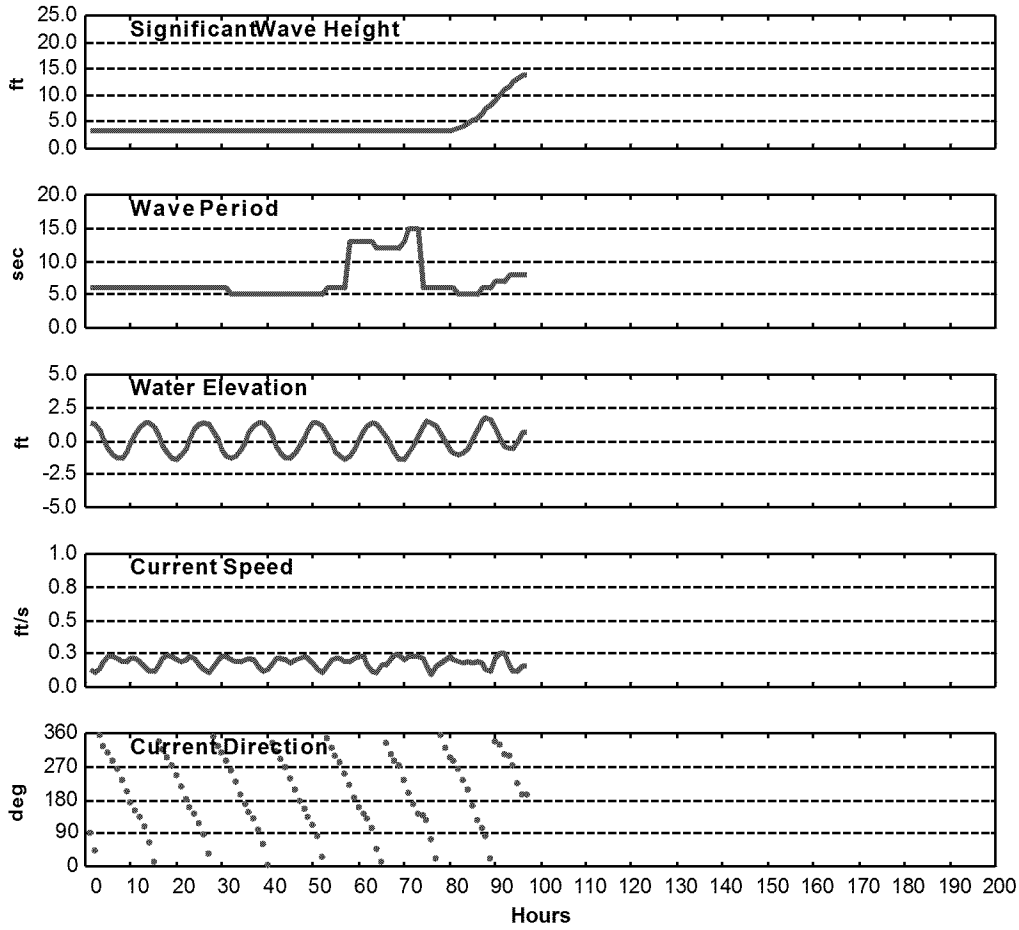

Figure 21. Storm 748 (1976 Hurricane Belle) Time Series of Significant Wave Height, Wave Period, Sea Surface Elevation, Current Speed and Direction for Site W.

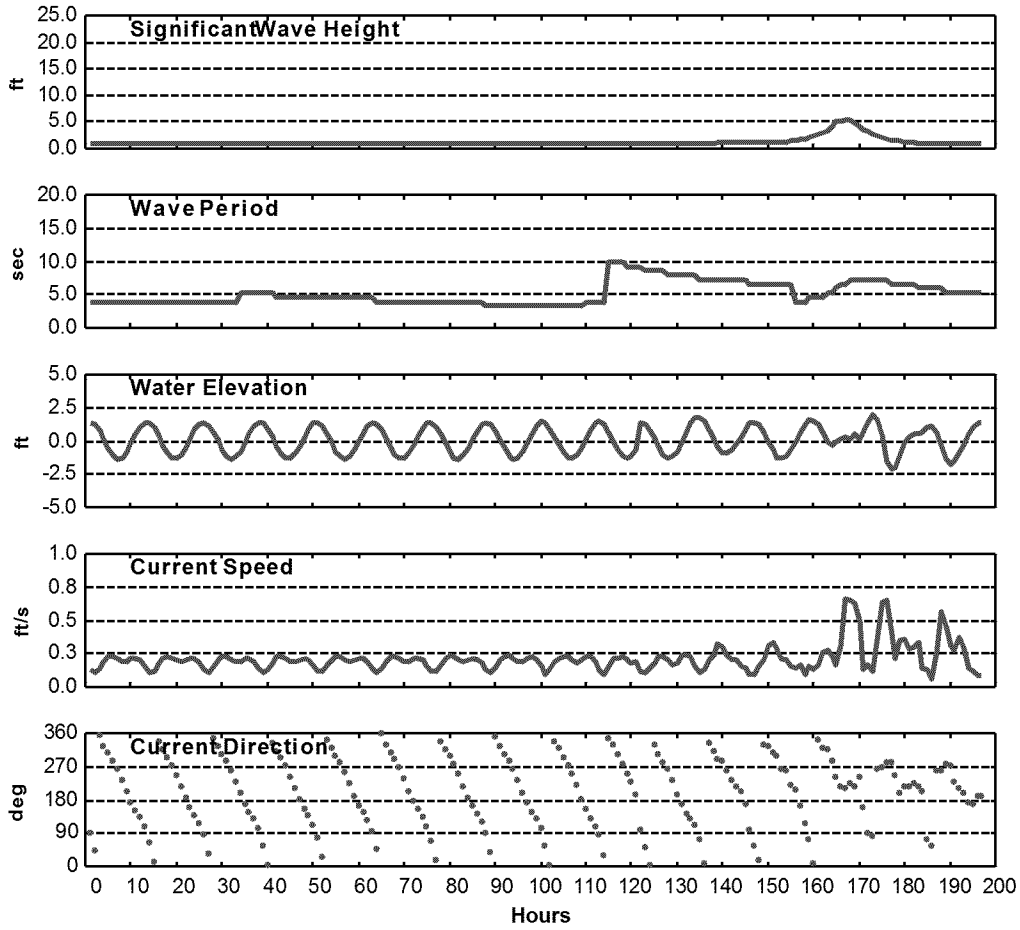

Figure 22. Storm H1.7 Time Series of Significant Wave Height, Wave Period, Sea Surface Elevation, Current Speed and Direction for Site W.

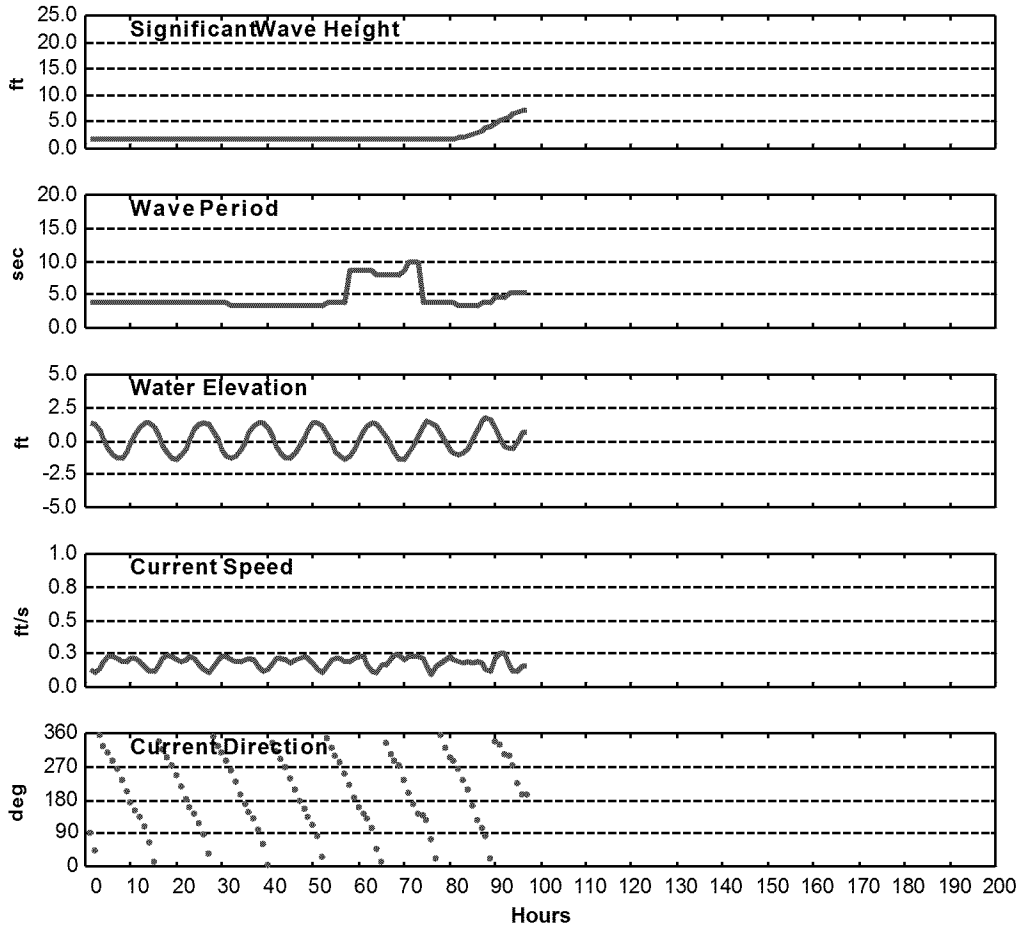

Figure 23. Storm H2.5 Time Series of Significant Wave Height, Wave Period, Sea Surface Elevation, Current Speed and Direction for Site W.

Each simulated mound was configured as an idealized cone frustum, with a volume equal to 0.88 million cubic yards. The mounds were configured with a central height of 18 ft above the seafloor, the height necessary to hold the requisite material assuming a shoulder slope of 1:20 and a 10 % margin between mounds and between the mounds and the site boundary (Figure 24).

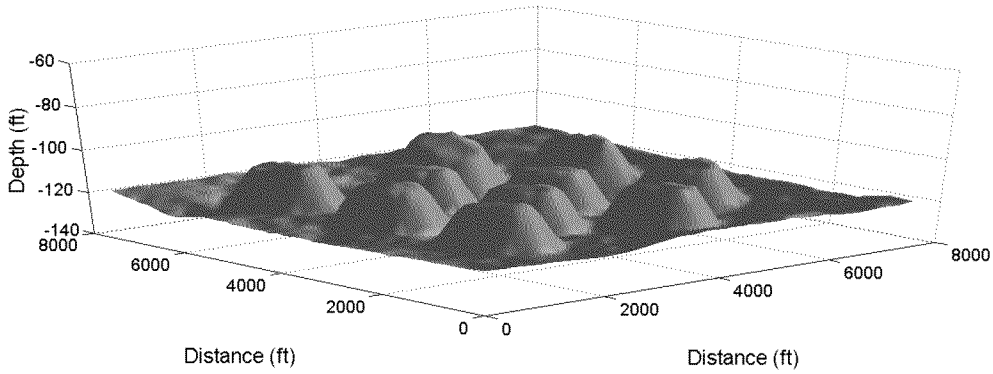

Figure 24. Bathymetry of Site W Showing Configuration of Proposed Dredged Material Mounds.

LTFATE is sensitive to geotechnical parameters of the sediments, also known as erosion potential parameters. These parameters are normally derived from laboratory measurements using undisturbed sediment cores collected in the field. These measurements are used to characterize the resistance to erosion and the rates of erosion as a function of depth in the sediment core and are a measure of the critical shear stress above which sediments are mobilized. The measurements are complicated to make, but are necessary to calibrate cohesive sediment transport models like LTFATE. Such geotechnical data are available for only a very few harbor locations. Erosion potential parameters measured in a field and laboratory study for the Portland Maine Disposal Site were used in the LTFATE model simulations described here (WES, 1998). Erosion potential parameters are also available for Providence River sediments (Gailani *et al.*, 2001); however, the samples used in that study were extremely cohesive compared to typical harbor sediment. This resulted in dubiously low predictions of erosion relative to typical dredged material. While the erosion potential parameter data for Portland sediments are not specific to the Rhode Island Sound alternative sites, they represent the best available data for New England (Tom Fredette, Corps, personal communication), and are reasonably representative of potential dredged material to be placed in the alternative sites (Table 12). The use of non-site specific parameters, where no local data are available is valid given that the models are intended to show the relative differences between the two alternative sites.

Table 12. Cohesive Sediments Erosion Potential Parameter from flume measurements made on Portland Disposal Site sediments.

Layer	Depth below sediment/water interface (ft)	A_0 ($g/cm^2/s$)	τ_{cr} ($dynes/cm^2$)
1	0.0-0.2	3.9×10^{-6}	0.24
2	0.2-0.4	2.0×10^{-6}	0.48
3	0.4-0.6	4.9×10^{-7}	2.40
4	0.6-1.0	4.9×10^{-8}	4.80
5	1.0-1.6	3.7×10^{-8}	9.60
6	1.6-2.0	2.5×10^{-8}	9.60
7	2.0-9.0	9.8×10^{-9}	9.60

7.3 Results

The results of LTFATE model simulations are described below for each of the alternative disposal sites. A number of model simulations failed to execute when LTFATE became unstable or terminated with fatal errors.

7.3.1 Site W

The array of disposal material mounds modeled was overlain on high-resolution bathymetry of Site W. The bathymetry data were collected in the summer of 2002. The model predicted erosion and deposition for a storm simulation with a peak wave height of 5.4 ft shows a small amount of erosion on the crests of the mounds and a small amount of deposition in the troughs between mounds (Figure 25). The average depth of erosion was 0.02 ft and the net volume of erosion, defined as the net mass of sediment eroded and deposited outside of the site was 11,200 CY (see Table 13). This represents a very small degree of resuspension of bottom sediments (0.1% of the deposited material). This simulation was chosen because it corresponds approximately to the 5 ft wave height events seen during the May and June 2002 field observations. The model results show a slight elevation in suspended material, which corresponds well with slight elevation in the turbidity when surface floc was resuspended by 5 ft high waves.

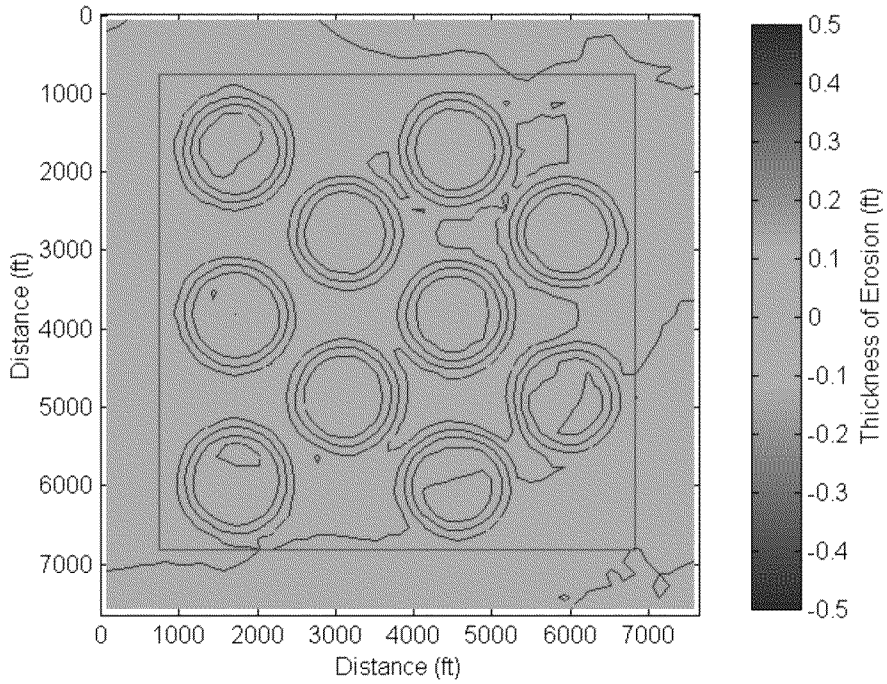

Note: Positive values indicate erosion.

Figure 25. Change in Bathymetry at the Site W Predicted for 5.4 ft Peak Wave Height Storm Simulation.

Table 13. Model Predicted Erosion and Deposition over Site W for Four Storm Scenarios.

Storm ID	Average Depth Change (ft)	Average Depth Erosion (ft)	Max Depth Erosion (ft)	Average Depth Deposition (ft)	Max Depth Deposition (ft)	Site Net Erosion (CY)	Site Gross Erosion (CY)	Site Gross Deposition (CY)
H1.7	0.01	0.02	0.07	-0.01	-0.02	11,200	16,692	-5,492
H2.5	0.05	0.07	0.21	-0.02	-0.05	63,092	66,908	-3,817
748 (Belle)	0.15	0.18	0.43	-0.04	-0.12	210,608	215,608	-5,000
712 (Agnes)	0.45	0.45	0.69	0	0	632,817	632,817	0
712 (Agnes) No Mounds	0.03	0.03	0.07	-0.02	0	42,575	42,575	0

The erosion on the crests of the mounds for a storm simulation with a peak wave height of 7.1 ft is clearly visible (Figure 26), with deposition between the mounds particularly in the southeast part of the site where water depths are deepest. The total amount of erosion is still small, with a predicted maximum erosion depth of 0.21 ft on the highest edge of the mounds and an average erosion depth over the model grid of 0.07 ft. The net volume of erosion was approximately 63,000 CY or 0.7% of the deposited material.

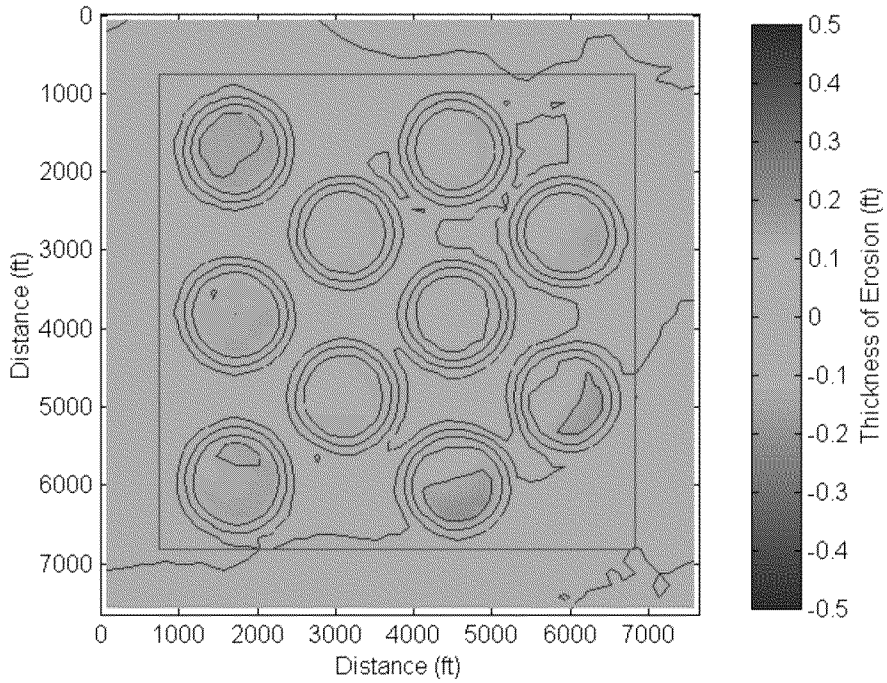

Note: Positive values indicate erosion.

Figure 26. Change in Bathymetry at the Site W Predicted for 7.1 ft Peak Wave Height Storm Simulation.

Finally, the model predicted erosion and deposition for the Hurricane Belle simulation, during which the maximum significant wave height reached 13.7 ft (Figure 27). Hurricane Belle represents a storm with a return period of 5 to 10 years. Erosion is predicted across the crests in the mounds and deposition predicted within the troughs concentrated primarily in the southeast part of the site where the bathymetric depression is located. The predicted average depth of erosion was 0.18 ft, with the maximum depth of erosion of 0.43 ft concentrated on the shallowest portions of the mounds. The total volume of material transported out of the site was 210,000 CY, or approximately 2 percent of the total volume of dredged material in the mounds. The Hurricane Agnes simulation (figure not shown) resulted in a net erosion of 632,000 CY of sediments from the site, or 7% of the total volume of dredged material. Hurricane Agnes approximates a storm with a return period of 15 years. For comparison, Hurricane Agnes simulation was also run with no mounds present, using the natural bathymetry (Figure 28), which resulted in a net erosion of approximately 43,000 CY of sediments from the site, or 0.5% of the total volume of dredged material. All attempts to model the 1936 Storm failed when LTFATE simulations became unstable.

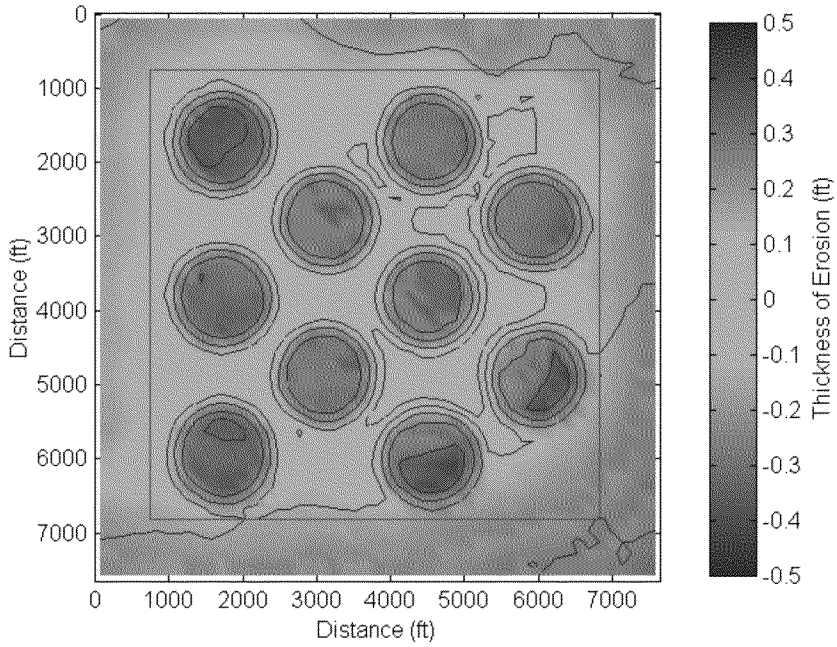

Note: Positive values indicate erosion.

Figure 27. Change in Bathymetry at the Site W Predicted for 13.7 ft Peak Wave Height Storm Simulation, Hurricane Belle.

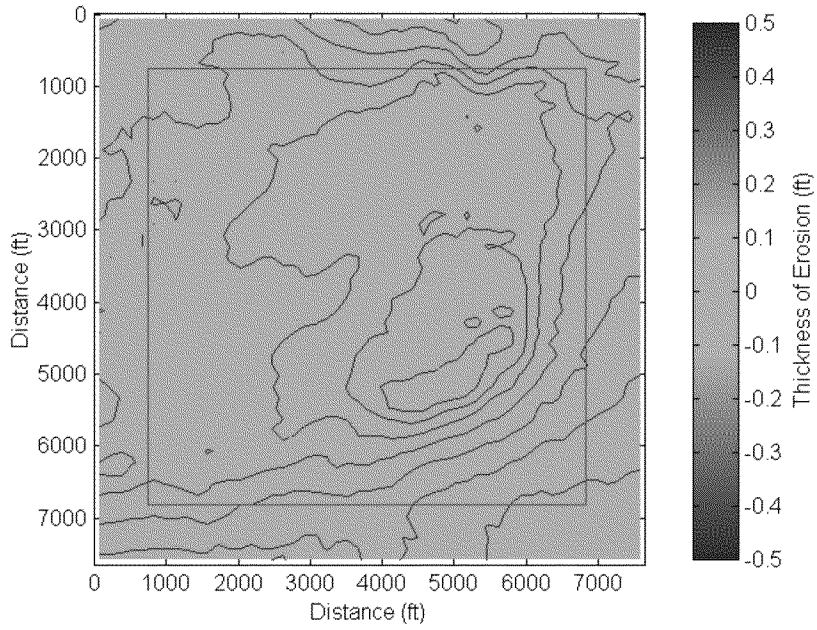

Note: Positive values indicate erosion.

Figure 28. Change in Bathymetry at the Site W Predicted for 14.9 ft Peak Wave Height Storm Simulation, Hurricane Agnes with no disposal mounds present.

7.3.2 Site E

Using the same mound configuration and storm scenarios for Site W, LTFATE simulations were developed for Site E. There were two differences in the set of simulations created for the two alternative sites. The first is the differences in the natural bathymetry of the two sites and the second is the difference in wave heights, which are slightly higher at Site E because of the site's greater potential for exposure to storm winds and waves from the south and southwest (Section 3). For the purposes of the model simulations, wave heights in Site E were set 8 percent higher and wave periods 5 percent longer than those in Site W. As for Site W, ten 18-ft high mounds were overlain on recent high-resolution bathymetry at Site E.

The model predicts a small amount of erosion on the crests of the mounds and a small amount of deposition in the troughs between mounds for a storm simulation with a peak wave height of 5.8 ft (Figure 29). The average erosion depth was only 0.02 ft, with net erosion out of the site of 9,900 CY or approximately 0.1% (Table 14).

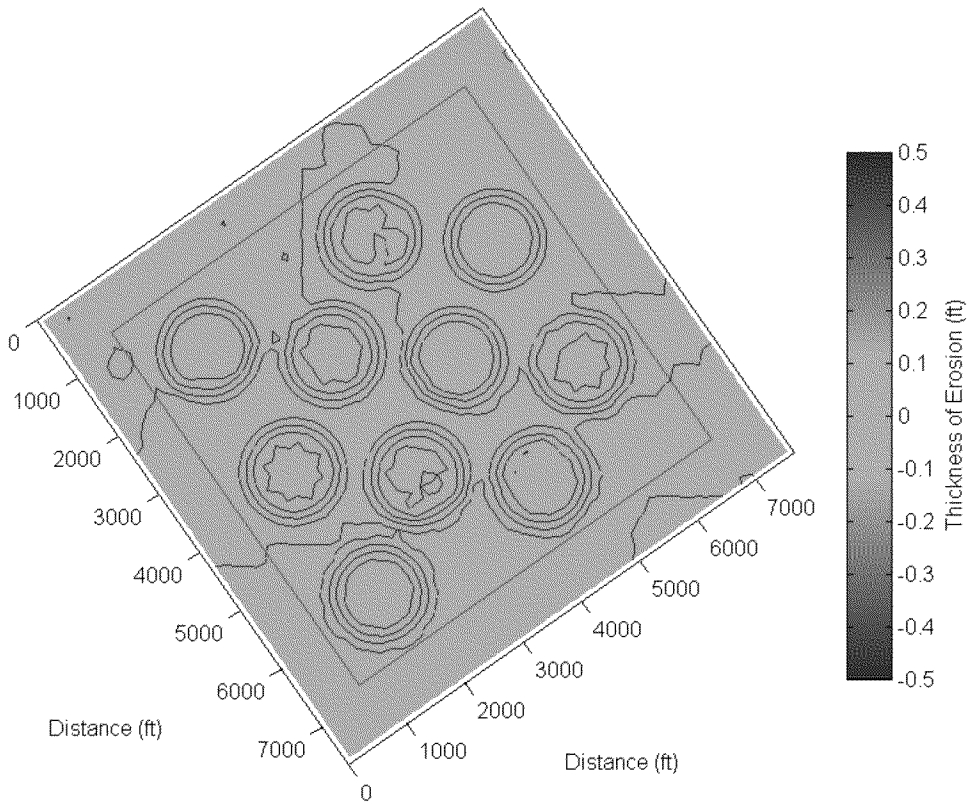

Note: Positive values indicate erosion.

Figure 29. Change in Bathymetry at the Site E Predicted for 5.8 ft Peak Wave Height Storm Simulation.

Table 14. Model Predicted Erosion and Deposition over Site E for Four Storm Scenarios.

Storm ID	Average Depth Change (ft)	Average Depth Erosion (ft)	Max Depth Erosion (ft)	Average Depth Deposition (ft)	Max Depth Deposition (ft)	Site Net Erosion (CY)	Site Gross Erosion (CY)	Site Gross Deposition (CY)
H1.7	0.01	0.02	0.04	-0.01	-0.01	9,917	12,542	-2,625
H2.5	0.07	0.09	0.25	-0.02	-0.05	101,342	103,900	-2,558
748 (Belle)	0.23	0.23	0.49	-0.03	-0.05	315,442	315,650	-208
712 (Agnes)	0.44	0.47	0.76	0	0	634,142	634,142	0
712 (Agnes) No Mounds	0.05	0.05	0.08	-0.02	0	73,442	73,442	0

The model predicts erosion on the crests of the mounds and deposition between the mounds for a storm simulation with a peak wave height of 7.6 ft (Figure 30). The highest erosion occurs on the shallowest mounds to the north. The total amount of erosion is small, with a predicted maximum erosion depth of 0.25 ft and an average erosion depth of 0.09 ft. The net volume of erosion over the entire site was approximately 101,000 CY (1.1%).

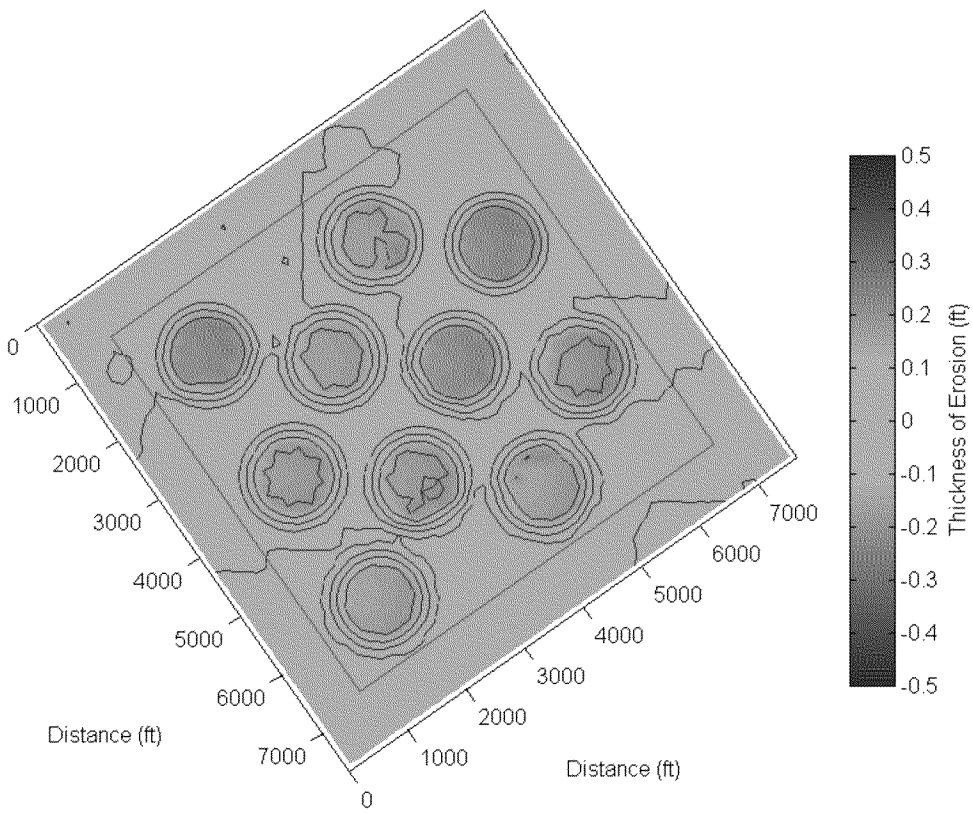

Note: Positive values indicate erosion.

Figure 30. Change in Bathymetry at the Site E Predicted for 7.6 ft Peak Wave Height Storm Simulation.

Finally, the model predicted erosion and deposition for the Hurricane Belle simulation, during which the maximum significant wave height reached 14.7 ft (Figure 31). Significant erosion is predicted to occur throughout the site, except for a small amount of deposition between the troughs in the east central portion of the site. The average erosion depth was 0.23 ft, with a predicted maximum erosion depth of about 0.5 ft concentrated on the shallowest portions of the mounds. The total volume of material transported out of the site was 316,000 CY, or approximately 3.5% of the total volume of dredged material in the mounds. The Hurricane Agnes simulation (figure not shown) resulted in a net erosion of 634,142 CY of sediments from the site, or 7 percent of the total volume of dredged material in the mounds. For comparison, Hurricane Agnes simulation was also run with no mounds present, using the natural bathymetry (Figure 32), which resulted in a net erosion of approximately 73,000 CY of sediments from the site, or 0.8% of the total volume of dredged material. All attempts to model the 1936 Storm failed when LTFATE simulations became unstable.

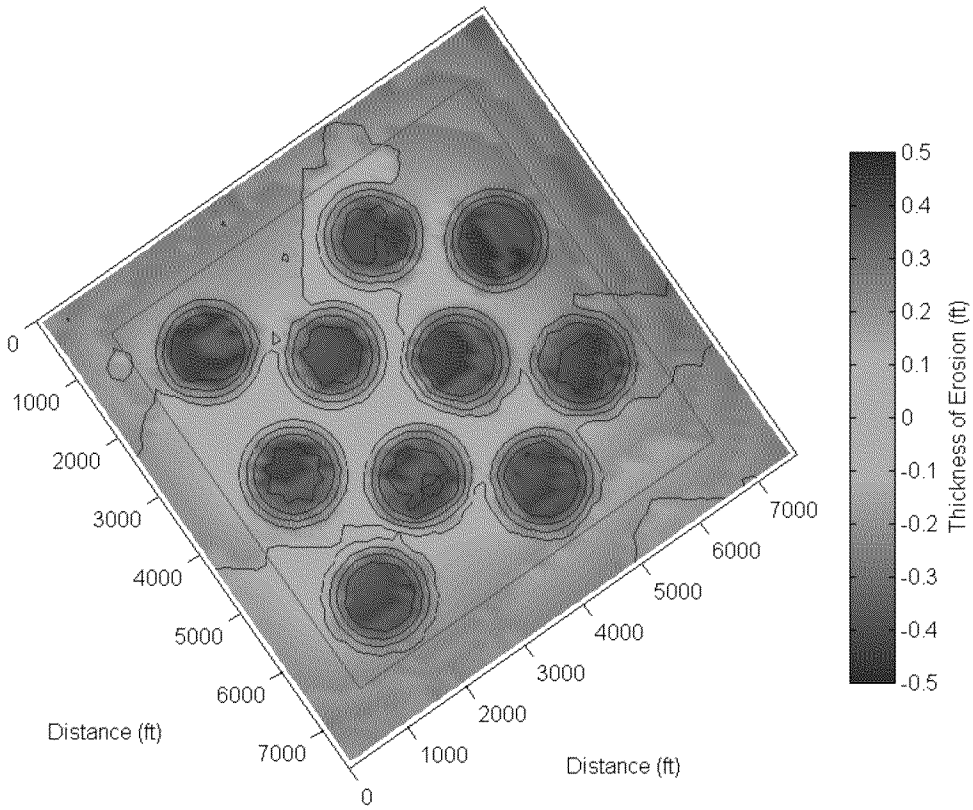

Note: Positive values indicate erosion.

Figure 31. Change in Bathymetry at the Site E Predicted for 14.7 ft Peak Wave Height Storm Simulation, Hurricane Belle.

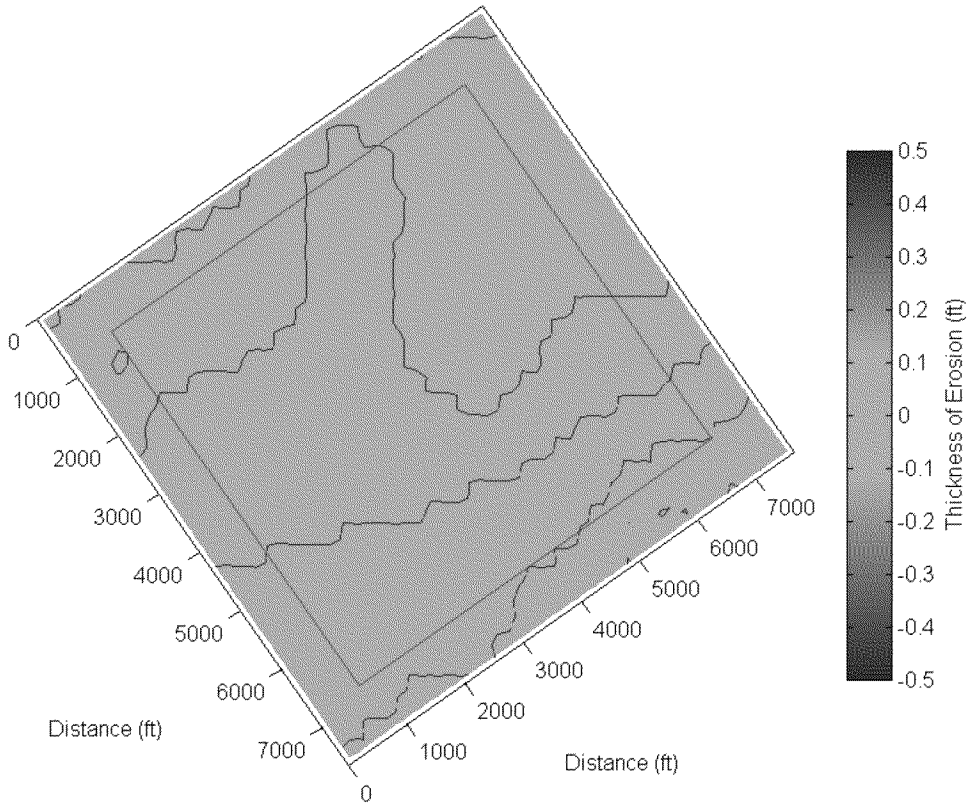

Note: Positive values indicate erosion.

Figure 32. Change in Bathymetry at the Site E Predicted for 16.0 ft Peak Wave Height Storm Simulation, Hurricane Agnes with no disposal mounds present.

Numerical model predictions of sediment transport by storm waves and currents show that frequent, moderately-sized storms resuspend and transport fine bottom sediment, but the total volume of material eroded is very small (probably limited to only the upper 1 or 2 mm). This result is consistent with field observations of near-bottom turbidity and surface waves. Model predictions suggest that during storm conditions expected to occur in Rhode Island Sound three to five times per year (maximum wave height of 8.2-8.9 ft, approximately 5 percent frequency of occurrence of storm conditions [Section 3]), under a worst case scenario of 18 ft high disposal mounds, an average of up to 0.21 ft of disposal mound will erode in Site W and 0.25 ft in Site E. For the case of a storm with a return period of from 5 to 10 years, 18 ft high mounds will erode an average of 0.49 feet in Site E and 0.43 feet in Site W with a total of 4 percent of the 8.8 MCY of dredged material predicted to be eroded at Site E and 2 percent at Site W.

All simulations showed some deposition of dredged material in the troughs between disposal mounds and simulations using the natural bathymetry (no mounds) resulted in little net erosion. This is consistent with our understanding of processes at work and the importance of depth in determining resuspension under storm waves and currents. This suggests that sediment stability could be improved at both sites with a site management approach which limits the height of disposal mounds.

Numerical models are simple representation of physical reality and as such have a limited ability to predict quantitative results. Modeling sediment transport is complicated by uncertainty in the current speed, particle size, shape, density, sediment cohesiveness and friction terms. In this case, the model results compare well with a short record of field observations which provides additional credibility to the model predictions. The model predictions provide an opportunity to qualitatively compare the two alternative sites. The relative differences between the predicted results indicate that Site E has a slightly higher potential for resuspension of dredged material from storms than Site W.

8.0 REFERENCES

Beardsley, R.C. and W.C. Boicourt. 1981. On Estuarine and Continental-shelf Circulation in the Middle Atlantic Bight in: Evolution of Physical Oceanography. B.A. Warren and C. Wunsch, (Eds.) MIT Press.

Brandsma, M. G., and Divoky, D. J. 1976. "Development of Models for Prediction of Short Term Fate of Dredged Material Discharged in the Estuarine Environment," CR D 76 5, US Army Engineer Waterways Experiment Station (USAE WES), Vicksburg, MS.

Corps. 1979. Disposal Area Monitoring System (DAMOS) Annual Data Report - 1978 Supplement E Brenton Reef Disposal Site. U.S. Army Corps of Engineers, New England Division. Waltham, MA. 36 pp.

Corps. 2001a. Letter Report: Evaluation of Existing Physical Oceanographic Data. Prepared under Contract No. DACW33-01-D-0004, Delivery Order No. 2 by Battelle for the U.S. Army Corps of Engineers.

Corps. 2001b. Providence River and Harbor Maintenance Dredging Project Final Environmental Impact Statement. Prepared under Contract No. DACW33-01-D-0004, Delivery Order No. 37 by Battelle for the U.S. Army Corps of Engineers, New England Division. Concord, MA.

Corps, 2001c. Final Data Report for Laboratory Testing in Support of Environmental Assessment, Environmental Sampling and Testing – New Haven, CT. Submitted to U.S. Army Corps of Engineers, New England Division. Contract DACW22-01-D-0004. Delivery Order 11.

Corps, 2001d. Final Data Report for Laboratory Testing in Support of Environmental Assessment, Environmental Sampling and Testing – Norwalk, CT. Submitted to U.S. Army Corps of Engineers, New England Division. Contract DACW22-01-D-0004. Delivery Order 8.

Corps, 2001e. Final Data Report for Laboratory Testing in Support of Environmental Assessment, Environmental Sampling and Testing – Guilford Harbor, CT. Submitted to U.S. Army Corps of Engineers, New England Division. Contract DACW22-01-D-0004. Delivery Order 11.

Corps. 2003. Final Survey Report for Winter 2002 Physical Oceanography Data Collection Survey. Rhode Island Region Long-term Dredged Material Disposal Site Evaluation Project. Prepared under Contract No. DACW33-01-D-0004, Delivery Order No. 2 by Battelle for the U.S. Army Corps of Engineers.

Corps. 2004. Data Report for 1999 and 2002 Physical Oceanography. Rhode Island Region Long-term Dredged Material Disposal Site Evaluation Project. Prepared under Contract

No. DACW33-01-D-0004, Delivery Order No. 2 by Battelle for the U.S. Army Corps of Engineers.

Csanady, G.T. 1973. Turbulent Diffusion in the Environment. Reidel. 248 pp.

Dragos, P. and D. Lewis. 1993. Plume Tracking/Model Verification Project (Draft Final Report). Prepared by Battelle Ocean Sciences, Duxbury, MA, for EPA Region II under EPA Contract No. 68-C2-0134, Work Assignment No. 222.

Dyer, K., 1986, Coastal and estuarine sediment dynamics. John Wiley & Sons, Inc., New York.

Ecker R.M. and Downing, J. P. 1987. Review of State-Of-The-Art modeling of Ocean-Dumped Wastes. Prepared by Battelle Ocean Sciences, Duxbury, MA, for EPA under Contract No. 68-03-3319, Work Assignment No. 9. 90pp

EPA and Corps. 1991. Evaluation of Dredged Material Proposed for Ocean Disposal Testing Manual. EPA Report No. EPA-503-8-91/001. U.S. Environmental Protection Agency, Office of Marine and Estuarine Protection and Department of the Army, U.S. Army Corps of Engineers. Washington, DC.

Gailani, J.Z., S.J. Smith, N.W. Scheffner, and W. Vanadit-Ellis. 2001. Dredged Material Fate Modeling of Proposed Providence River Confined Aquatic Disposal (CAD) Cells and Ocean Dredged Material Disposal Site (ODMDS), Prepared for the U.S. Army Engineer District, New England.

Grant, W. D., and O. S. Madsen. 1986. The continental-shelf bottom boundary layer. *Annual Review of Fluid Mechanics*. 18:265-305.

Hicks, S.D. 1959. The physical oceanography of Narragansett Bay. *Limnology and Oceanography*. 4:316-327.

Koh, R. C. Y., and Chang, Y. C. 1973. "Mathematical Model for Barged Ocean Disposal of Waste," Environmental Protection Technology Series EPA 660/2 73 029, US Environmental Protection Agency, Washington, DC.

Kraus, N. C., Ed. 1991. "Mobile, Alabama, Field Data Collection Project, 18 August - 2 September 1989 Report 1: Dredged Material Plume Survey Data Report" TR DRP 91 3, USAE WES, Vicksburg, MS.

Lavelle, J. W., Mofjeld, H. O., and Baker, E. T. 1984. "An in situ erosion rate for a fine-grained marine sediment," *J. Geophys. Res*. 89(C4), 6543-6552.

Luettich, R.A., Westerink, J.J., and N.W. Scheffner (1992). ADCIRC: An Advanced Three-Dimensional Circulation Model for Shelves, Coasts and Estuaries, Report 1, Theory and Methodology of ADCIRC 2DDI and ADCIRC-3DL, Technical Report DRP-92-6, U.S. Army Corps of Engineers, Vicksburg, MS.

Madsen, O. S., and P. N. Wikramanayake. 1991. Simple models for turbulent wave and current bottom boundary layer flow, Contract Rep. DRP-91-1, 150 pp., U.S. Army Corps of Eng., Coastal Eng. Res. Cent., Vicksburg, Miss.

Mayer, D.A., D.V. Hansen, and D.A. Ortmann. 1979. Long-term current and temperature observations on the Middle Atlantic Shelf. *Journal of Geophysical Research.* 84(C4):1776-1792.

Rhoads, D. C. 1994. Analysis of the Contribution of Dredged Material to Sediments and Contaminant Fluxes in Long Island Sound. DAMOS Report 88. Waltham, MA, U.S. Army Corps of Engineers, New England Division.

Riley, G.A. 1948. The Hydrography of the Western Atlantic. Woods Hole Oceanographic Institution Technical Report No. 11.

SAIC. 1988. Distribution of Dredged Material at the Rockland Disposal Sites, May 1985. DAMOS Report 50. Waltham, MA, U.S. Army Corps of Engineers, New England Division.

Scheffner, N. W., Thevenot, M. M., Tallent, J. R., and Mason, J. M. 1995. "LTFATE: A model to investigate the long-term stability of dredged material disposal sites", Technical Report DRP-95-1, U.S. Army Engineer Waterways Experiment Station, Vicksburg, MS.

Scheffner, N. W. 1996. "Systematic analysis of long-term fate of disposed dredged material," *J. Waterways, Harbors and Coastal Eng. Div. Am. Soc. Civ. Eng.* 122(3), 127-133.

Scorer, R.S. 1957. Experiments on Convection of Isolated Masses of Buoyant Fluid. J. of Fluid Mechanics. 2:583.

Tavolaro, J. 1984. A Sediment Budget Study of Clamshell Dredging and Ocean Disposal Activities in the New York Bight. Environmental Geology 6:133-140.

Tsai, J.J., and J.R. Proni. 1985. Acoustic Study of Dredged-Material Dumping in the New York Bight In: Ketchum, B.H., J.M. Capuzzo, W.V. Burt, I.W. Duedall, P.K. Park, and D.R. Kester (eds), Wastes in the Ocean, Vol. 6, Nearshore Waste Disposal, pp. 357-381. John Wiley and Sons, New York, NY.

Waterways Experiment Station (WES), U.S. Army Engineer. 1998. A Predictive Model for Sediment Transport at the Portland Disposal Site, Maine. DAMOS Contribution No. 122. U.S. Army Corps of Engineers, New England District, Concord, MA, 23 pp.

Woodward, B. 1959. Motion In and Around Isolated Thermals. Quarterly J. of the Royal Meteorological Society. 85:144.

Williams, R.G. 1969. Physical Oceanography of Block Island Sound. USL Report No.966. U.S. Navy Underwater Sound Laboratory. Fort Trumbull, New London, CT.

Appendix A

STFATE Model Simulation Results

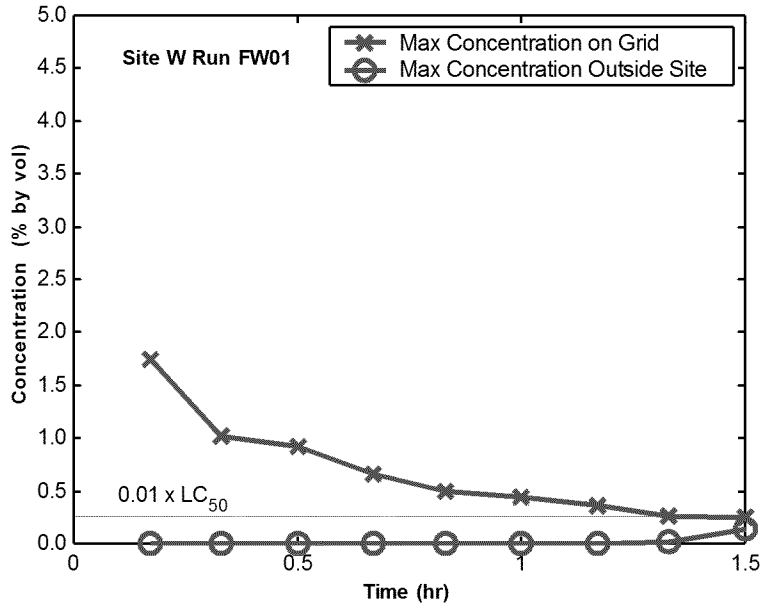

Figure A-1. Predicted Change in Dredged Material Plume Concentration after Release in Site W. Shown is the maximum concentration over the entire model grid and the maximum outside the site for a 3000 CY release with 40% clumps, 10% free water, and a 20 cm/s current. A water quality criteria of 0.26% dilution is also shown.

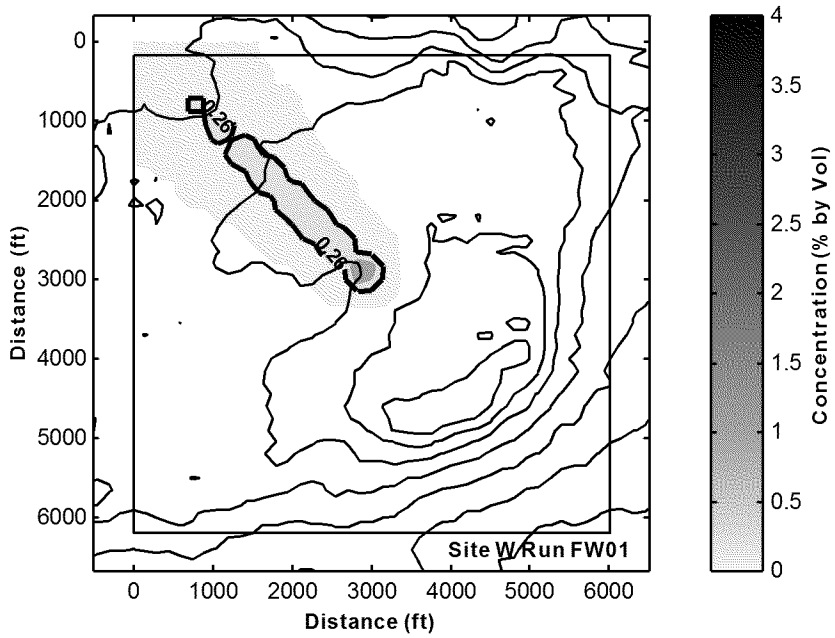

Figure A-2. Predicted depth-maximum plume concentration over the model grid after 90 min for a 3000 CY release in Site W with 40% clumps, 10% free water, and a 20 cm/s current. Bathymetric depth contour interval equals 2 ft.

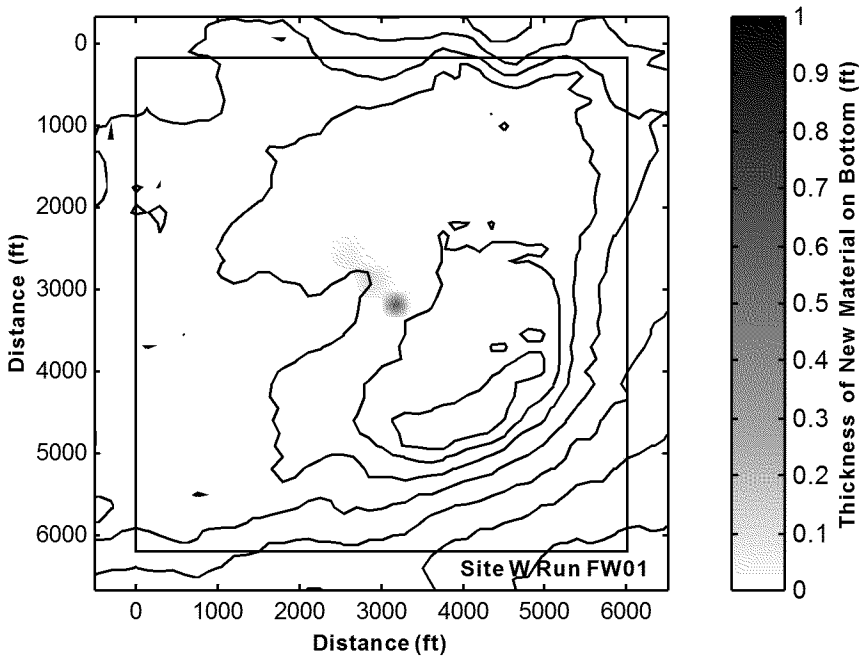

Figure A-3. Predicted total thickness of new material on the bottom for a 3000 CY release in Site W with 40% clumps, 10% free water, and a 20 cm/s current. Bathymetric depth contour interval equals 2 ft.

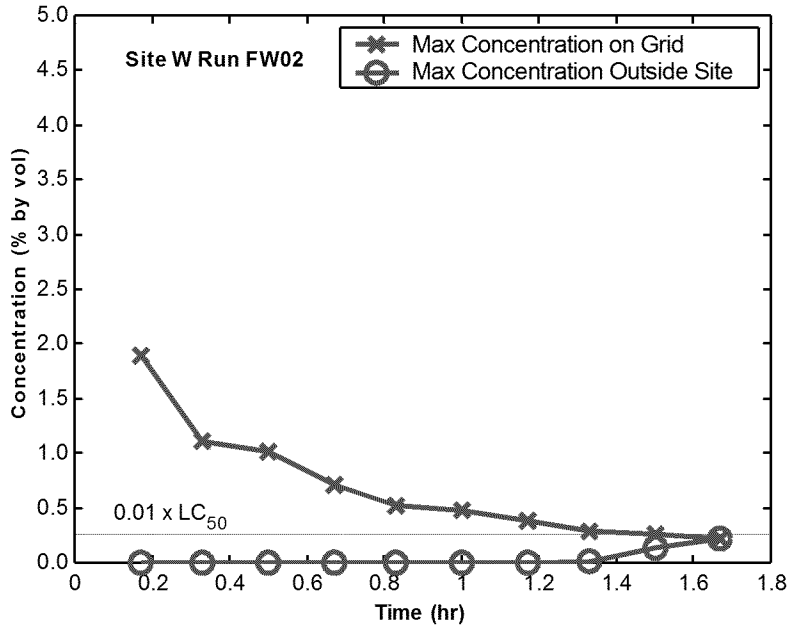

Figure A-4. Predicted change in dredged material plume concentration after release in Site W. Shown is the maximum concentration over the entire model grid and the maximum outside the site for a 3000 CY release with 60% clumps, 30% free water, and a 20 cm/s current. A water quality criteria of 0.26% dilution is also shown.

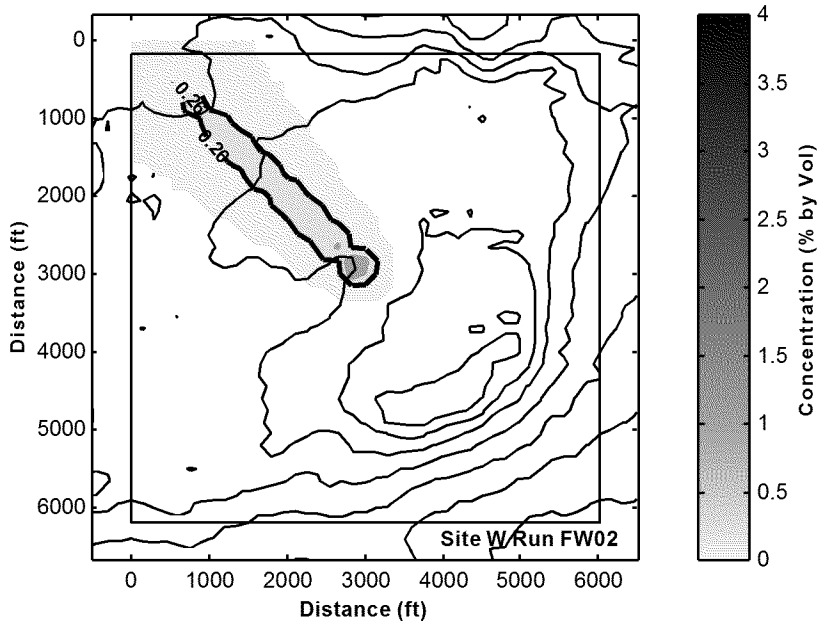

Figure A-5. Predicted depth-maximum plume concentration over the model grid after 100 min for a 3000 CY release in Site W with 60% clumps, 30% free water, and a 20 cm/s current. Bathymetric depth contour interval equals 2 ft.

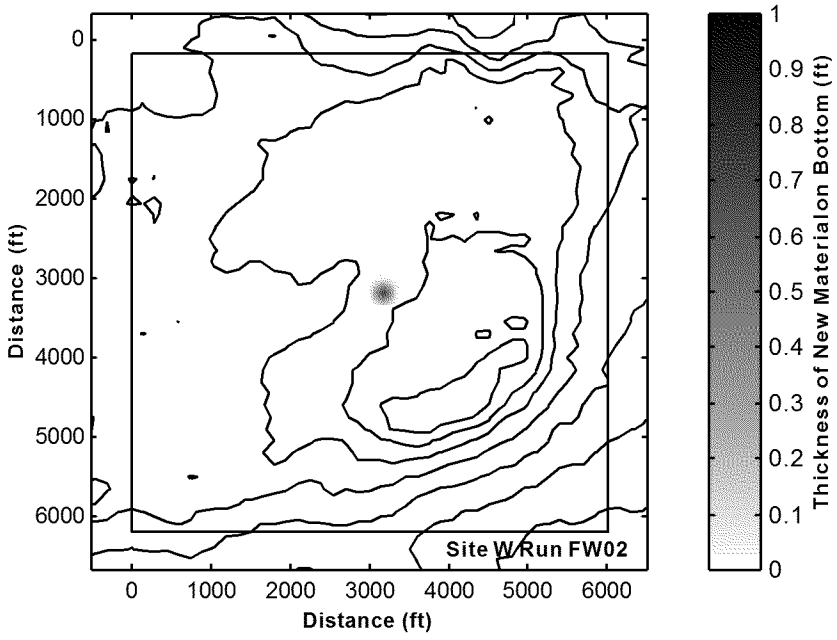

Figure A-6. Predicted total thickness of new material on the bottom for a 3000 CY release in Site W with 60% clumps, 30% free water, and a 20 cm/s current. Bathymetric depth contour interval equals 2 ft.

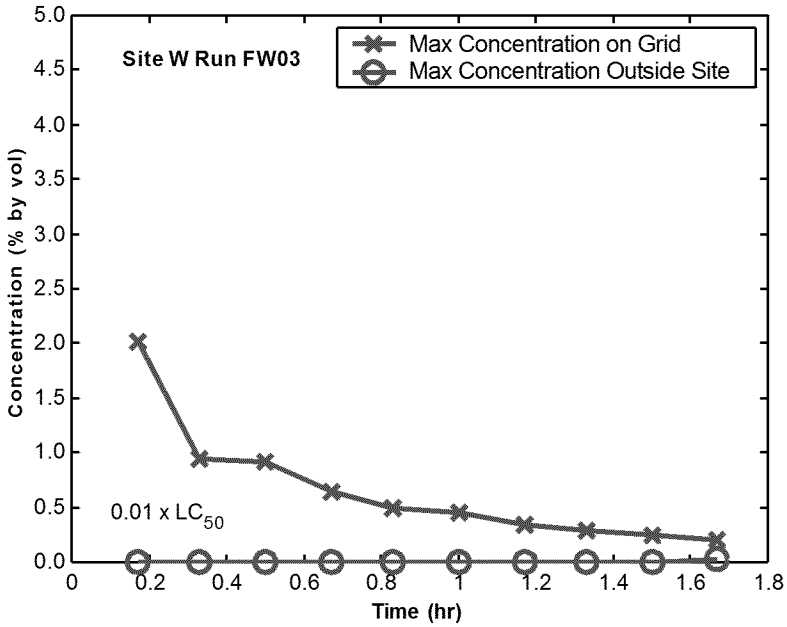

Figure A-7. Predicted change in dredged material plume concentration after release in Site W. Shown is the maximum concentration over the entire model grid and the maximum outside the site for a 3000 CY release with 40% clumps, 10% free water, and a 17 cm/s current. A water quality criteria of 0.26% dilution is also shown.

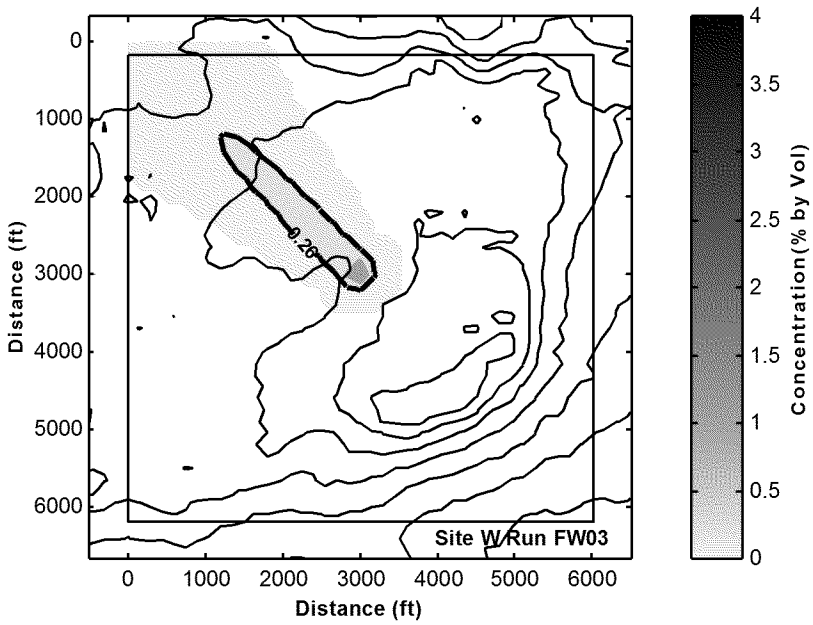

Figure A-8. Predicted depth-maximum plume concentration over the model grid after 100 min for a 3000 CY release in Site W with 40% clumps, 10% free water, and a 17 cm/s current. Bathymetric depth contour interval equals 2 ft.

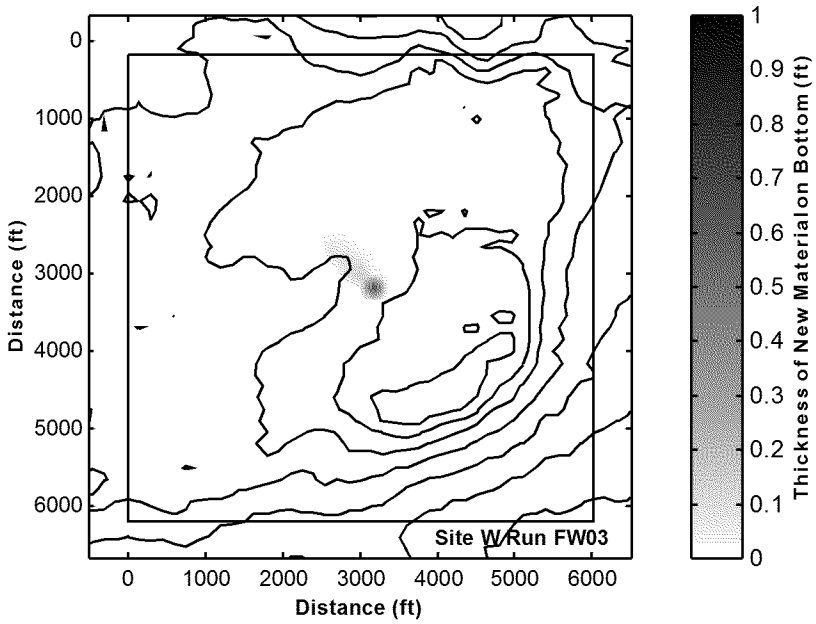

Figure A-9. Predicted total thickness of new material on the bottom for a 3000 CY release in Site W with 40% clumps, 10% free water, and a 17 cm/s current. Bathymetric depth contour interval equals 2 ft.

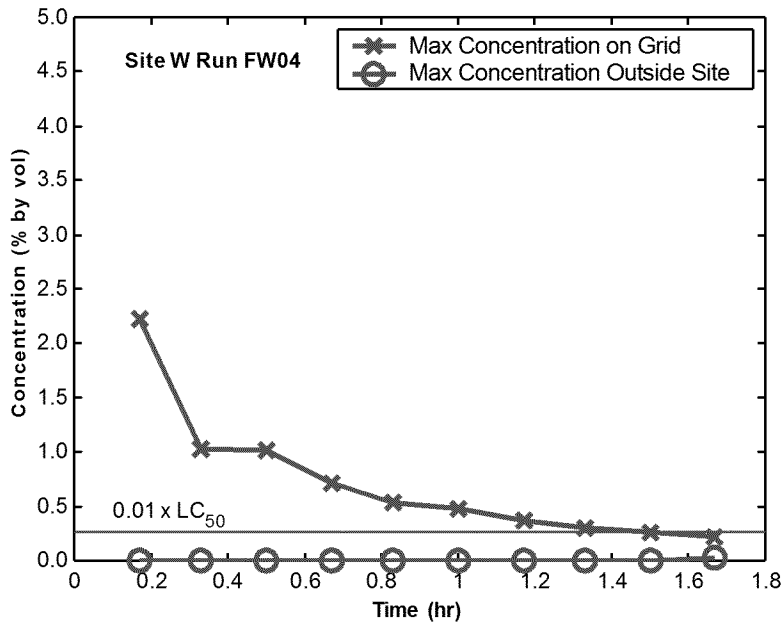

Figure A-10. Predicted change in dredged material plume concentration after release in Site W. Shown is the maximum concentration over the entire model grid and the maximum outside the site for a 3000 CY release with 60% clumps, 30% free water, and a 17 cm/s current. A water quality criteria of 0.26% dilution is also shown.

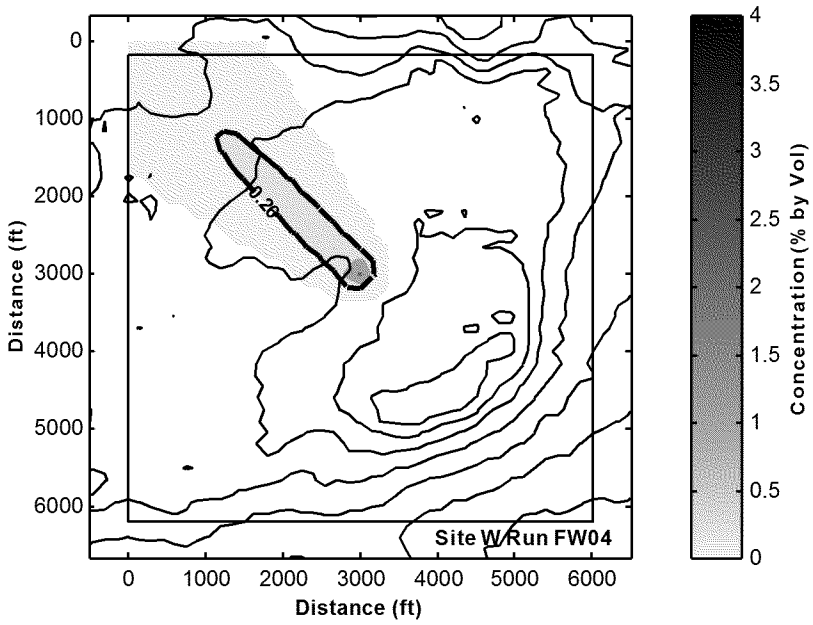

Figure A-11. Predicted depth-maximum plume concentration over the model grid after 100 min for a 3000 CY release in Site W with 60% clumps, 30% free water, and a 17 cm/s current. Bathymetric depth contour interval equals 2 ft.

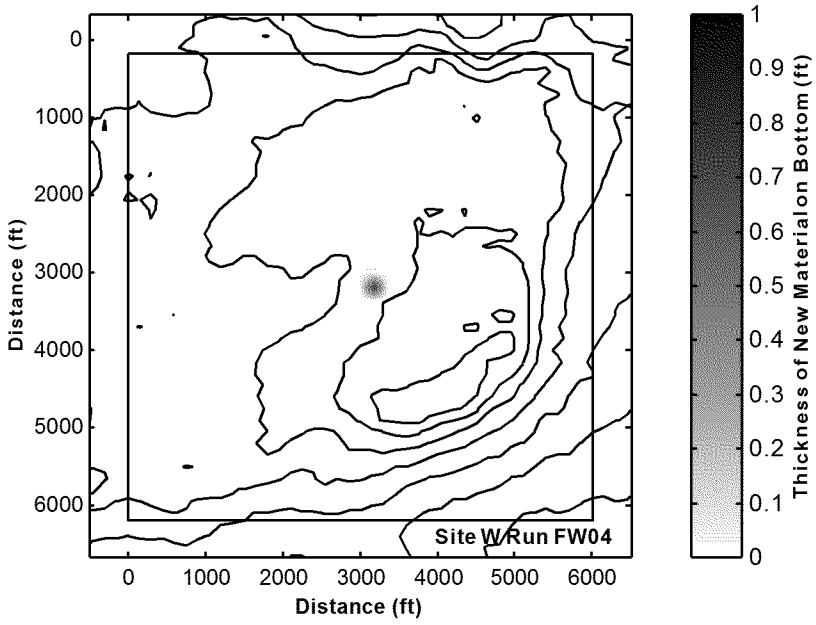

Figure A-12. Predicted total thickness of new material on the bottom for a 3000 CY release in Site W with 60% clumps, 30% free water, and a 17 cm/s current. Bathymetric depth contour interval equals 2 ft.

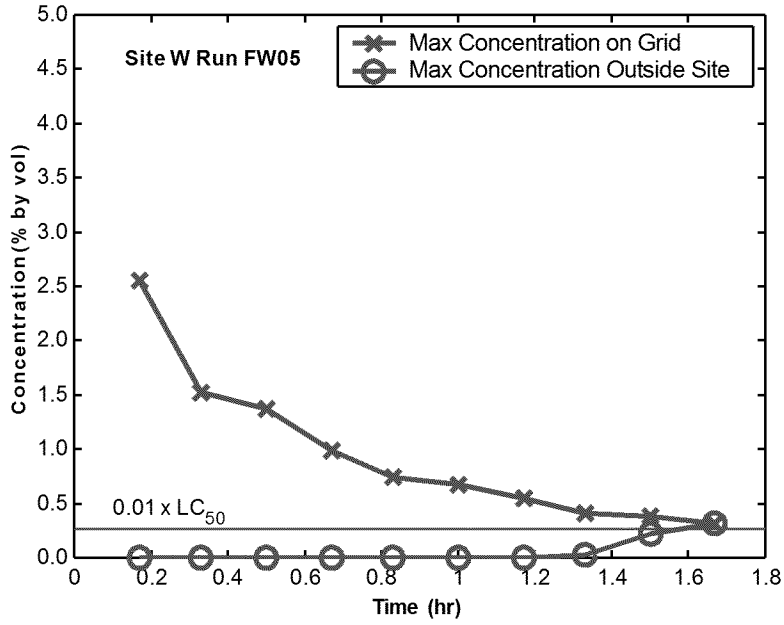

Figure A-13. Predicted change in dredged material plume concentration after release in Site W. Shown is the maximum concentration over the entire model grid and the maximum outside the site for a 5000 CY release with 40% clumps, 10% free water, and a 20 cm/s current. A water quality criteria of 0.26% dilution is also shown.

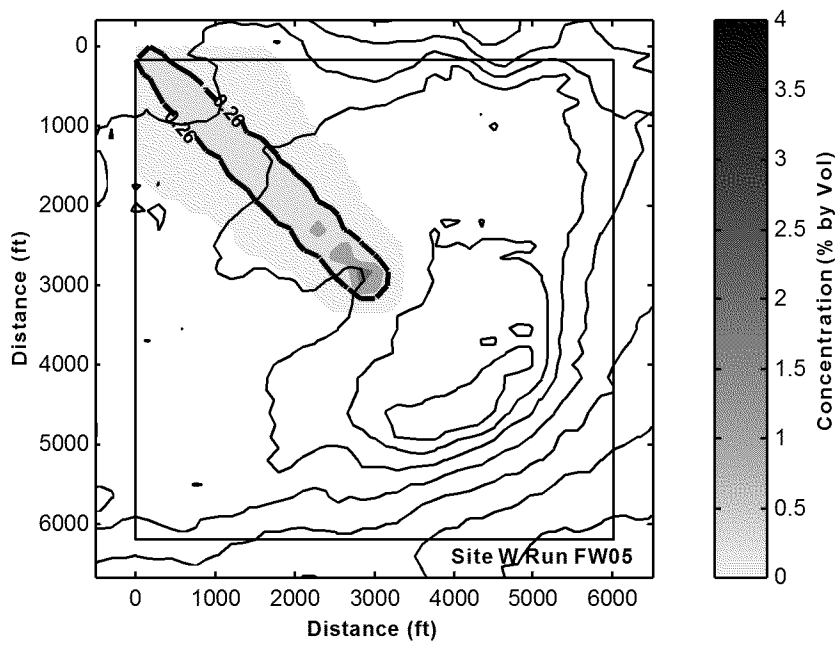

Figure A-14. Predicted depth-maximum plume concentration over the model grid after 100 min for a 5000 CY release in Site W with 40% clumps, 10% free water, and a 20 cm/s current. Bathymetric depth contour interval equals 2 ft.

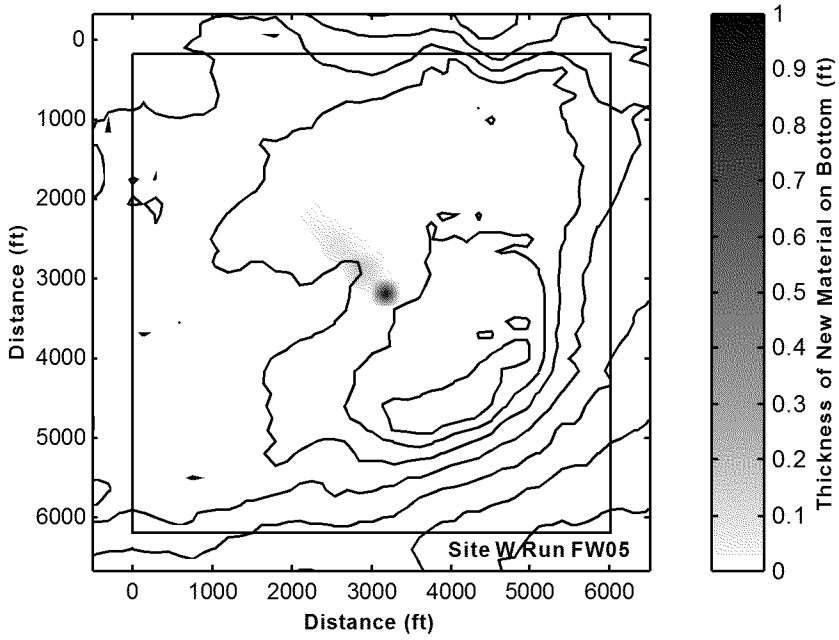

Figure A-15. Predicted total thickness of new material on the bottom for a 5000 CY release in Site W with 40% clumps, 10% free water, and a 20 cm/s current. Bathymetric depth contour interval equals 2 ft.

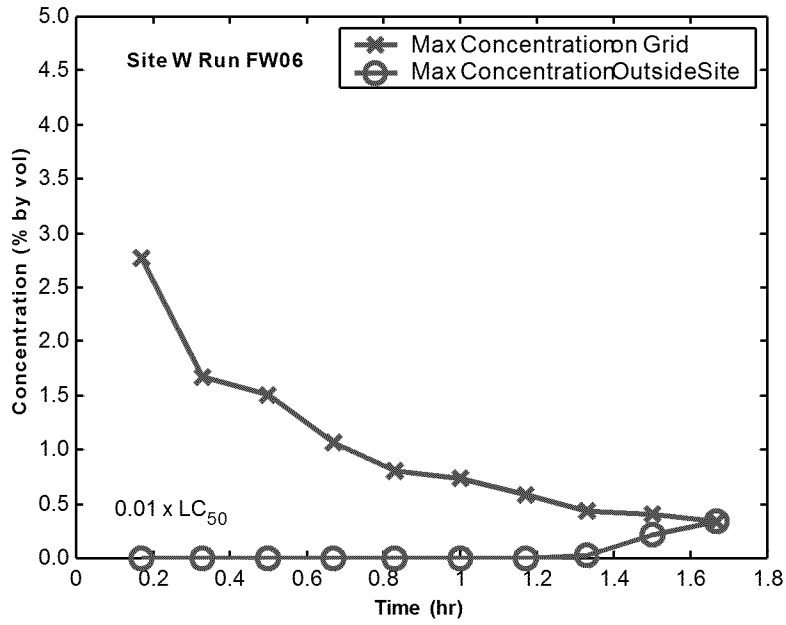

Figure A-16. Predicted change in dredged material plume concentration after release in Site W. Shown is the maximum concentration over the entire model grid and the maximum outside the site for a 5000 CY release with 60% clumps, 30% free water, and a 20 cm/s current. A water quality criteria of 0.26% dilution is also shown.

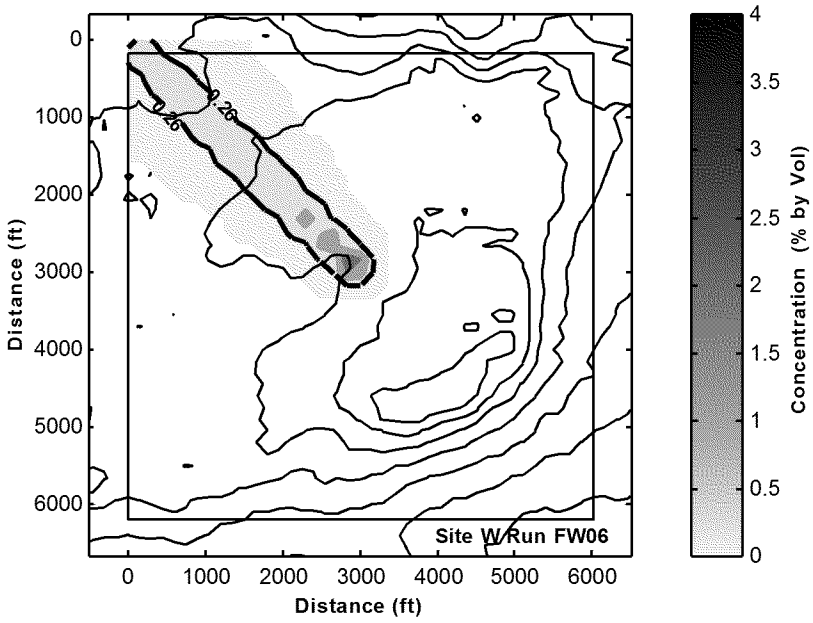

Figure A-17. Predicted depth-maximum plume concentration over the model grid after 100 min for a 5000 CY release in Site W with 60% clumps, 30% free water, and a 20 cm/s current. Bathymetric depth contour interval equals 2 ft.

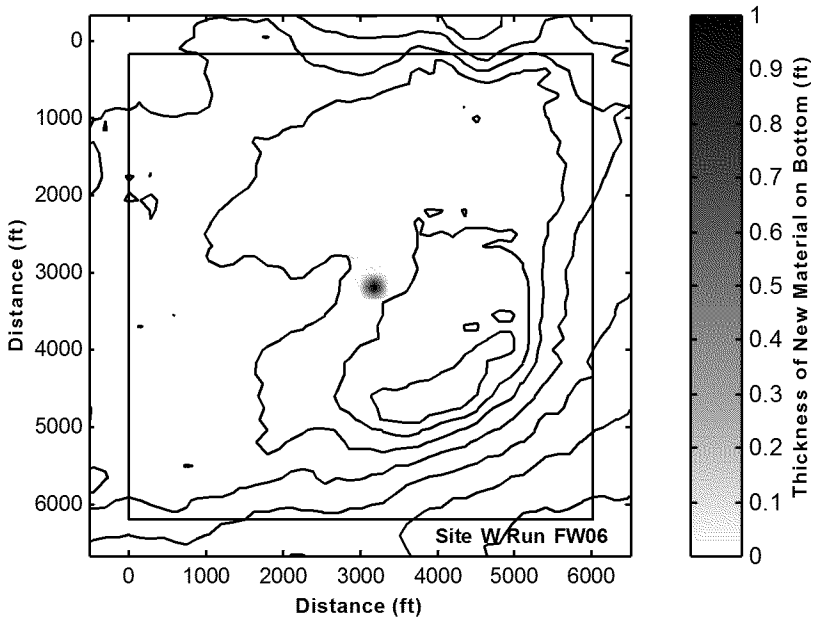

Figure A-18. Predicted total thickness of new material on the bottom for a 5000 CY release in Site W with 60% clumps, 30% free water, and a 20 cm/s current. Bathymetric depth contour interval equals 2 ft.

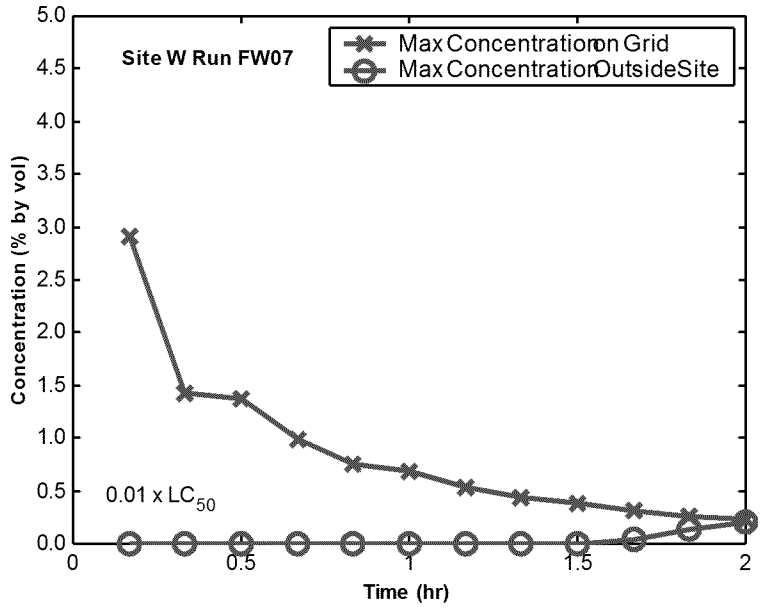

Figure A-19. Predicted change in dredged material plume concentration after release in Site W. Shown is the maximum concentration over the entire model grid and the maximum outside the site for a 5000 CY release with 40% clumps, 10% free water, and a 17 cm/s current. A water quality criteria of 0.26% dilution is also shown.

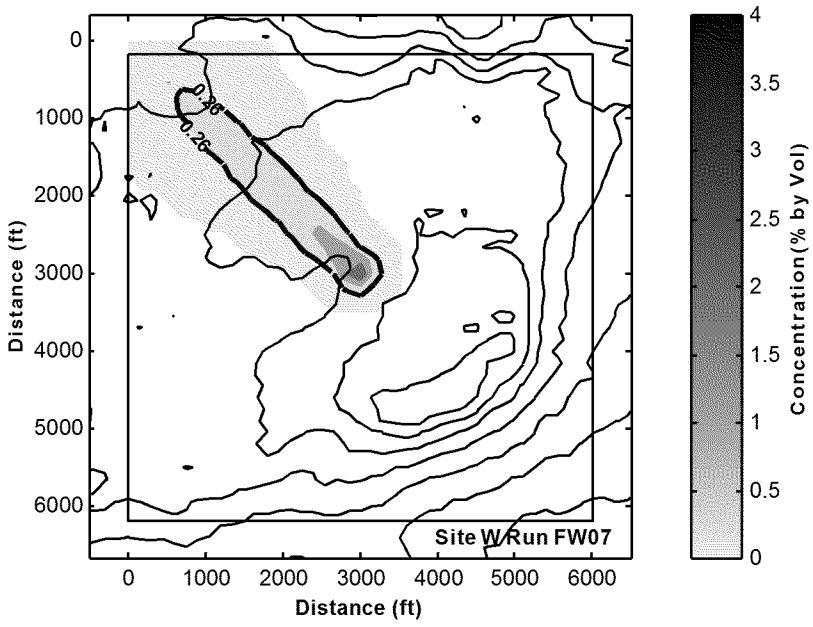

Figure A-20. Predicted depth-maximum plume concentration over the model grid after 120 min for a 5000 CY release in Site W with 40% clumps, 10% free water, and a 17 cm/s current. Bathymetric depth contour interval equals 2 ft.

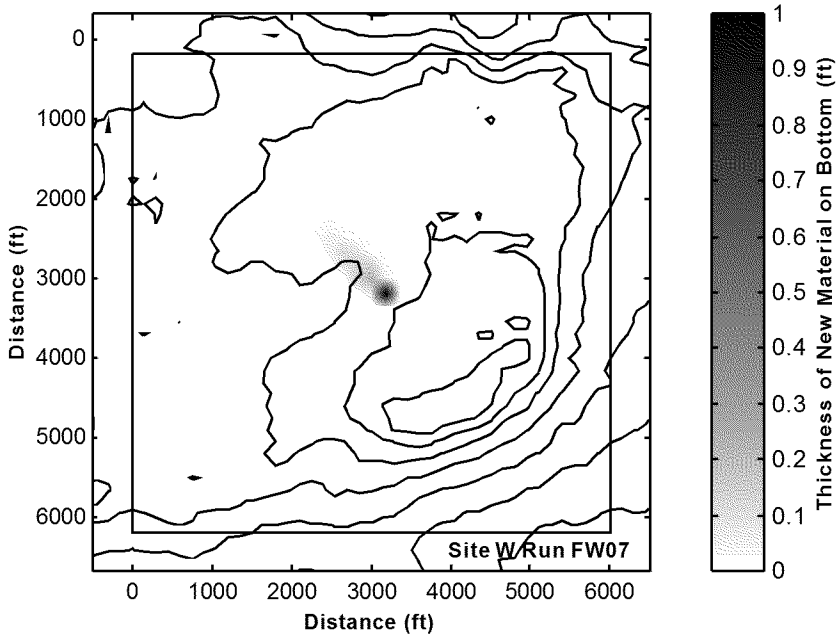

Figure A-21. Predicted total thickness of new material on the bottom for a 5000 CY release in Site W with 40% clumps, 10% free water, and a 17 cm/s current. Bathymetric depth contour interval equals 2 ft.

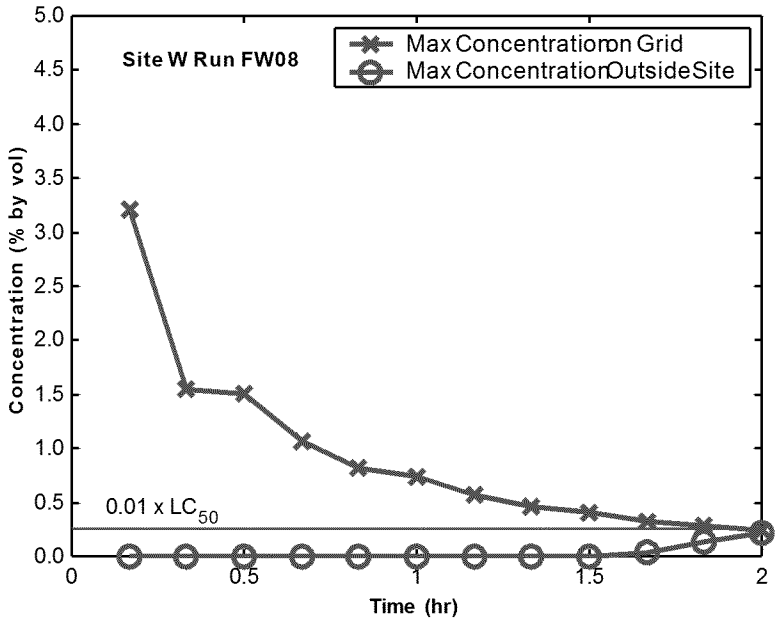

Figure A-22. Predicted change in dredged material plume concentration after release in Site W. Shown is the maximum concentration over the entire model grid and the maximum outside the site for a 5000 CY release with 60% clumps, 30% free water, and a 17 cm/s current. A water quality criteria of 0.26% dilution is also shown.

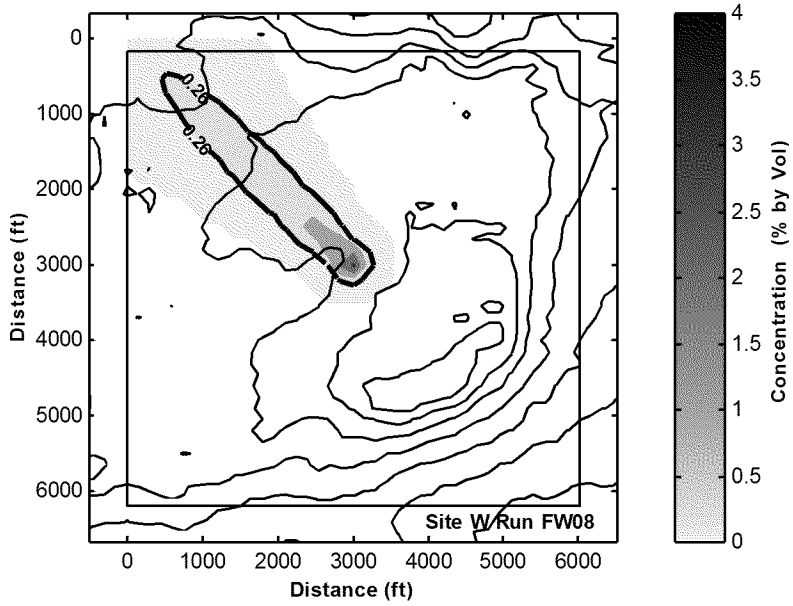

Figure A-23. Predicted depth-maximum plume concentration over the model grid after 120 min for a 5000 CY release in Site W with 60% clumps, 30% free water, and a 17 cm/s current. Bathymetric depth contour interval equals 2 ft.

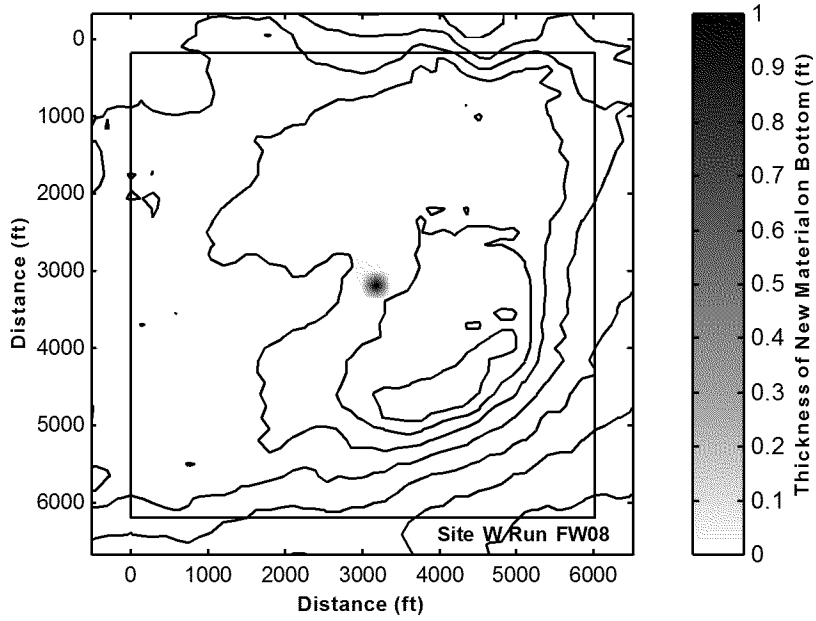

Figure A-24. Predicted total thickness of new material on the bottom for a 5000 CY release in Site W with 60% clumps, 30% free water, and a 17 cm/s current. Bathymetric depth contour interval equals 2 ft.

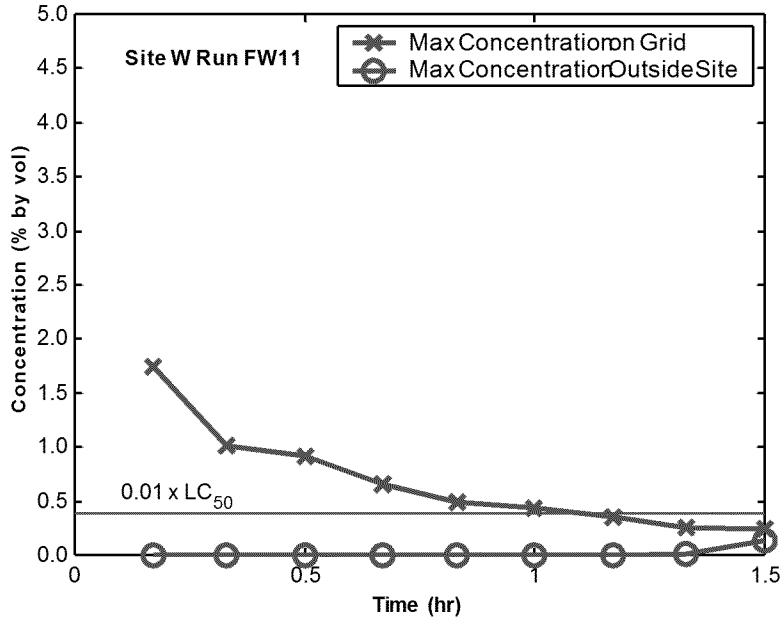

Figure A-25. Predicted change in dredged material plume concentration after release in Site W. Shown is the maximum concentration over the entire model grid and the maximum outside the site for a 3000 CY release with 40% clumps, 10% free water, and a 20 cm/s current. A water quality criteria of 0.38% dilution is also shown.

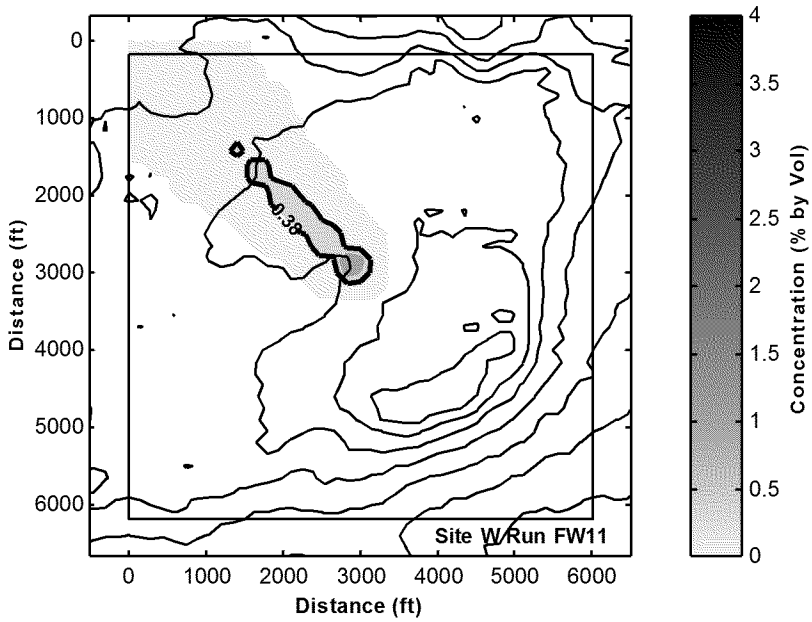

Figure A-26. Predicted depth-maximum plume concentration over the model grid after 90 min for a 3000 CY release in Site W with 40% clumps, 10% free water, and a 20 cm/s current. Bathymetric depth contour interval equals 2 ft.

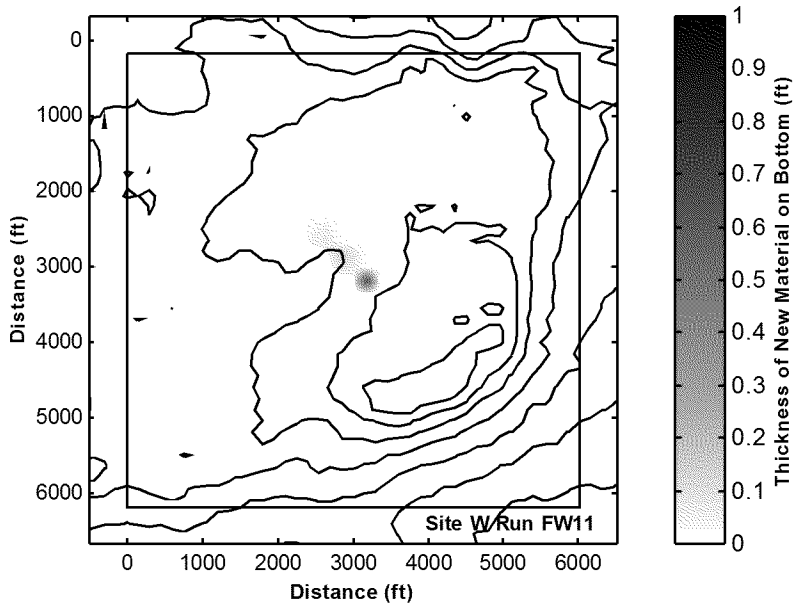

Figure A-27. Predicted total thickness of new material on the bottom for a 3000 CY release in Site W with 40% clumps, 10% free water, and a 20 cm/s current. Bathymetric depth contour interval equals 2 ft.

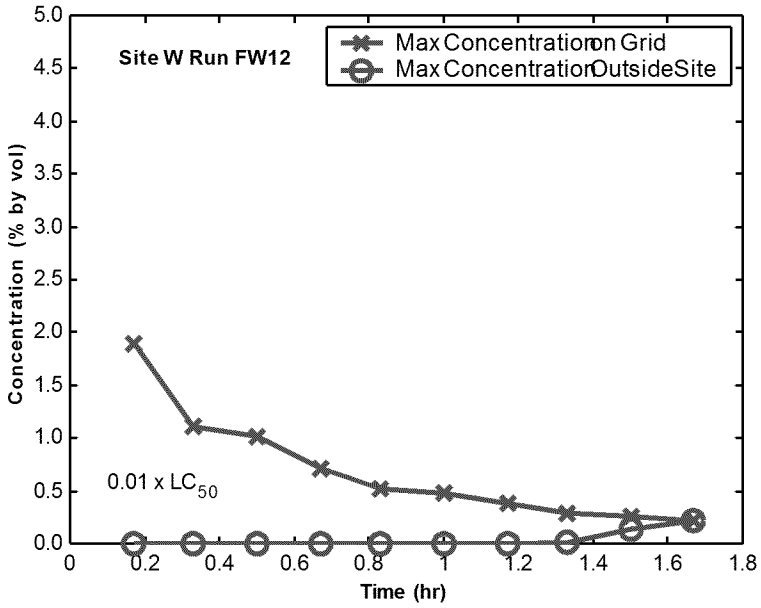

Figure A-28. Predicted change in dredged material plume concentration after release in Site W. Shown is the maximum concentration over the entire model grid and the maximum outside the site for a 3000 CY release with 60% clumps, 30% free water, and a 20 cm/s current. A water quality criteria of 0.38% dilution is also shown.

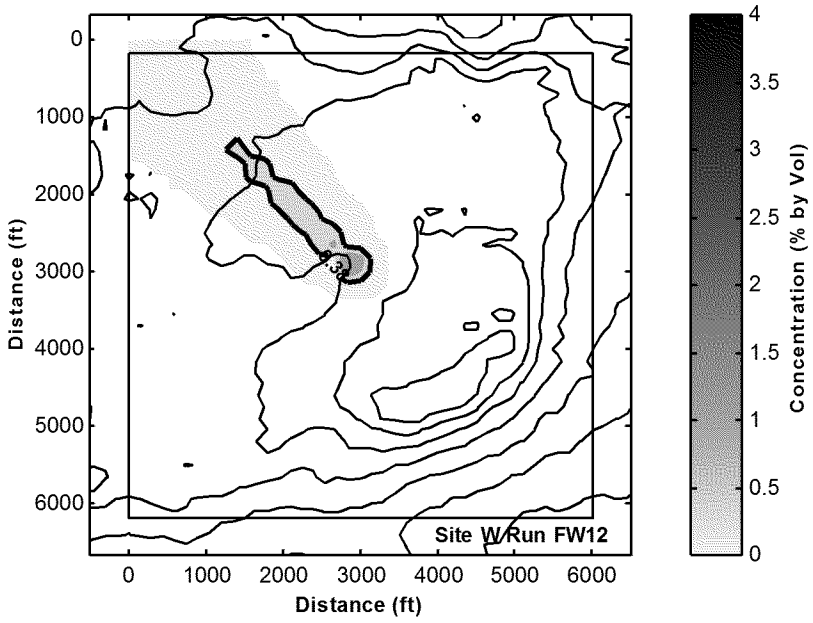

Figure A-29. Predicted depth-maximum plume concentration over the model grid after 100 min for a 3000 CY release in Site W with 60% clumps, 30% free water, and a 20 cm/s current. Bathymetric depth contour interval equals 2 ft.

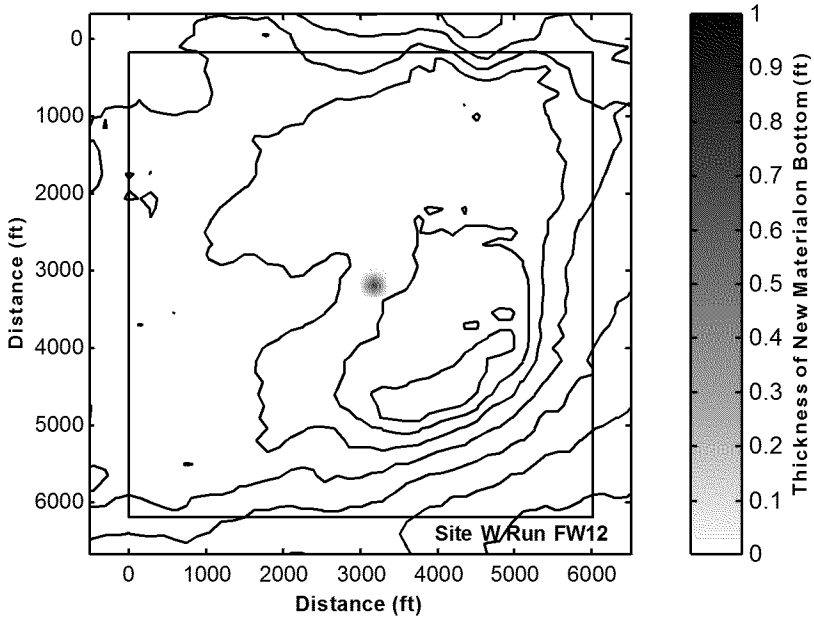

Figure A-30. Predicted total thickness of new material on the bottom for a 3000 CY release in Site W with 60% clumps, 30% free water, and a 20 cm/s current. Bathymetric depth contour interval equals 2 ft.

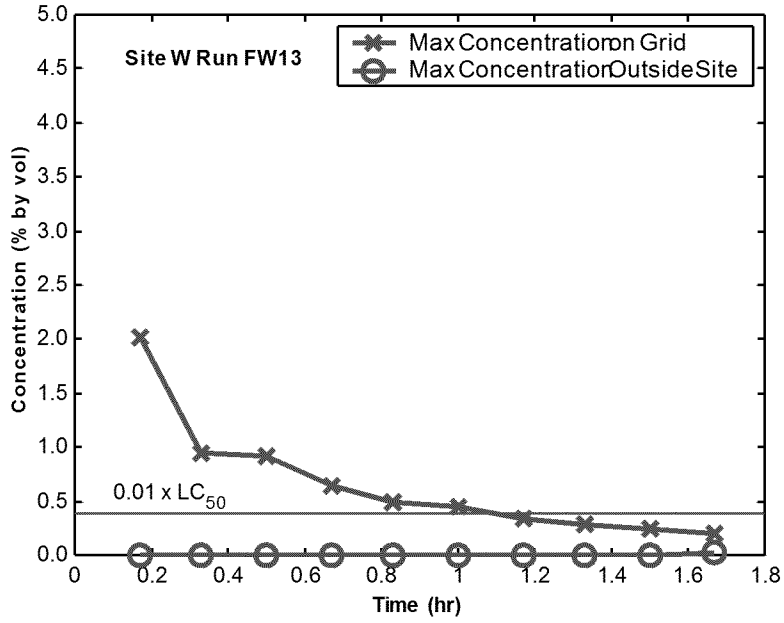

Figure A-31. Predicted change in dredged material plume concentration after release in Site W. Shown is the maximum concentration over the entire model grid and the maximum outside the site for a 3000 CY release with 40% clumps, 10% free water, and a 17 cm/s current. A water quality criteria of 0.38% dilution is also shown.

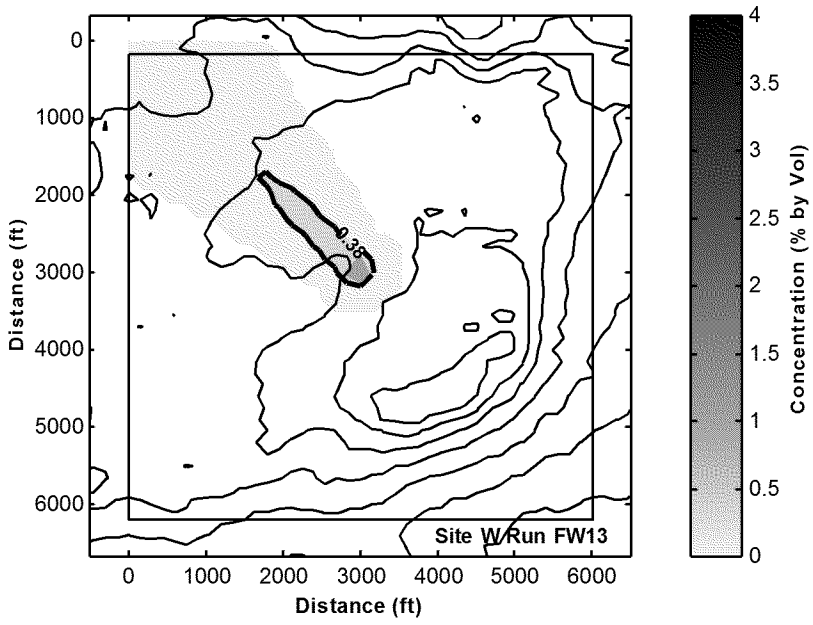

Figure A-32. Predicted depth-maximum plume concentration over the model grid after 100 min for a 3000 CY release in Site W with 40% clumps, 10% free water, and a 17 cm/s current. Bathymetric depth contour interval equals 2 ft.

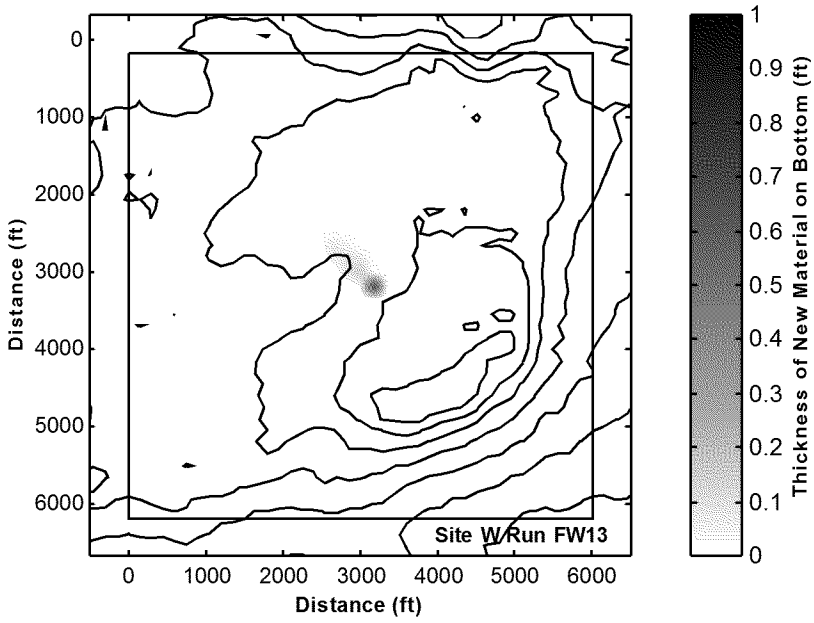

Figure A-33. Predicted total thickness of new material on the bottom for a 3000 CY release in Site W with 40% clumps, 10% free water, and a 17 cm/s current. Bathymetric depth contour interval equals 2 ft.

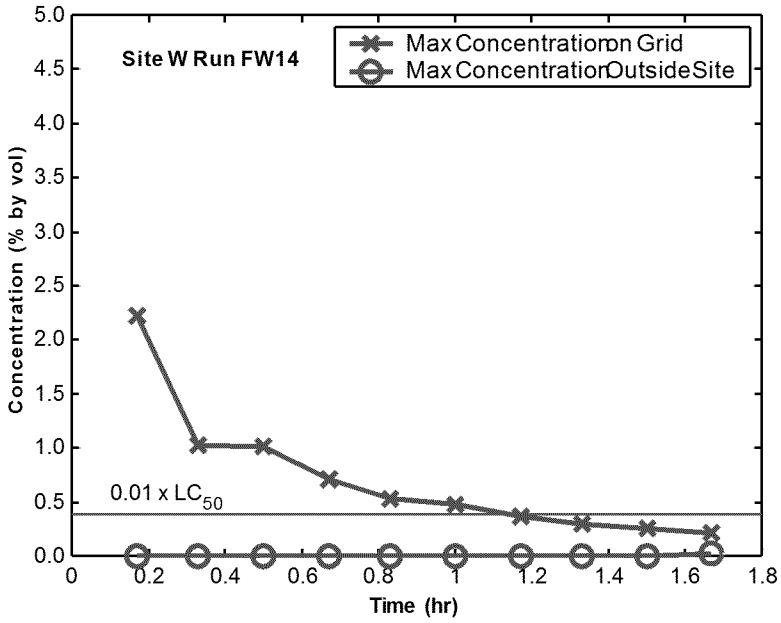

Figure A-34. Predicted change in dredged material plume concentration after release in Site W. Shown is the maximum concentration over the entire model grid and the maximum outside the site for a 3000 CY release with 60% clumps, 30% free water, and a 17 cm/s current. A water quality criteria of 0.38% dilution is also shown.

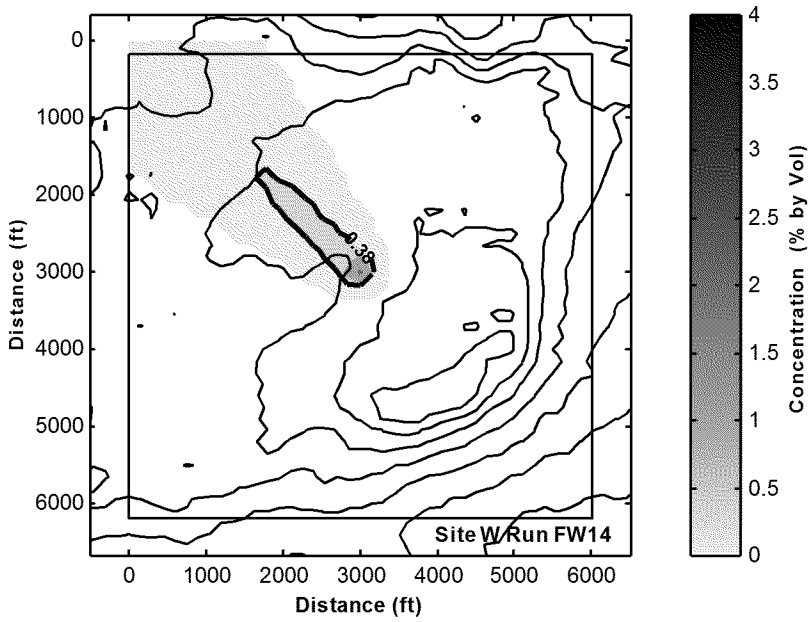

Figure A-35. Predicted depth-maximum plume concentration over the model grid after 100 min for a 3000 CY release in Site W with 60% clumps, 30% free water, and a 17 cm/s current. Bathymetric depth contour interval equals 2 ft.

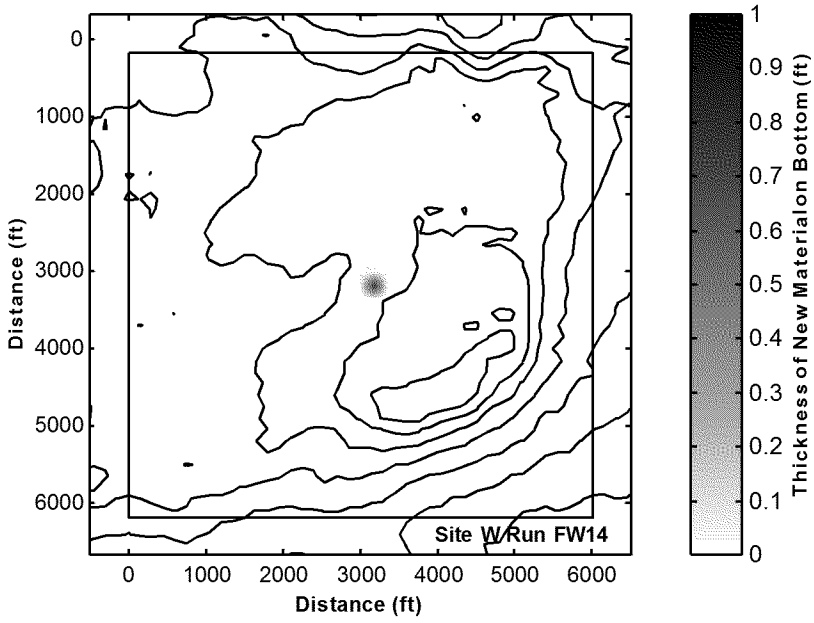

Figure A-36. Predicted total thickness of new material on the bottom for a 3000 CY release in Site W with 60% clumps, 30% free water, and a 17 cm/s current. Bathymetric depth contour interval equals 2 ft.

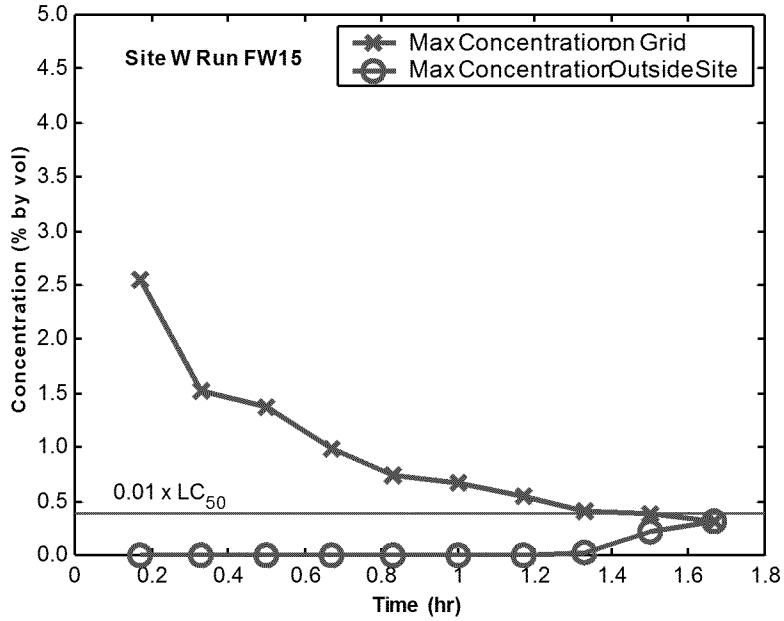

Figure A-37. Predicted change in dredged material plume concentration after release in Site W. Shown is the maximum concentration over the entire model grid and the maximum outside the site for a 5000 CY release with 40% clumps, 10% free water, and a 20 cm/s current. A water quality criteria of 0.38% dilution is also shown.

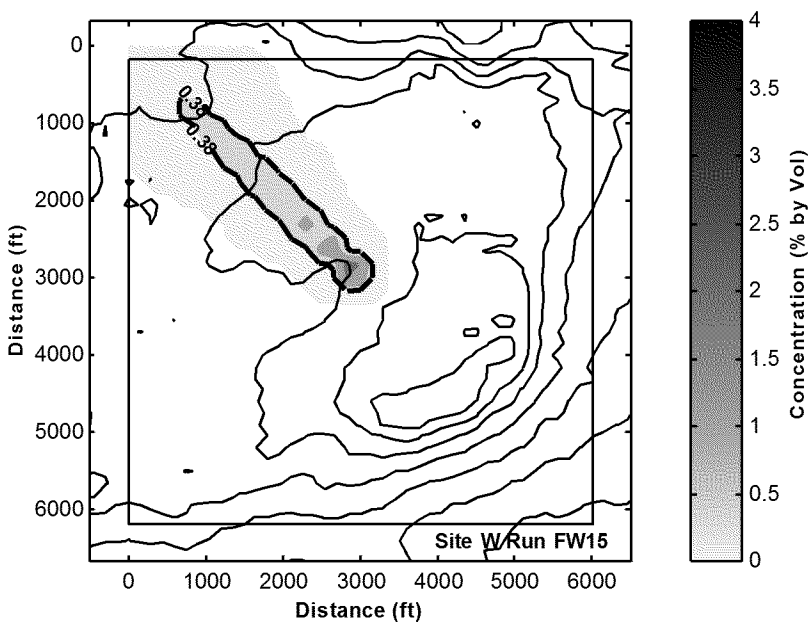

Figure A-38. Predicted depth-maximum plume concentration over the model grid after 100 min for a 5000 CY release in Site W with 40% clumps, 10% free water, and a 20 cm/s current. Bathymetric depth contour interval equals 2 ft.

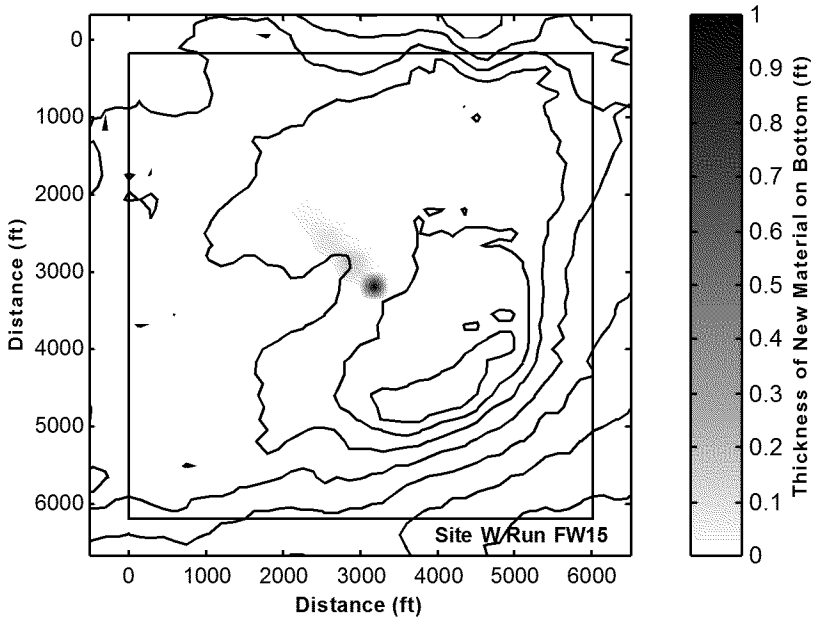

Figure A-39. Predicted total thickness of new material on the bottom for a 5000 CY release in Site W with 40% clumps, 10% free water, and a 20 cm/s current. Bathymetric depth contour interval equals 2 ft.

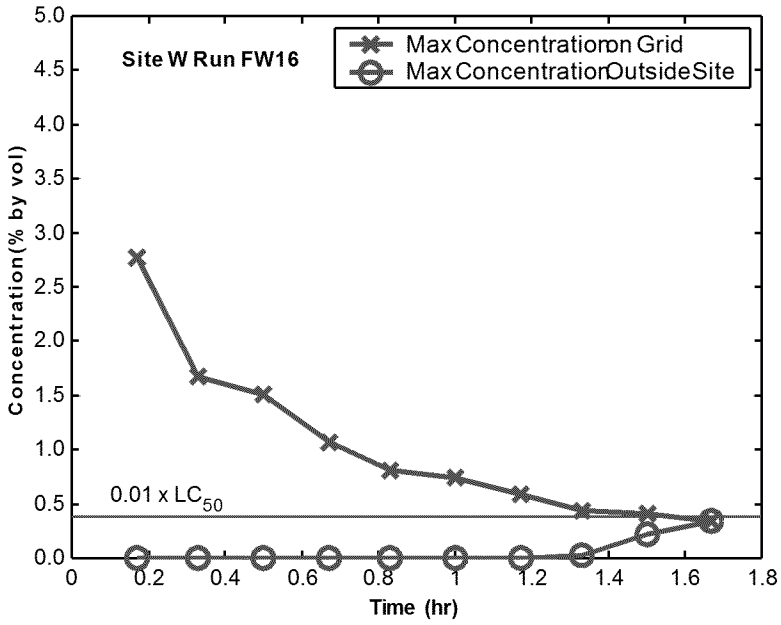

Figure A-40. Predicted change in dredged material plume concentration after release in Site W. Shown is the maximum concentration over the entire model grid and the maximum outside the site for a 5000 CY release with 60% clumps, 30% free water, and a 20 cm/s current. A water quality criteria of 0.38% dilution is also shown.

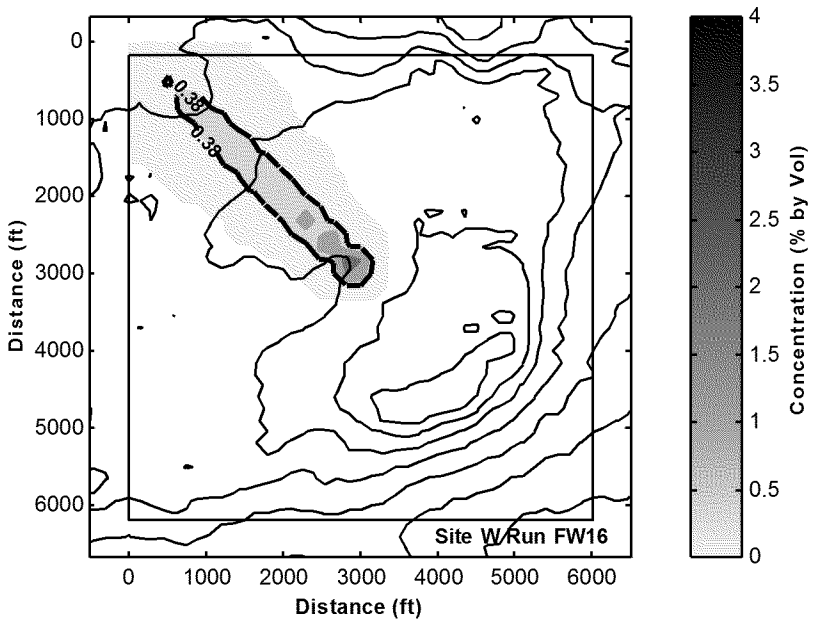

Figure A-41. Predicted depth-maximum plume concentration over the model grid after 100 min for a 5000 CY release in Site W with 60% clumps, 30% free water, and a 20 cm/s current. Bathymetric depth contour interval equals 2 ft.

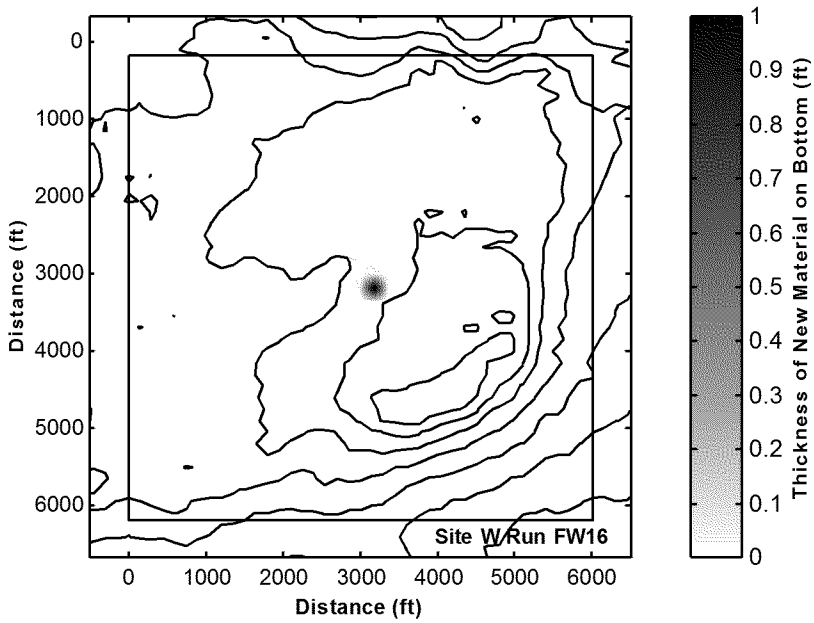

Figure A-42. Predicted total thickness of new material on the bottom for a 5000 CY release in Site W with 60% clumps, 30% free water, and a 20 cm/s current. Bathymetric depth contour interval equals 2 ft.

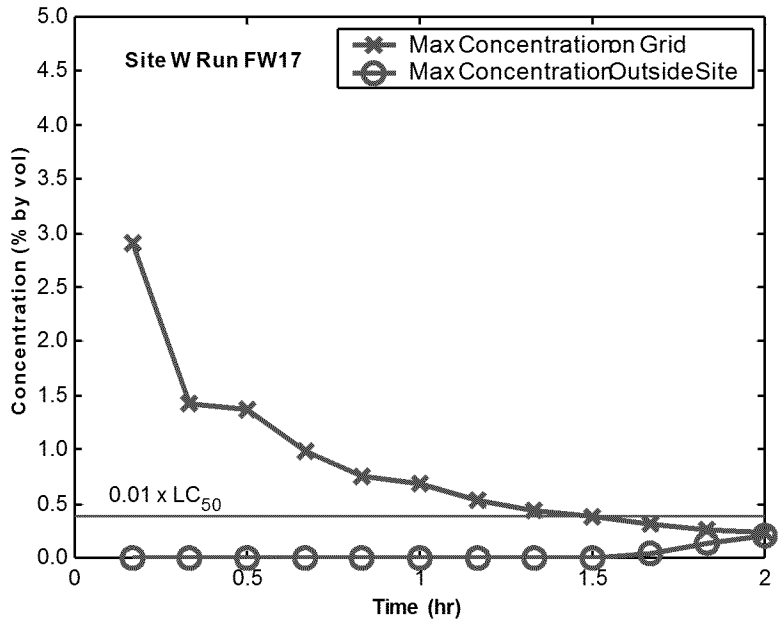

Figure A-43. Predicted change in dredged material plume concentration after release in Site W. Shown is the maximum concentration over the entire model grid and the maximum outside the site for a 5000 CY release with 40% clumps, 10% free water, and a 17 cm/s current. A water quality criteria of 0.38% dilution is also shown.

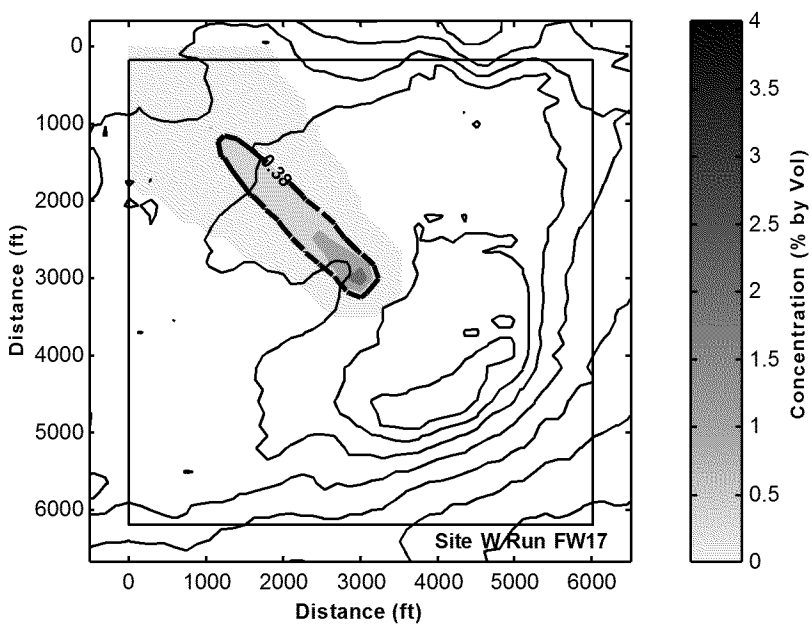

Figure A-44. Predicted depth-maximum plume concentration over the model grid after 120 min for a 5000 CY release in Site W with 40% clumps, 10% free water, and a 17 cm/s current. Bathymetric depth contour interval equals 2 ft.

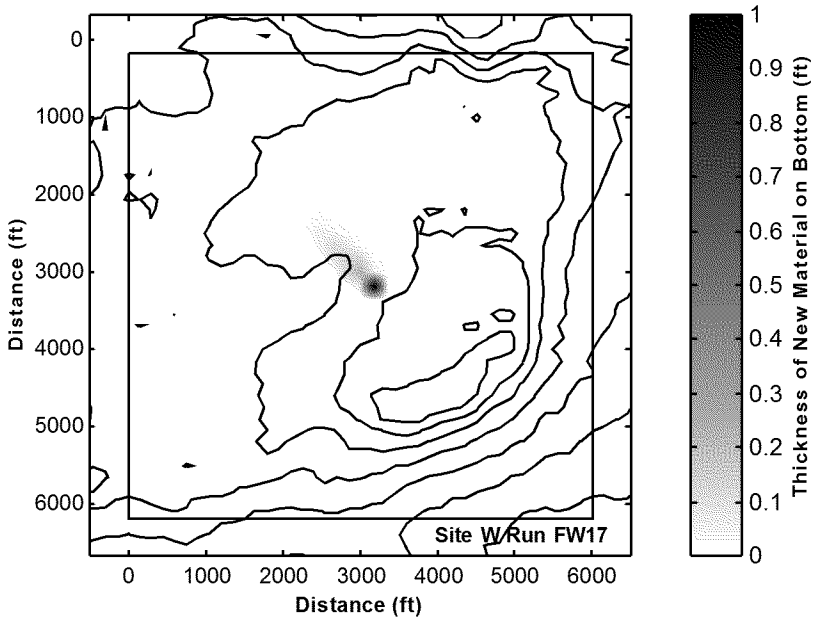

Figure A-45. Predicted total thickness of new material on the bottom for a 5000 CY release in Site W with 40% clumps, 10% free water, and a 17 cm/s current. Bathymetric depth contour interval equals 2 ft.

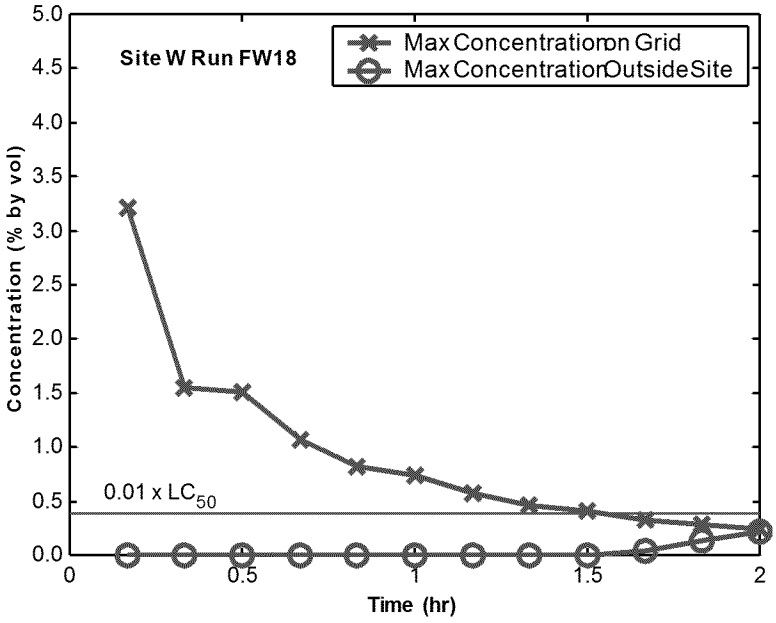

Figure A-46. Predicted change in dredged material plume concentration after release in Site W. Shown is the maximum concentration over the entire model grid and the maximum outside the site for a 5000 CY release with 60% clumps, 30% free water, and a 17 cm/s current. A water quality criteria of 0.38% dilution is also shown.

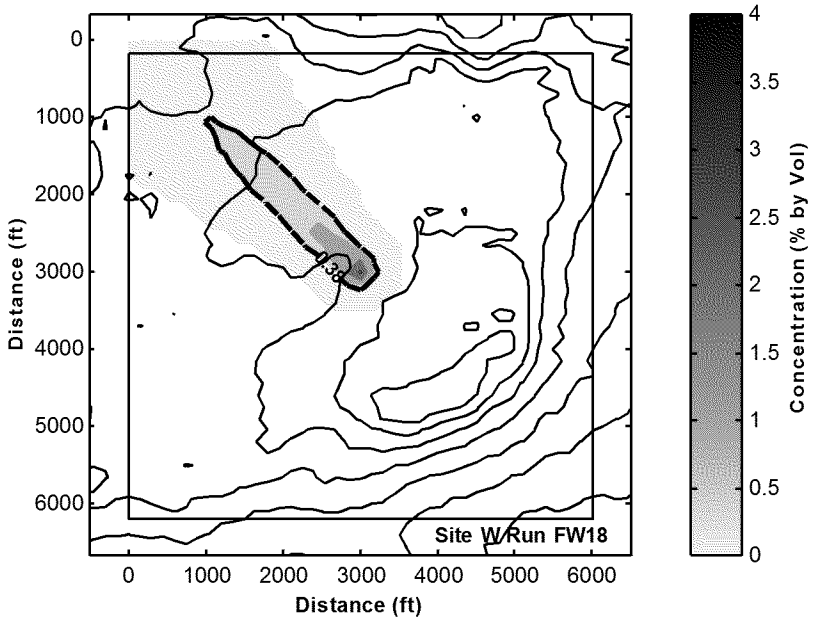

Figure A-47. Predicted depth-maximum plume concentration over the model grid after 120 min for a 5000 CY release in Site W with 60% clumps, 30% free water, and a 17 cm/s current. Bathymetric depth contour interval equals 2 ft.

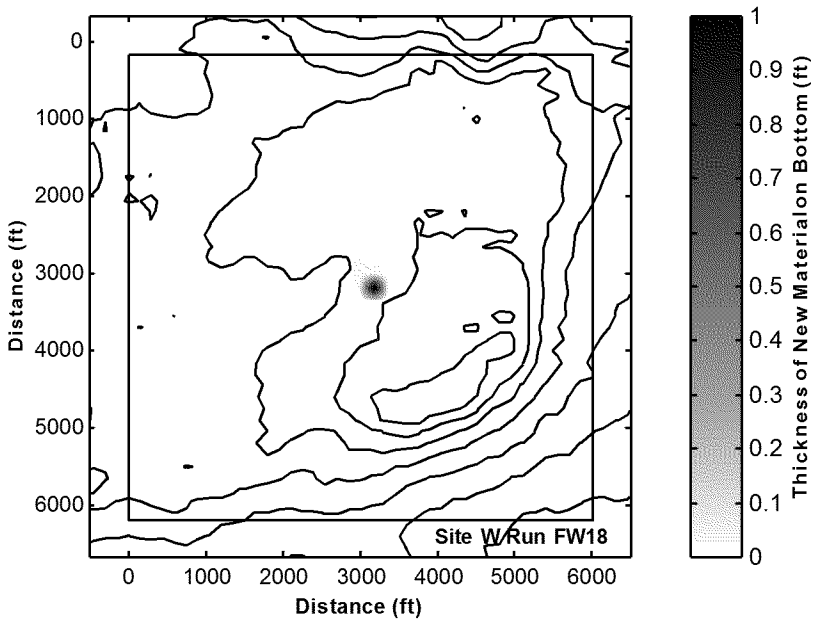

Figure A-48. Predicted total thickness of new material on the bottom for a 5000 CY release in Site W with 60% clumps, 30% free water, and a 17 cm/s current. Bathymetric depth contour interval equals 2 ft.

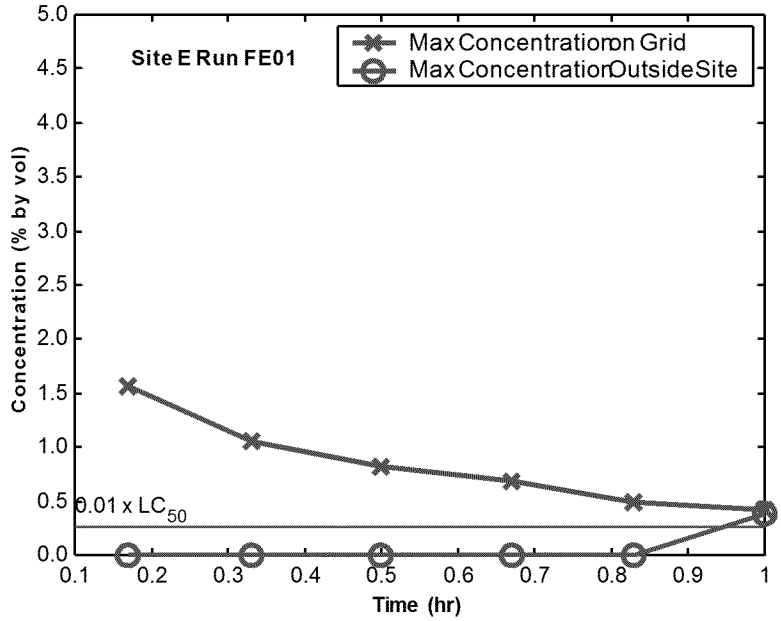

Figure A-49. Predicted change in dredged material plume concentration after release in Site E. Shown is the maximum concentration over the entire model grid and the maximum outside the site for a 3000 CY release with 40% clumps, 10% free water, and a 20 cm/s current. A water quality criteria of 0.26% dilution is also shown.

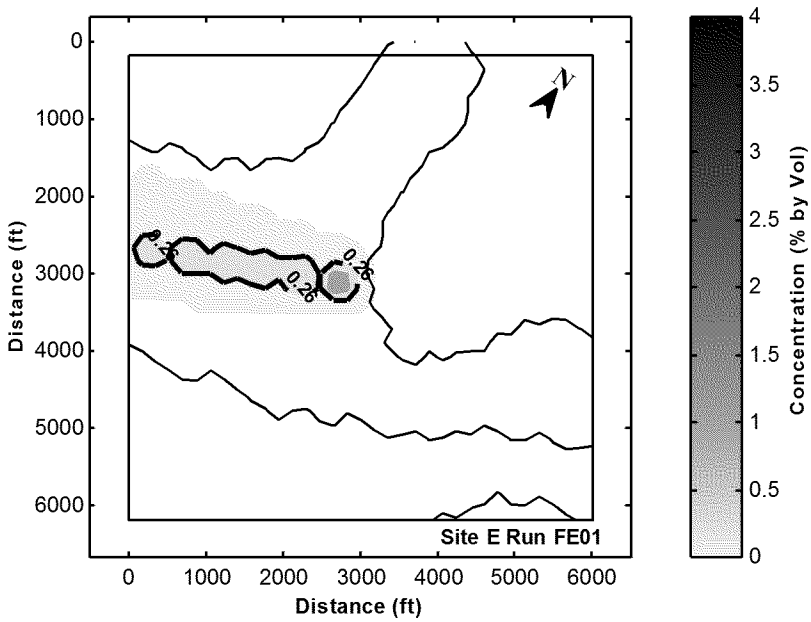

Figure A-50. Predicted depth-maximum plume concentration over the model grid after 90 min for a 3000 CY release in Site E with 40% clumps, 10% free water, and a 20 cm/s current. Bathymetric depth contour interval equals 2 ft.

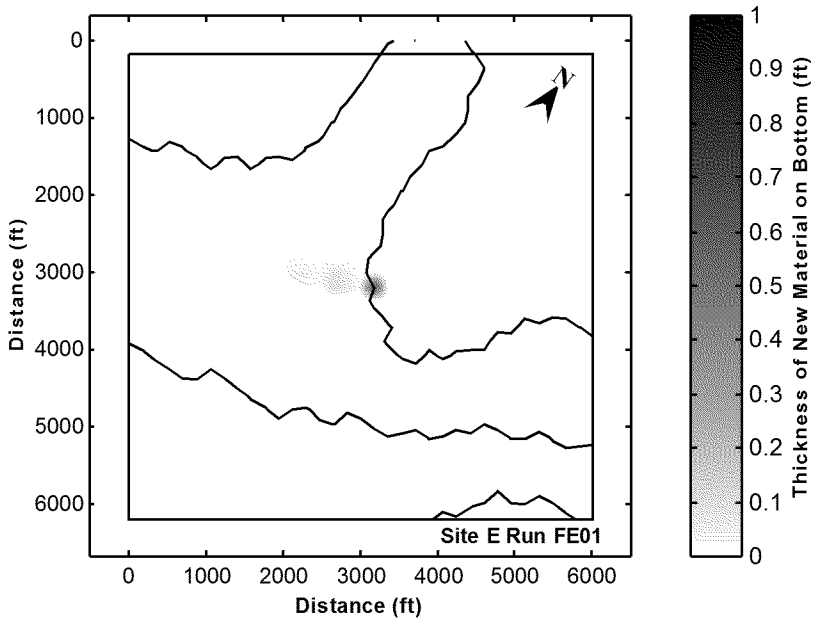

Figure A-51. Predicted total thickness of new material on the bottom for a 3000 CY release in Site E with 40% clumps, 10% free water, and a 20 cm/s current. Bathymetric depth contour interval equals 2 ft.

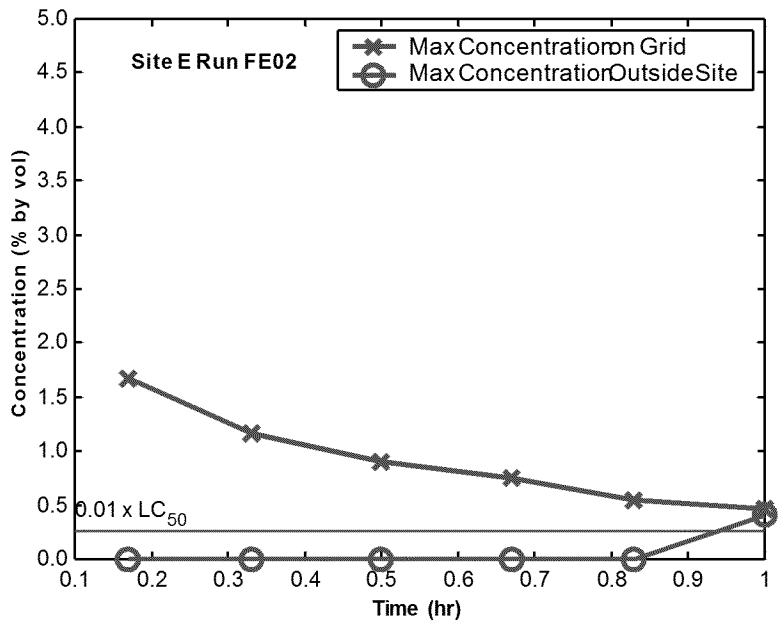

Figure A-52. Predicted change in dredged material plume concentration after release in Site E. Shown is the maximum concentration over the entire model grid and the maximum outside the site for a 3000 CY release with 60% clumps, 30% free water, and a 20 cm/s current. A water quality criteria of 0.26% dilution is also shown.

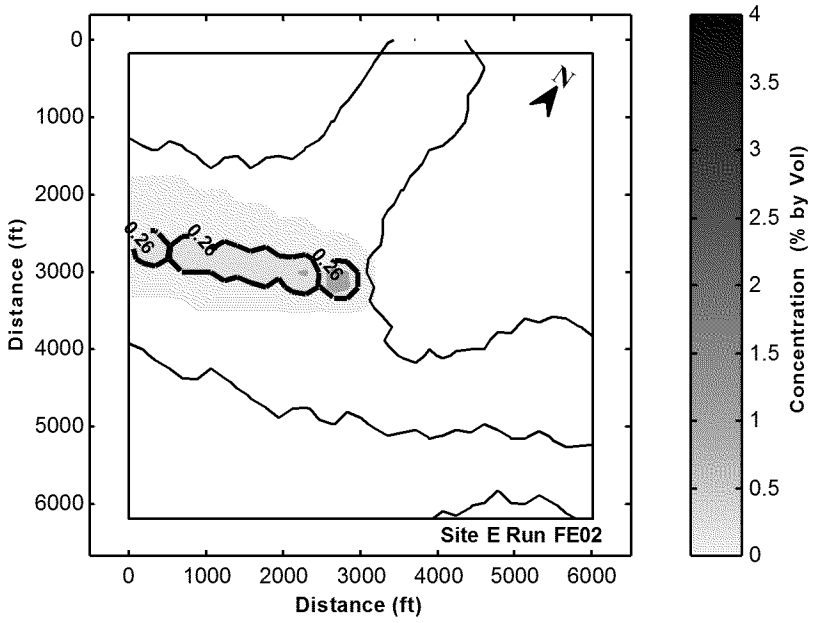

Figure A-53. Predicted depth-maximum plume concentration over the model grid after 100 min for a 3000 CY release in Site E with 60% clumps, 30% free water, and a 20 cm/s current. Bathymetric depth contour interval equals 2 ft.

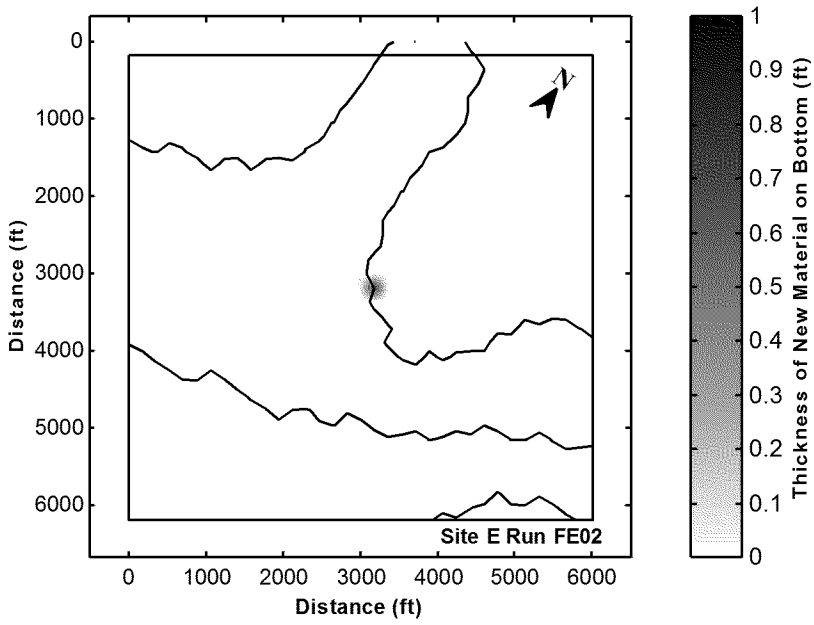

Figure A-54. Predicted total thickness of new material on the bottom for a 3000 CY release in Site E with 60% clumps, 30% free water, and a 20 cm/s current. Bathymetric depth contour interval equals 2 ft.

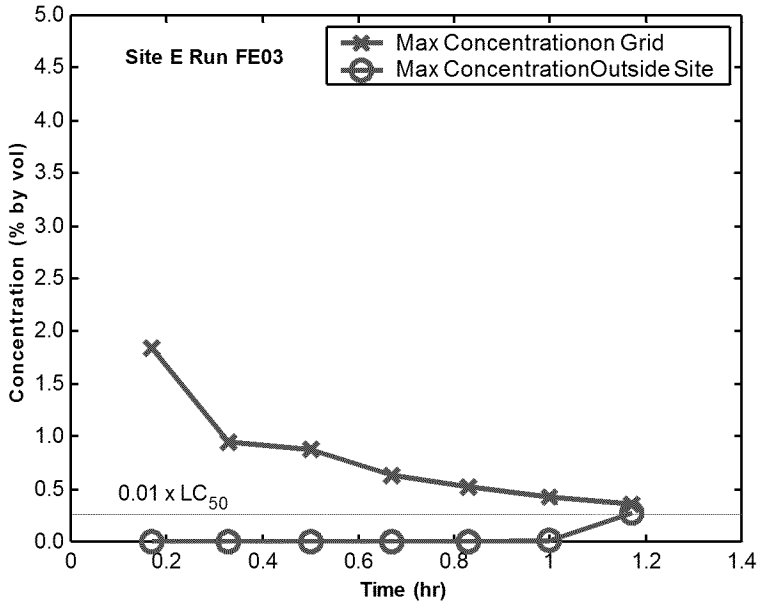

Figure A-55. Predicted change in dredged material plume concentration after release in Site E. Shown is the maximum concentration over the entire model grid and the maximum outside the site for a 3000 CY release with 40% clumps, 10% free water, and a 17 cm/s current. A water quality criteria of 0.26% dilution is also shown.

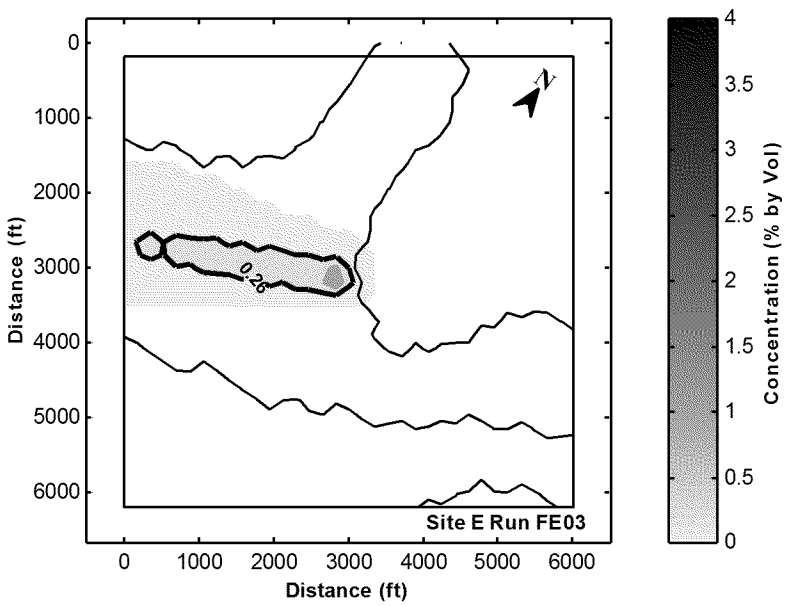

Figure A-56. Predicted depth-maximum plume concentration over the model grid after 100 min for a 3000 CY release in Site E with 40% clumps, 10% free water, and a 17 cm/s current. Bathymetric depth contour interval equals 2 ft.

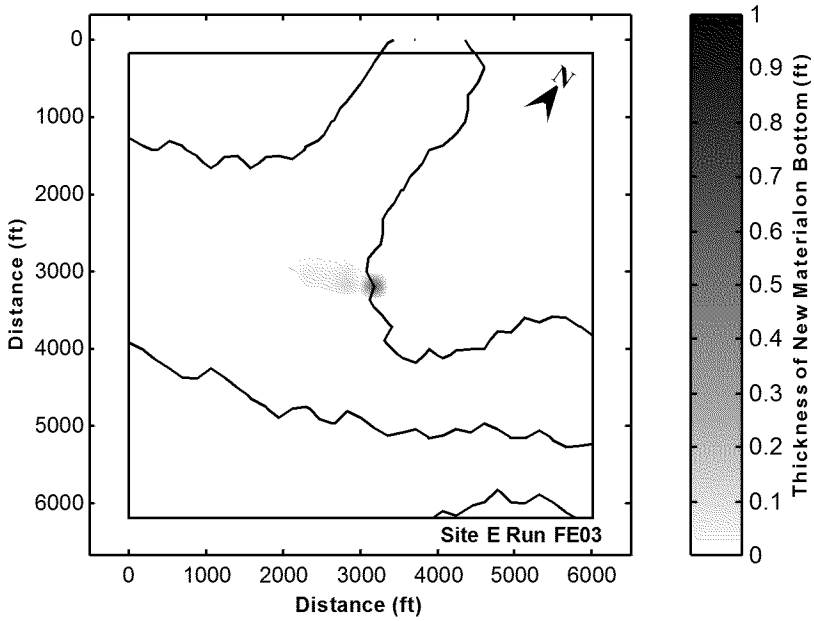

Figure A-57. Predicted total thickness of new material on the bottom for a 3000 CY release in Site E with 40% clumps, 10% free water, and a 17 cm/s current. Bathymetric depth contour interval equals 2 ft.

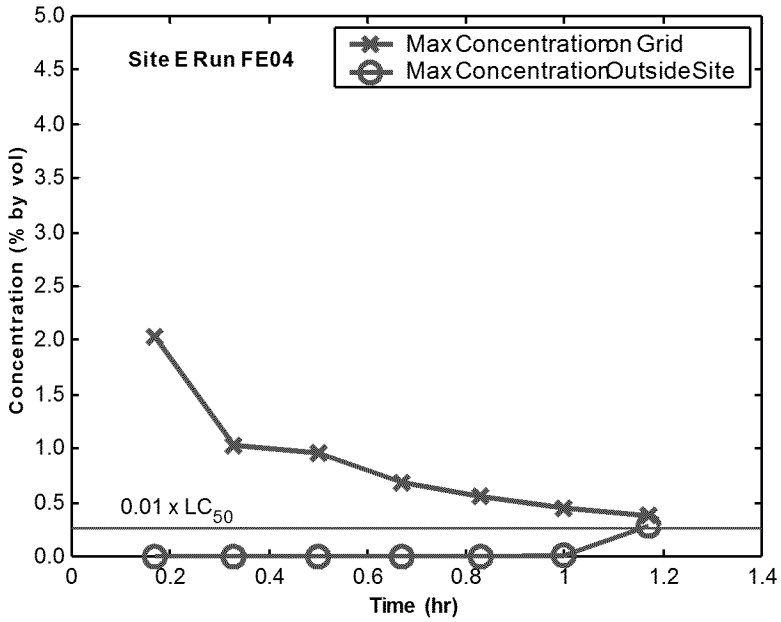

Figure A-58. Predicted change in dredged material plume concentration after release in Site E. Shown is the maximum concentration over the entire model grid and the maximum outside the site for a 3000 CY release with 60% clumps, 30% free water, and a 17 cm/s current. A water quality criteria of 0.26% dilution is also shown.

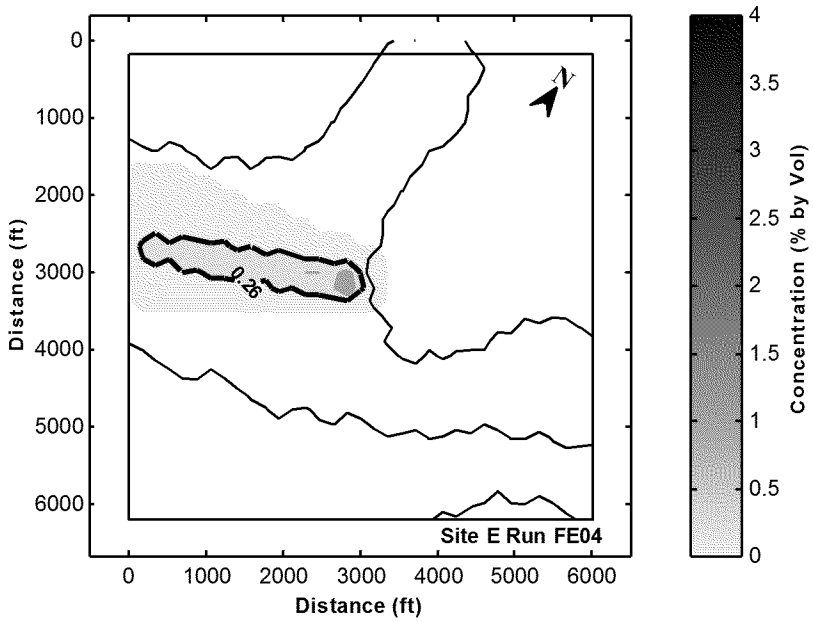

Figure A-59. Predicted depth-maximum plume concentration over the model grid after 100 min for a 3000 CY release in Site E with 60% clumps, 30% free water, and a 17 cm/s current. Bathymetric depth contour interval equals 2 ft.

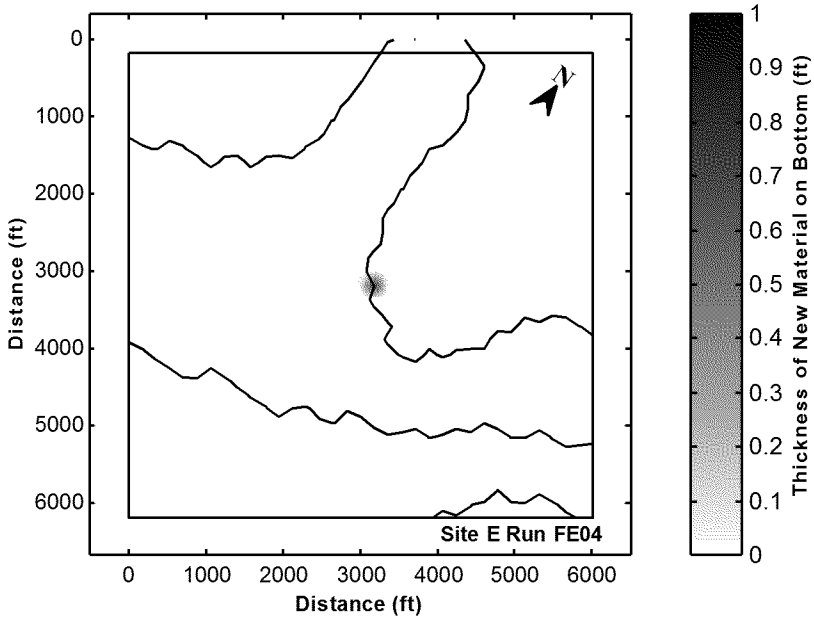

Figure A-60. Predicted total thickness of new material on the bottom for a 3000 CY release in Site E with 60% clumps, 30% free water, and a 17 cm/s current. Bathymetric depth contour interval equals 2 ft.

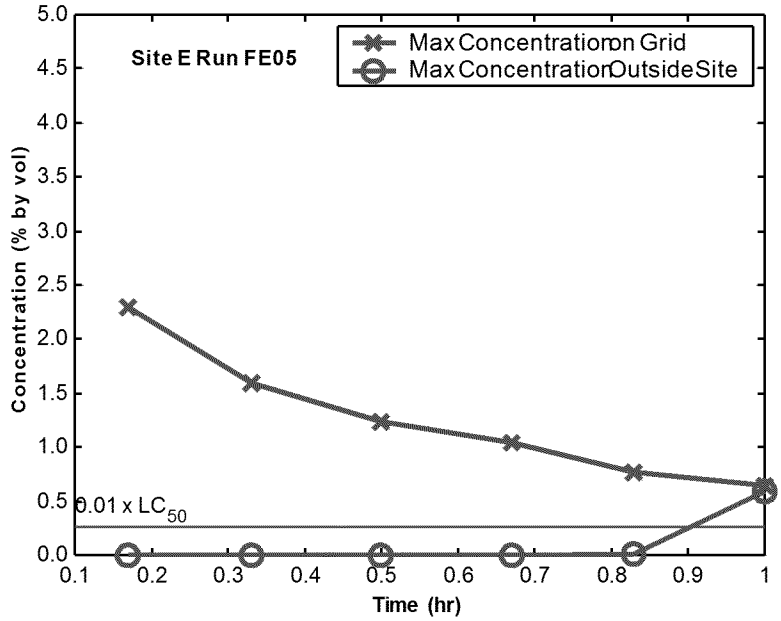

Figure A-61. Predicted change in dredged material plume concentration after release in Site E. Shown is the maximum concentration over the entire model grid and the maximum outside the site for a 5000 CY release with 40% clumps, 10% free water, and a 20 cm/s current. A water quality criteria of 0.26% dilution is also shown.

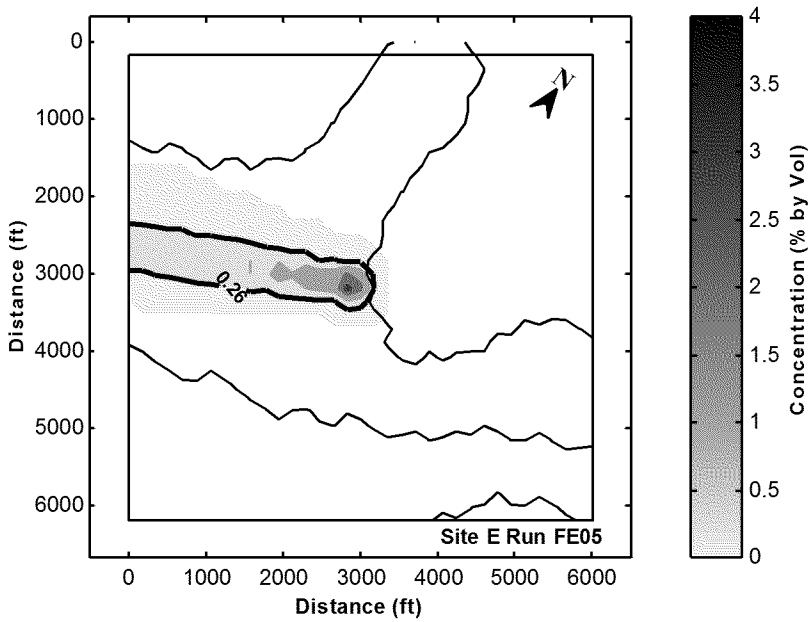

Figure A-62. Predicted depth-maximum plume concentration over the model grid after 100 min for a 5000 CY release in Site E with 40% clumps, 10% free water, and a 20 cm/s current. Bathymetric depth contour interval equals 2 ft.

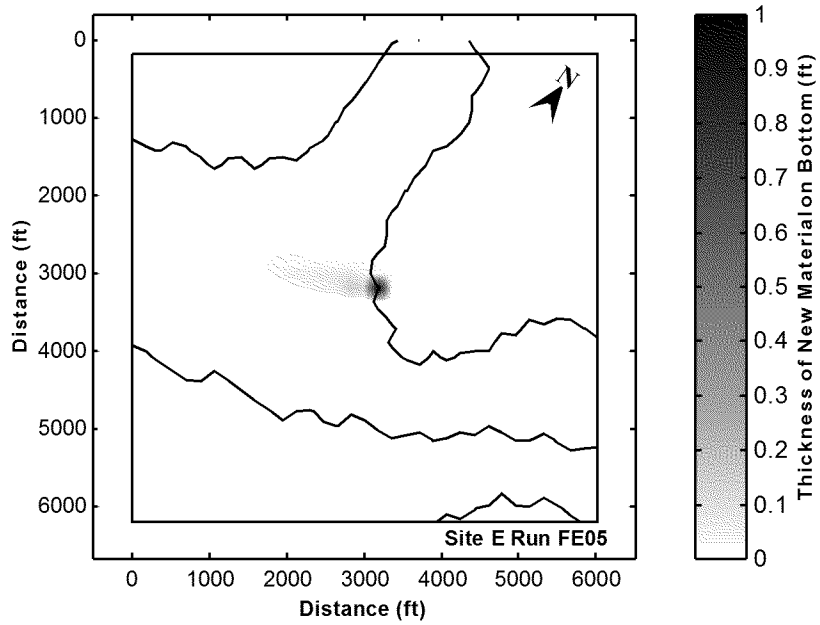

Figure A-63. Predicted total thickness of new material on the bottom for a 5000 CY release in Site E with 40% clumps, 10% free water, and a 20 cm/s current. Bathymetric depth contour interval equals 2 ft.

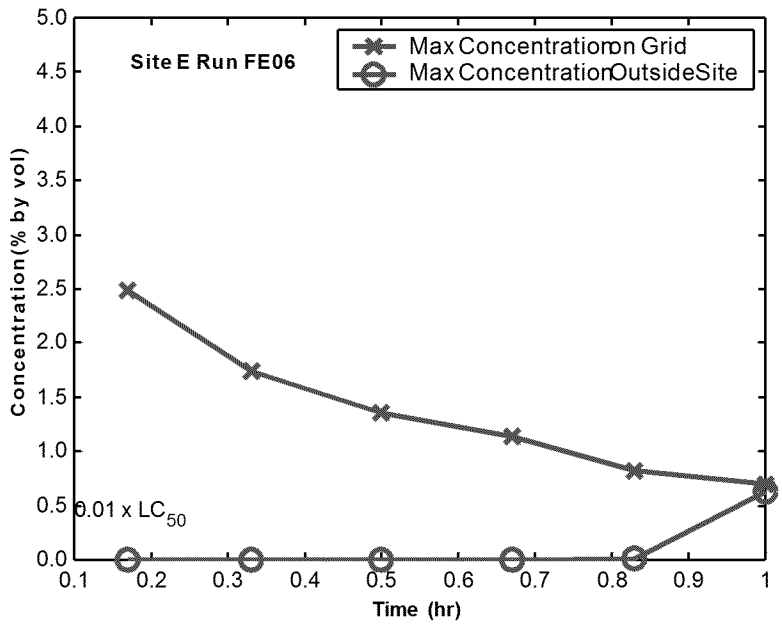

Figure A-64. Predicted change in dredged material plume concentration after release in Site E. Shown is the maximum concentration over the entire model grid and the maximum outside the site for a 5000 CY release with 60% clumps, 30% free water, and a 20 cm/s current. A water quality criteria of 0.26% dilution is also shown.

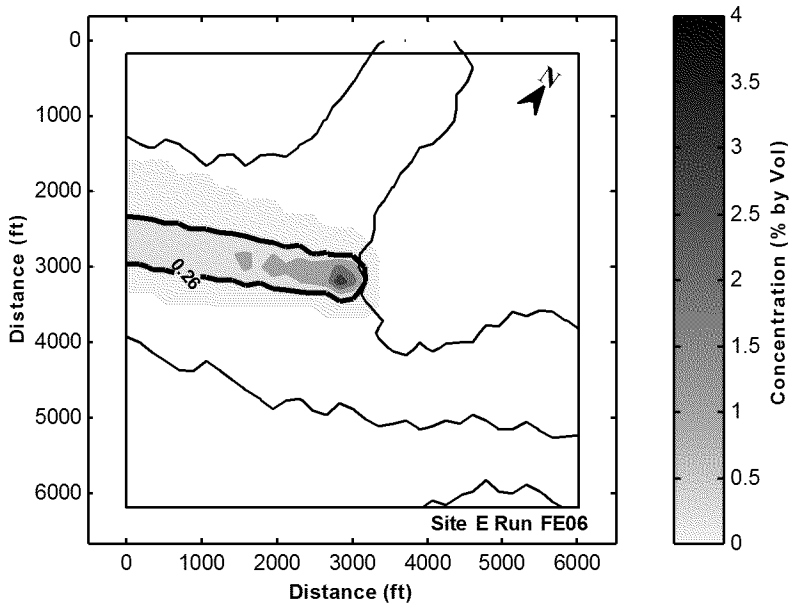

Figure A-65. Predicted depth-maximum plume concentration over the model grid after 100 min for a 5000 CY release in Site E with 60% clumps, 30% free water, and a 20 cm/s current. Bathymetric depth contour interval equals 2 ft.

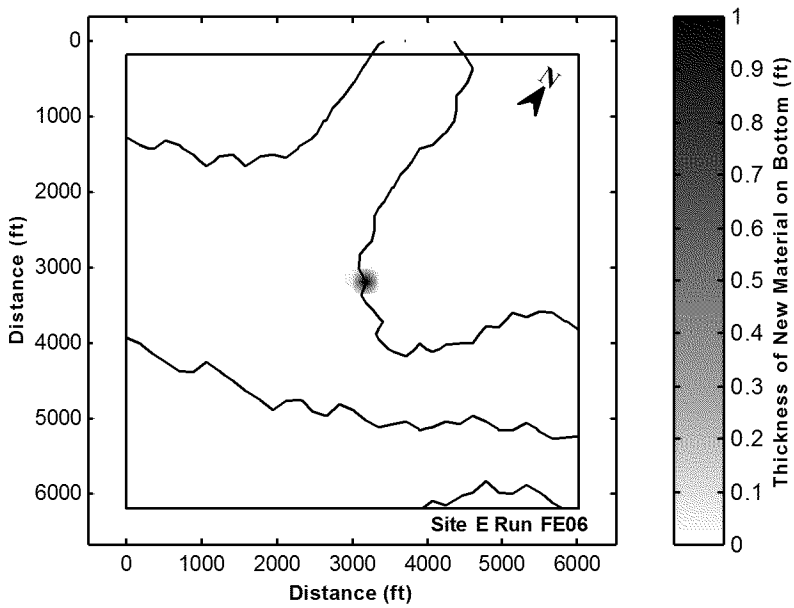

Figure A-66. Predicted total thickness of new material on the bottom for a 5000 CY release in Site E with 60% clumps, 30% free water, and a 20 cm/s current. Bathymetric depth contour interval equals 2 ft.

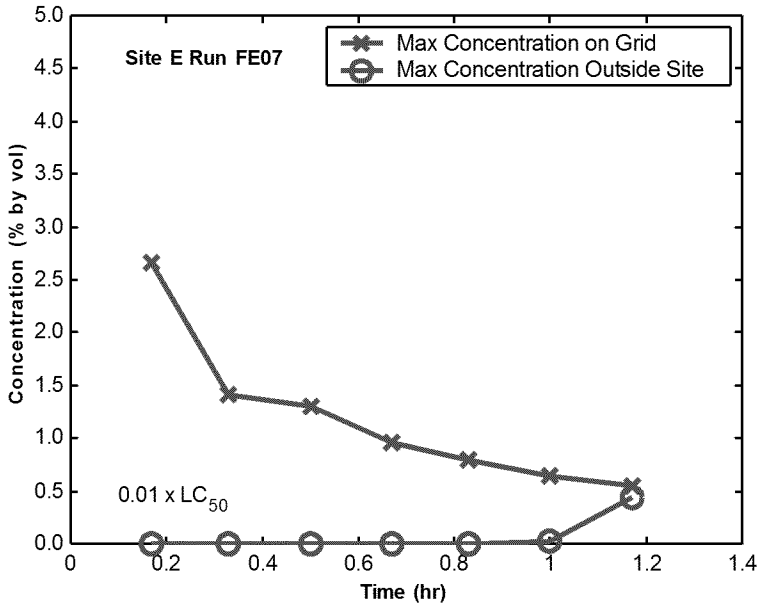

Figure A-67. Predicted change in dredged material plume concentration after release in Site E. Shown is the maximum concentration over the entire model grid and the maximum outside the site for a 5000 CY release with 40% clumps, 10% free water, and a 17 cm/s current. A water quality criteria of 0.26% dilution is also shown.

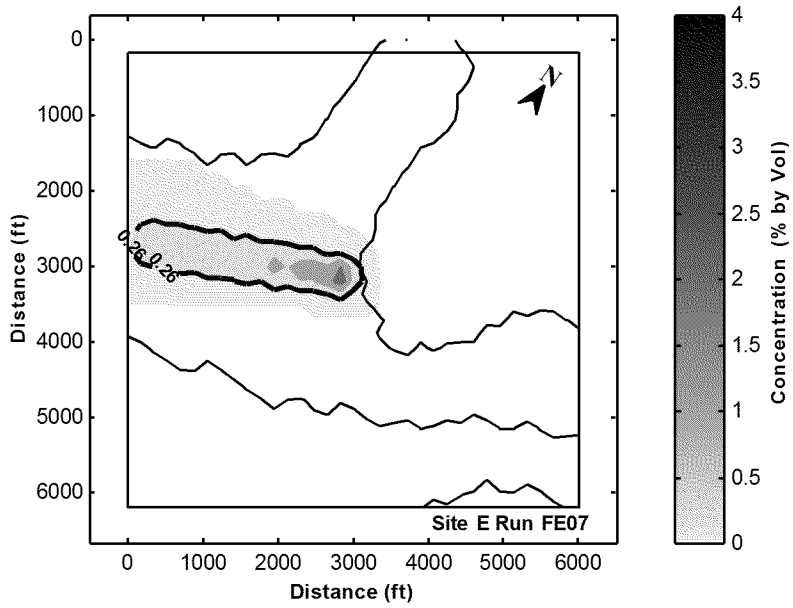

Figure A-68. Predicted depth-maximum plume concentration over the model grid after 120 min for a 5000 CY release in Site E with 40% clumps, 10% free water, and a 17 cm/s current. Bathymetric depth contour interval equals 2 ft.

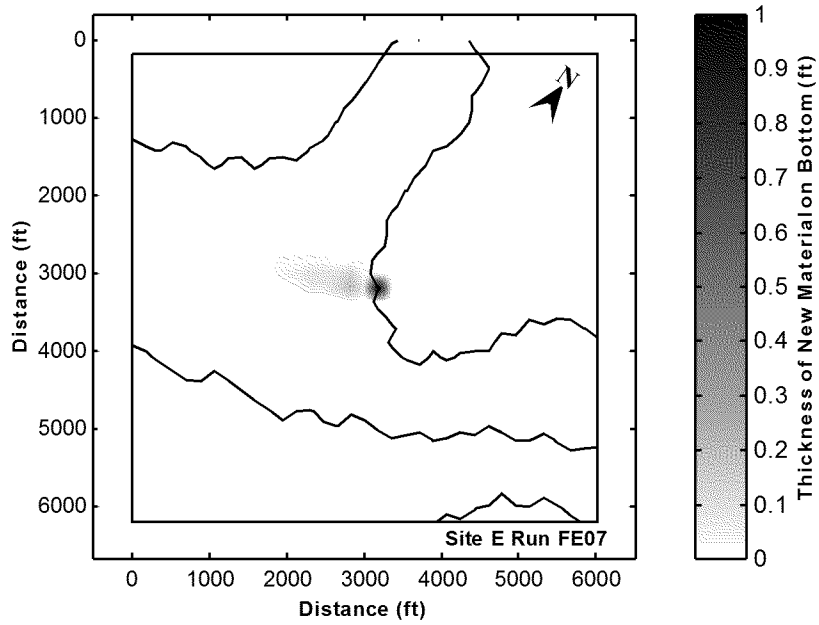

Figure A-69. Predicted total thickness of new material on the bottom for a 5000 CY release in Site E with 40% clumps, 10% free water, and a 17 cm/s current. Bathymetric depth contour interval equals 2 ft.

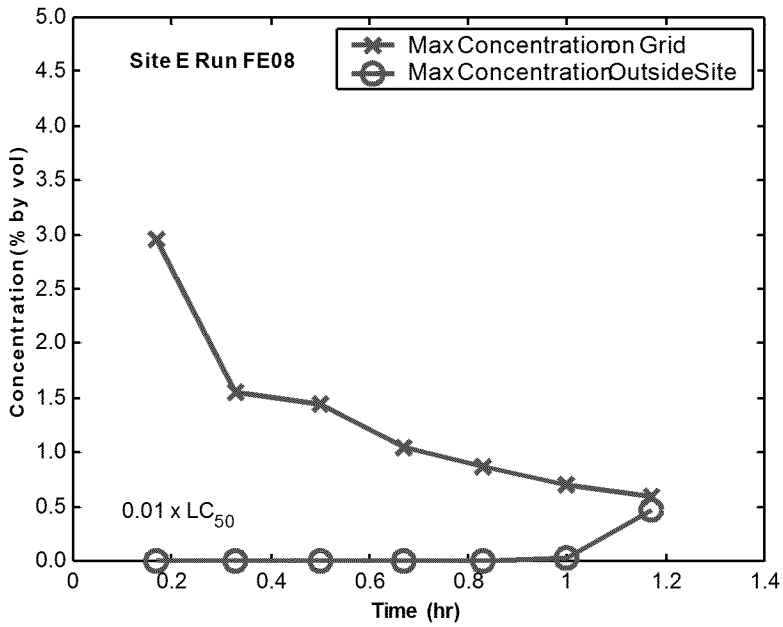

Figure A-70. Predicted change in dredged material plume concentration after release in Site E. Shown is the maximum concentration over the entire model grid and the maximum outside the site for a 5000 CY release with 60% clumps, 30% free water, and a 17 cm/s current. A water quality criteria of 0.26% dilution is also shown.

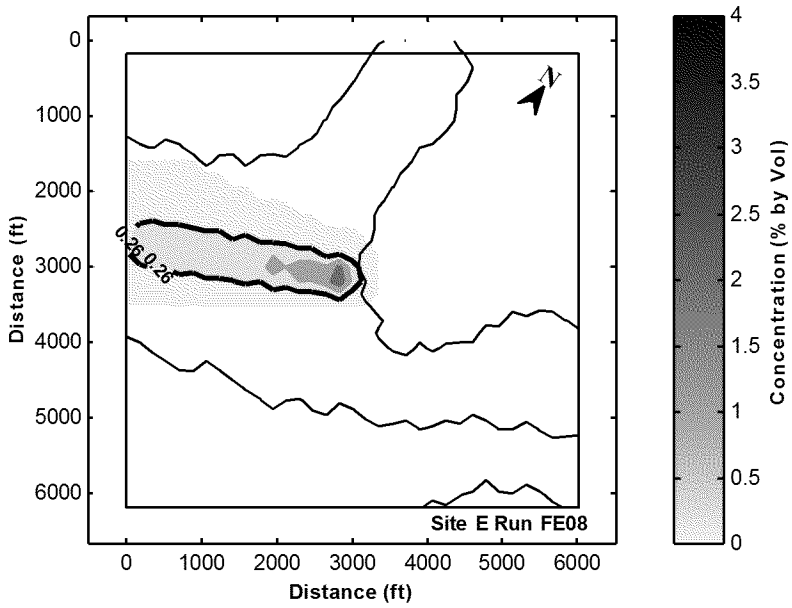

Figure A-71. Predicted depth-maximum plume concentration over the model grid after 120 min for a 5000 CY release in Site E with 60% clumps, 30% free water, and a 17 cm/s current. Bathymetric depth contour interval equals 2 ft.

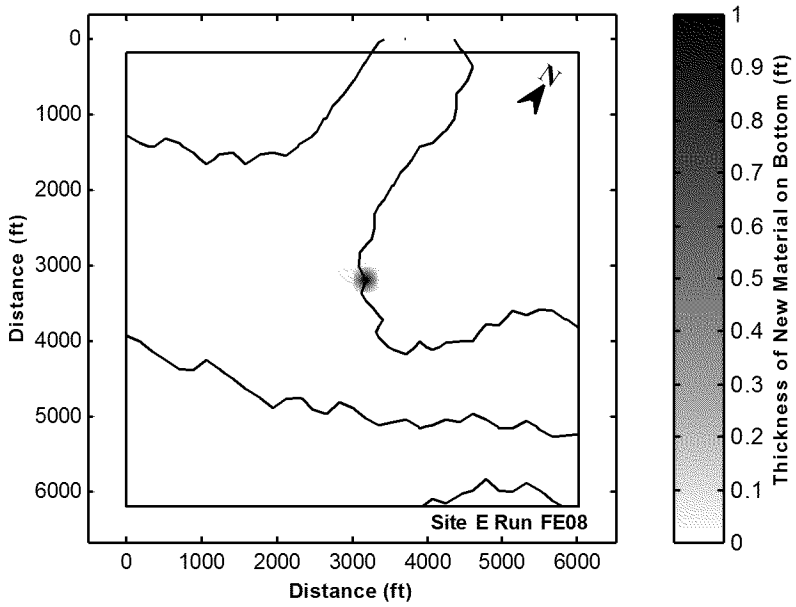

Figure A-72. Predicted total thickness of new material on the bottom for a 5000 CY release in Site E with 60% clumps, 30% free water, and a 17 cm/s current. Bathymetric depth contour interval equals 2 ft.

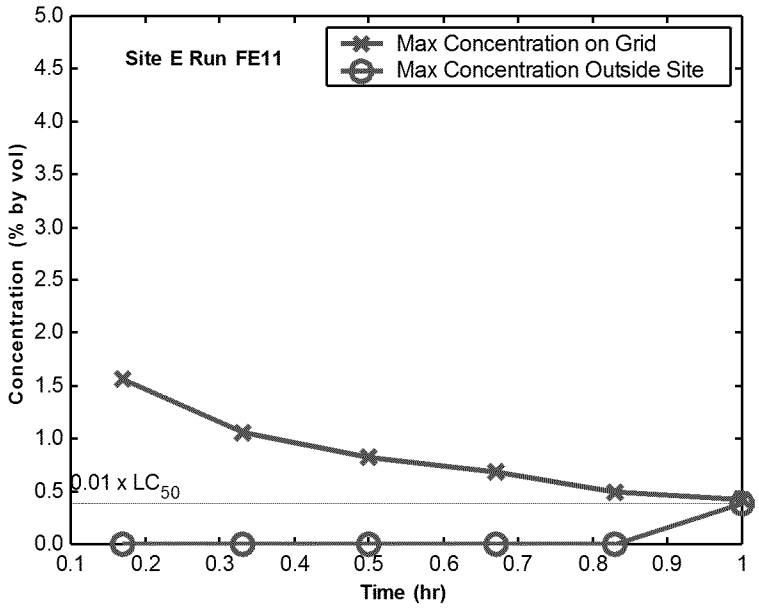

Figure A-73. Predicted change in dredged material plume concentration after release in Site E. Shown is the maximum concentration over the entire model grid and the maximum outside the site for a 3000 CY release with 40% clumps, 10% free water, and a 20 cm/s current. A water quality criteria of 0.38% dilution is also shown.

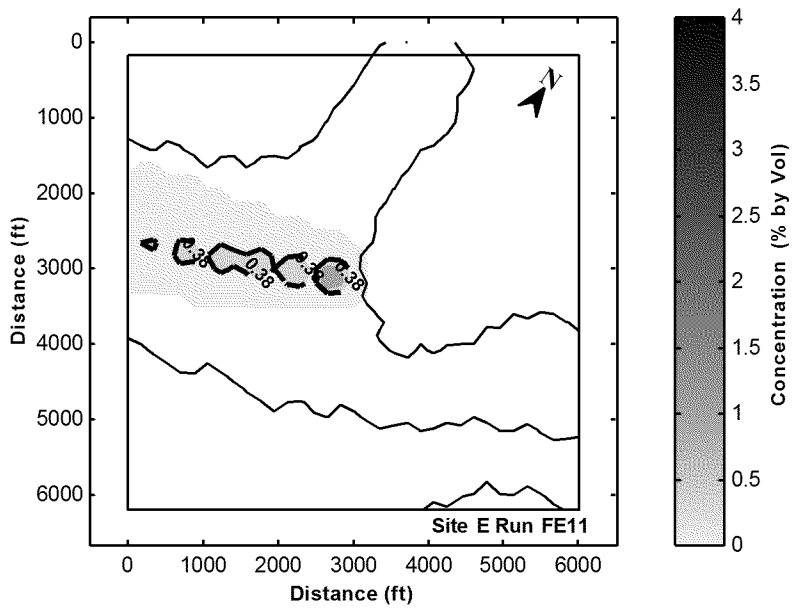

Figure A-74. Predicted depth-maximum plume concentration over the model grid after 90 min for a 3000 CY release in Site E with 40% clumps, 10% free water, and a 20 cm/s current. Bathymetric depth contour interval equals 2 ft.

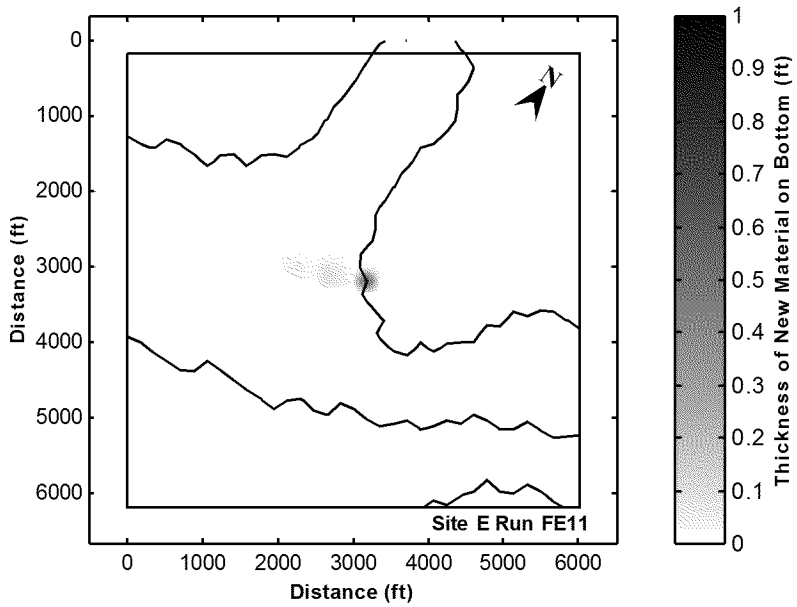

Figure A-75. Predicted total thickness of new material on the bottom for a 3000 CY release in Site E with 40% clumps, 10% free water, and a 20 cm/s current. Bathymetric depth contour interval equals 2 ft.

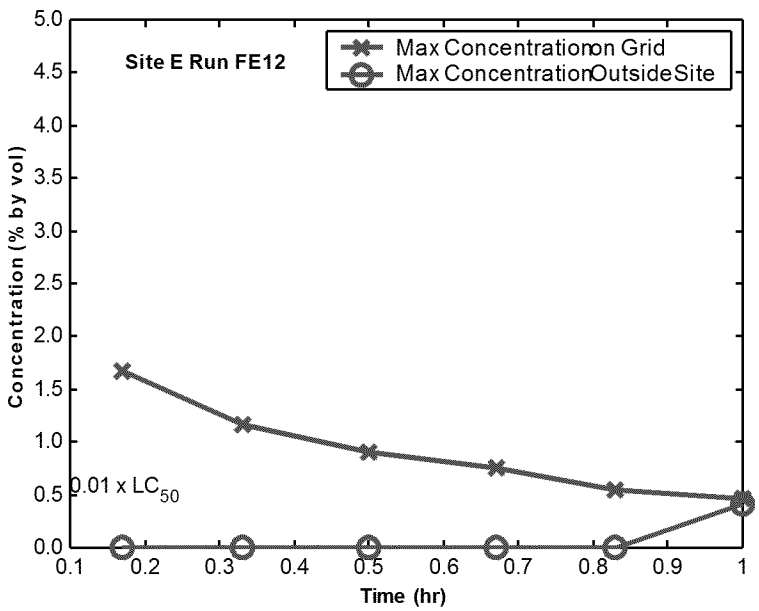

Figure A-76. Predicted change in dredged material plume concentration after release in Site E. Shown is the maximum concentration over the entire model grid and the maximum outside the site for a 3000 CY release with 60% clumps, 30% free water, and a 20 cm/s current. A water quality criteria of 0.38% dilution is also shown.

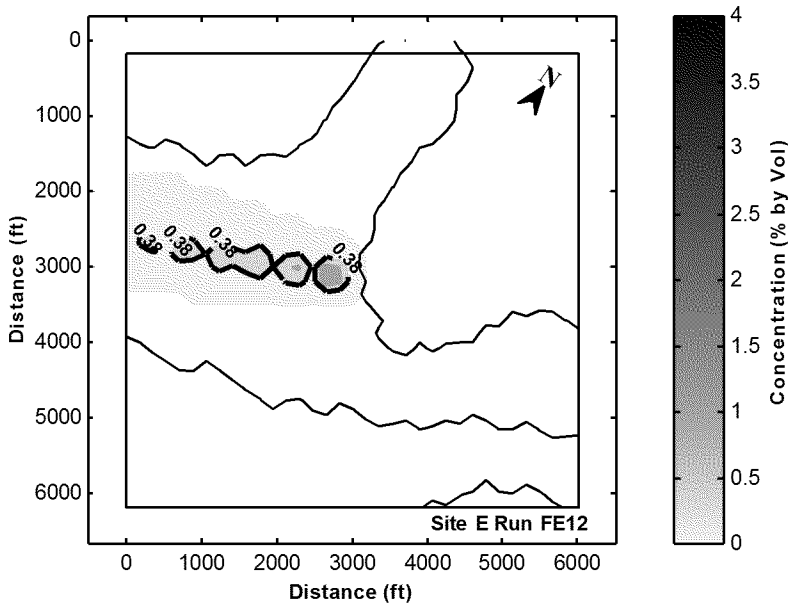

Figure A-77. Predicted depth-maximum plume concentration over the model grid after 100 min for a 3000 CY release in Site E with 60% clumps, 30% free water, and a 20 cm/s current. Bathymetric depth contour interval equals 2 ft.

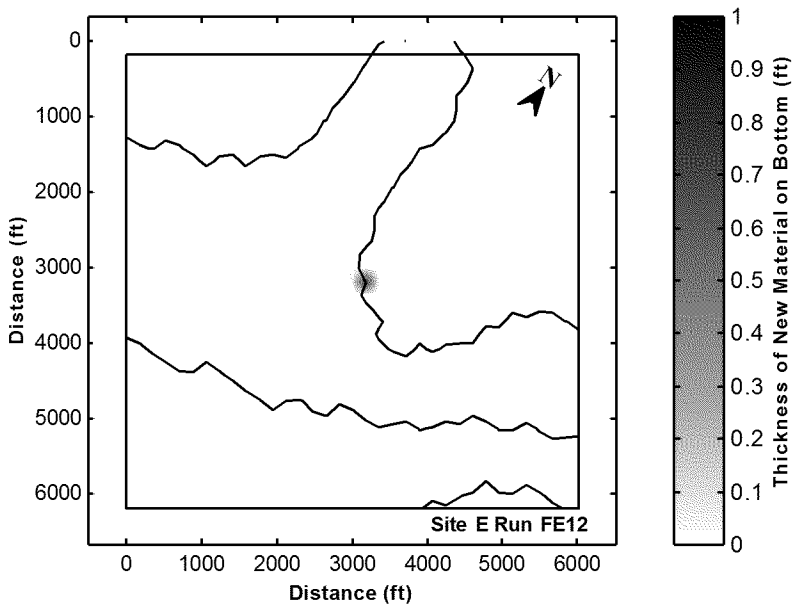

Figure A-78. Predicted total thickness of new material on the bottom for a 3000 CY release in Site E with 60% clumps, 30% free water, and a 20 cm/s current. Bathymetric depth contour interval equals 2 ft.

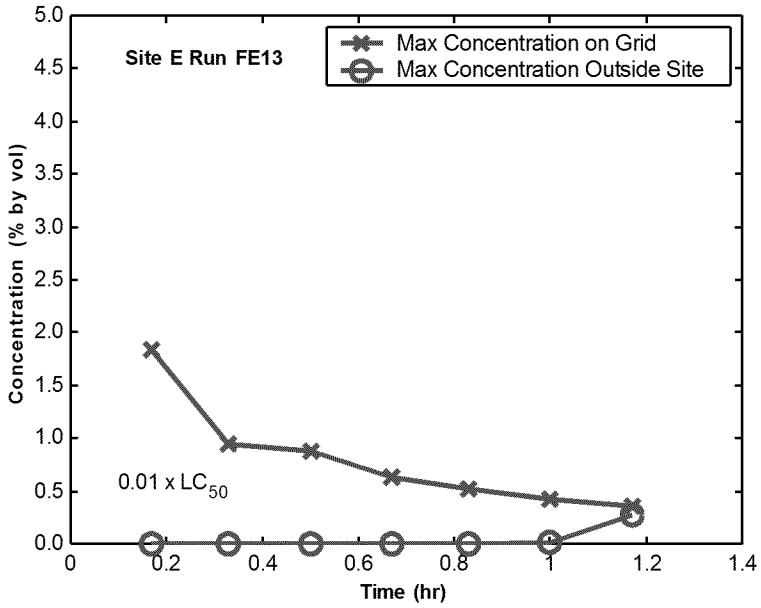

Figure A-79. Predicted change in dredged material plume concentration after release in Site E. Shown is the maximum concentration over the entire model grid and the maximum outside the site for a 3000 CY release with 40% clumps, 10% free water, and a 17 cm/s current. A water quality criteria of 0.38% dilution is also shown.

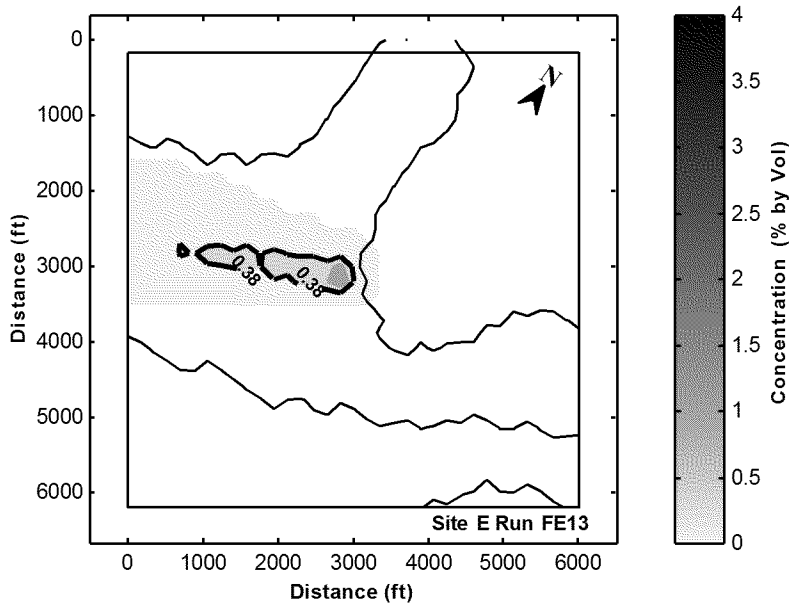

Figure A-80. Predicted depth-maximum plume concentration over the model grid after 100 min for a 3000 CY release in Site E with 40% clumps, 10% free water, and a 17 cm/s current. Bathymetric depth contour interval equals 2 ft.

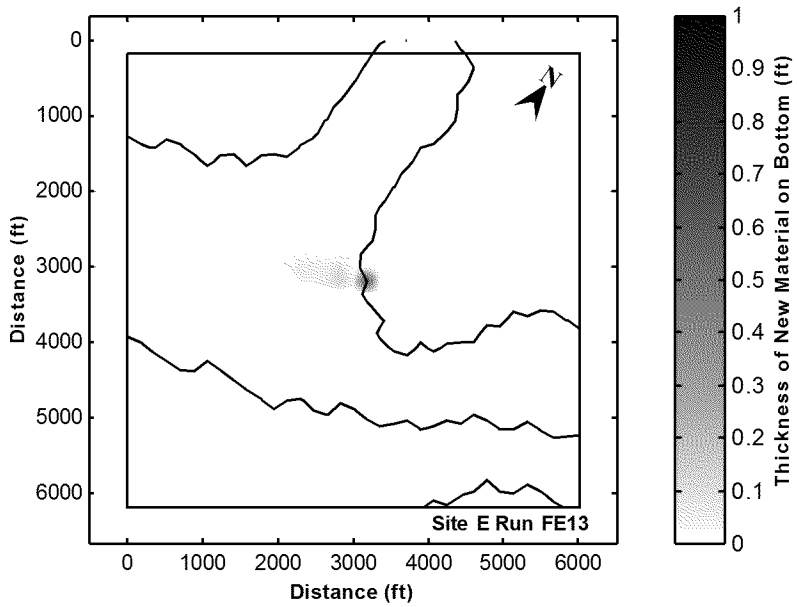

Figure A-81. Predicted total thickness of new material on the bottom for a 3000 CY release in Site E with 40% clumps, 10% free water, and a 17 cm/s current. Bathymetric depth contour interval equals 2 ft.

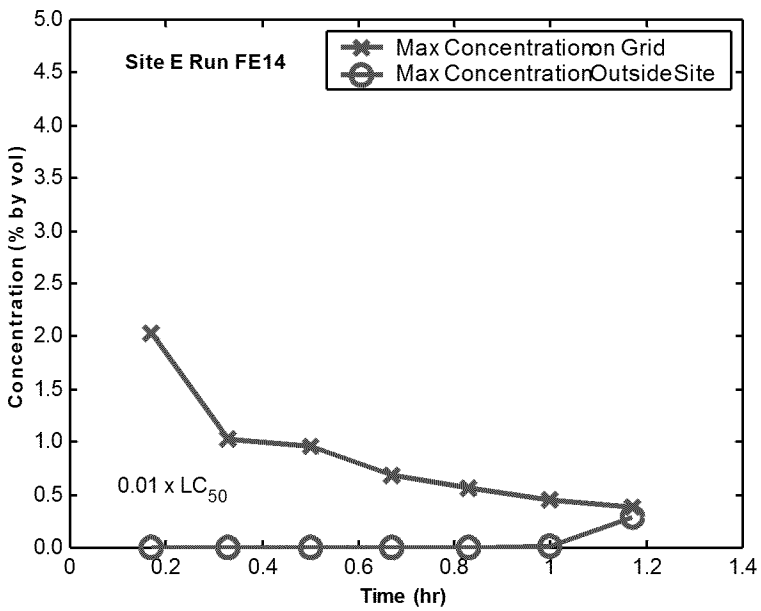

Figure A-82. Predicted change in dredged material plume concentration after release in Site E. Shown is the maximum concentration over the entire model grid and the maximum outside the site for a 3000 CY release with 60% clumps, 30% free water, and a 17 cm/s current. A water quality criteria of 0.38% dilution is also shown.

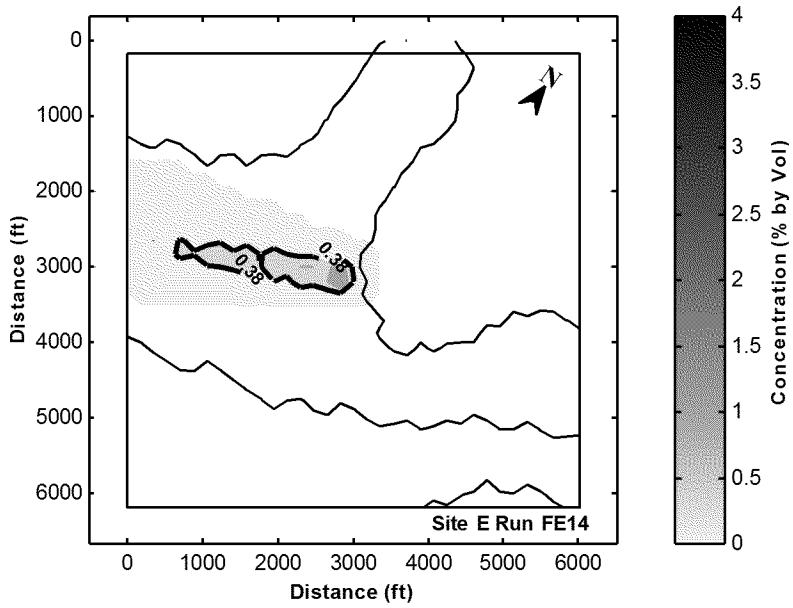

Figure A-83. Predicted depth-maximum plume concentration over the model grid after 100 min for a 3000 CY release in Site E with 60% clumps, 30% free water, and a 17 cm/s current. Bathymetric depth contour interval equals 2 ft.

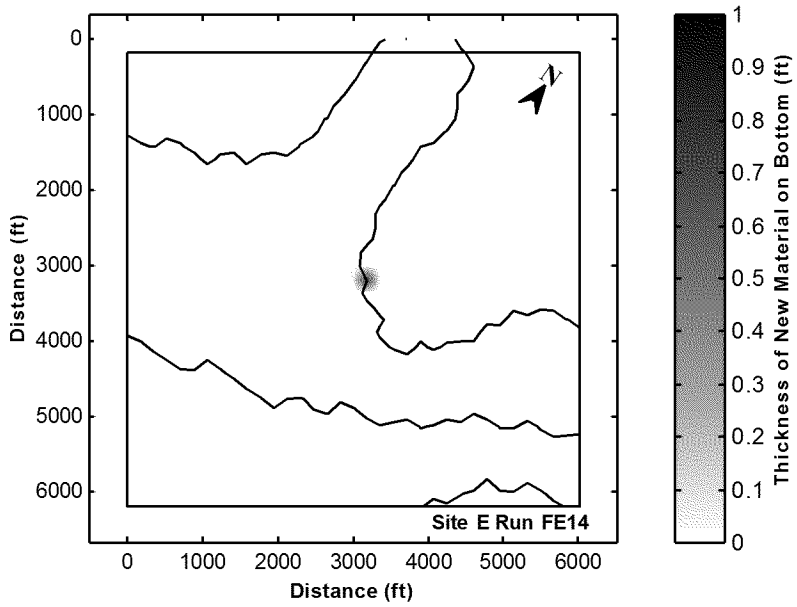

Figure A-84. Predicted total thickness of new material on the bottom for a 3000 CY release in Site E with 60% clumps, 30% free water, and a 17 cm/s current. Bathymetric depth contour interval equals 2 ft.

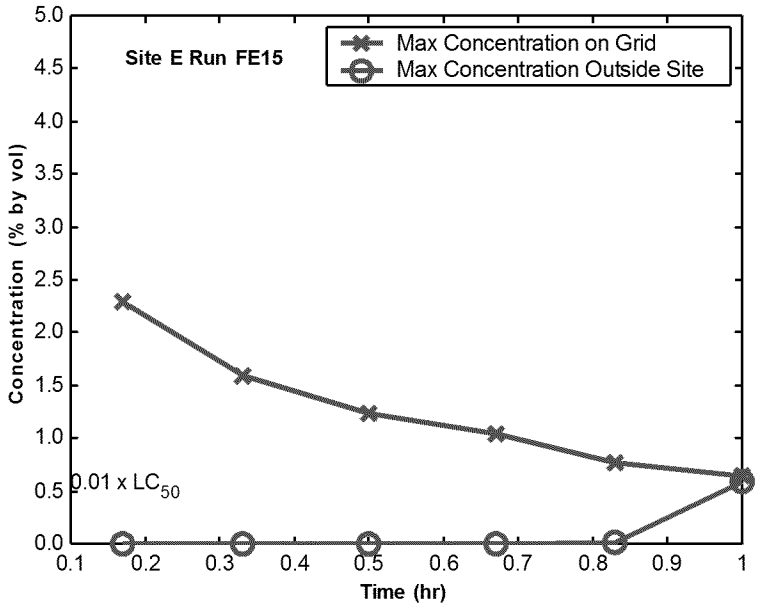

Figure A-85. Predicted change in dredged material plume concentration after release in Site E. Shown is the maximum concentration over the entire model grid and the maximum outside the site for a 5000 CY release with 40% clumps, 10% free water, and a 20 cm/s current. A water quality criteria of 0.38% dilution is also shown.

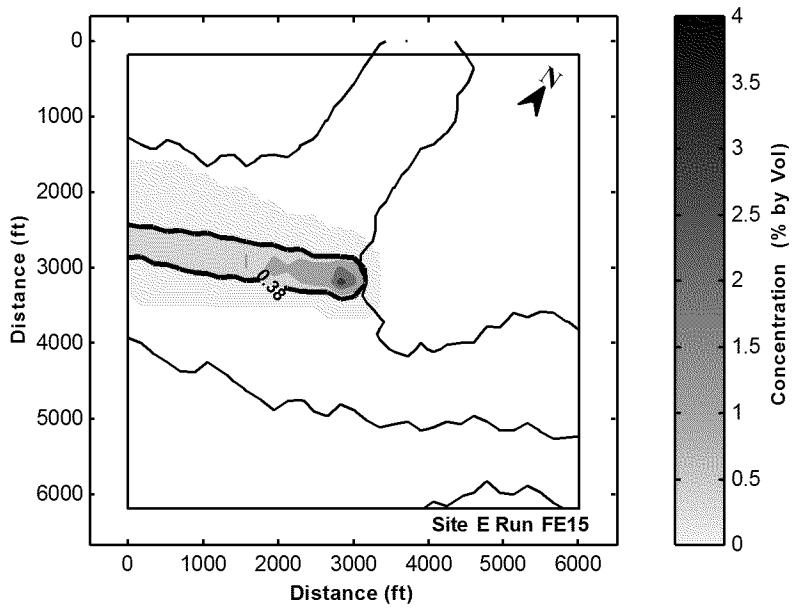

Figure A-86. Predicted depth-maximum plume concentration over the model grid after 100 min for a 5000 CY release in Site E with 40% clumps, 10% free water, and a 20 cm/s current. Bathymetric depth contour interval equals 2 ft.

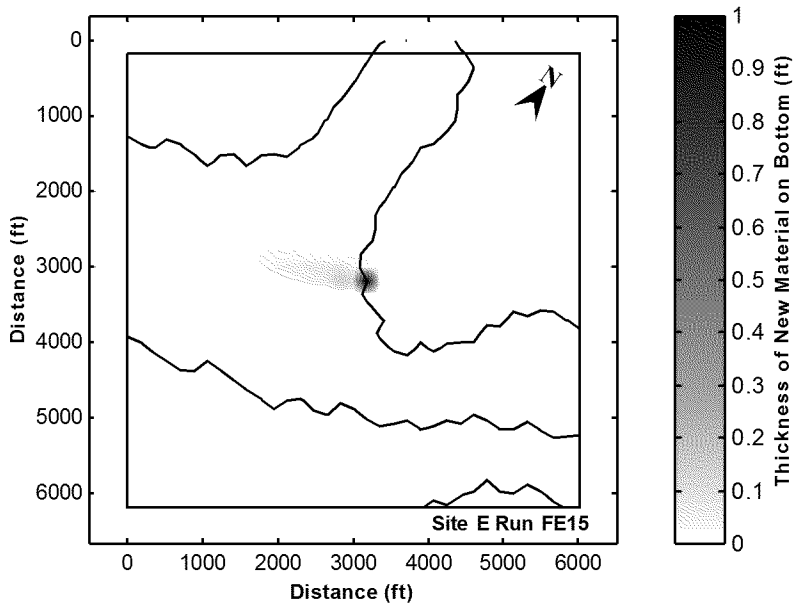

Figure A-87. Predicted total thickness of new material on the bottom for a 5000 CY release in Site E with 40% clumps, 10% free water, and a 20 cm/s current. Bathymetric depth contour interval equals 2 ft.

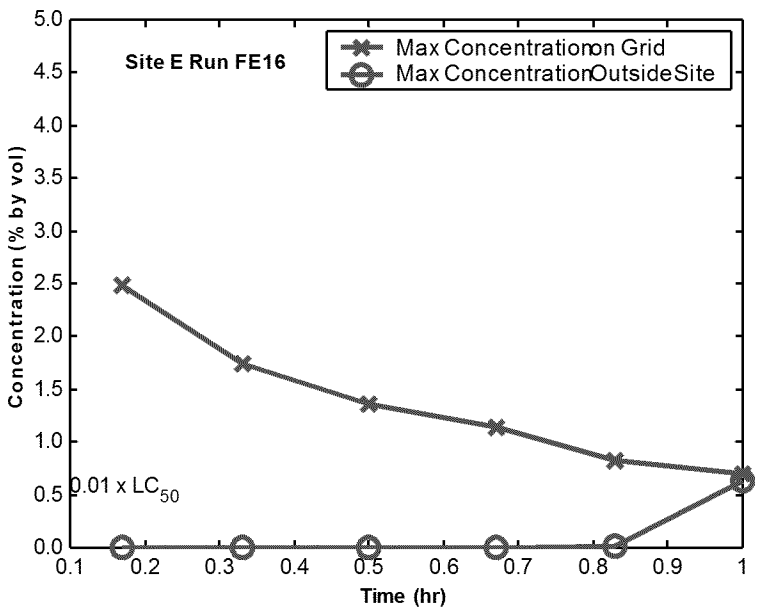

Figure A-88. Predicted change in dredged material plume concentration after release in Site E. Shown is the maximum concentration over the entire model grid and the maximum outside the site for a 5000 CY release with 60% clumps, 30% free water, and a 20 cm/s current. A water quality criteria of 0.38% dilution is also shown.

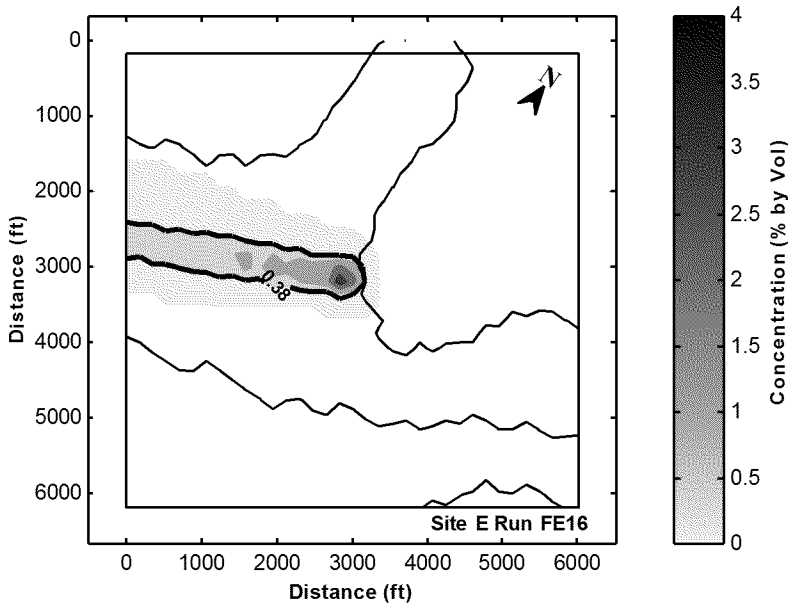

Figure A-89. Predicted depth-maximum plume concentration over the model grid after 100 min for a 5000 CY release in Site E with 60% clumps, 30% free water, and a 20 cm/s current. Bathymetric depth contour interval equals 2 ft.

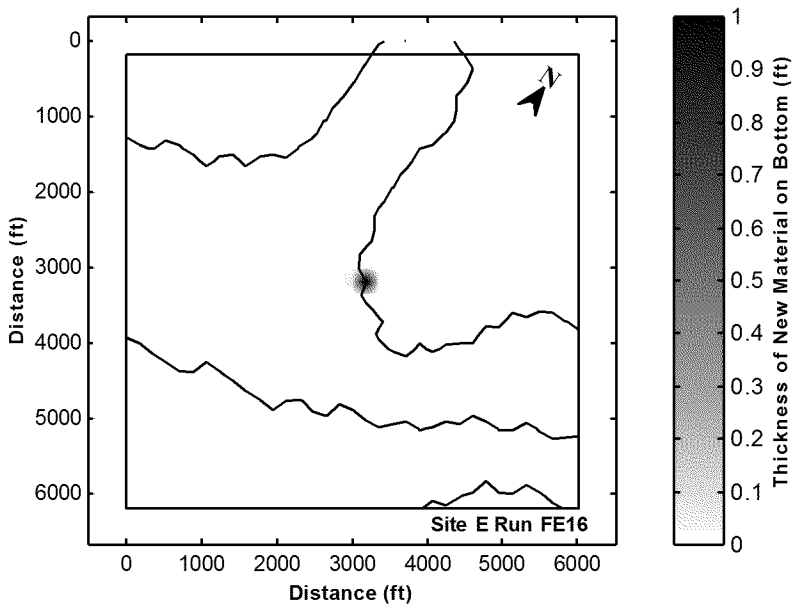

Figure A-90. Predicted total thickness of new material on the bottom for a 5000 CY release in Site E with 60% clumps, 30% free water, and a 20 cm/s current. Bathymetric depth contour interval equals 2 ft.

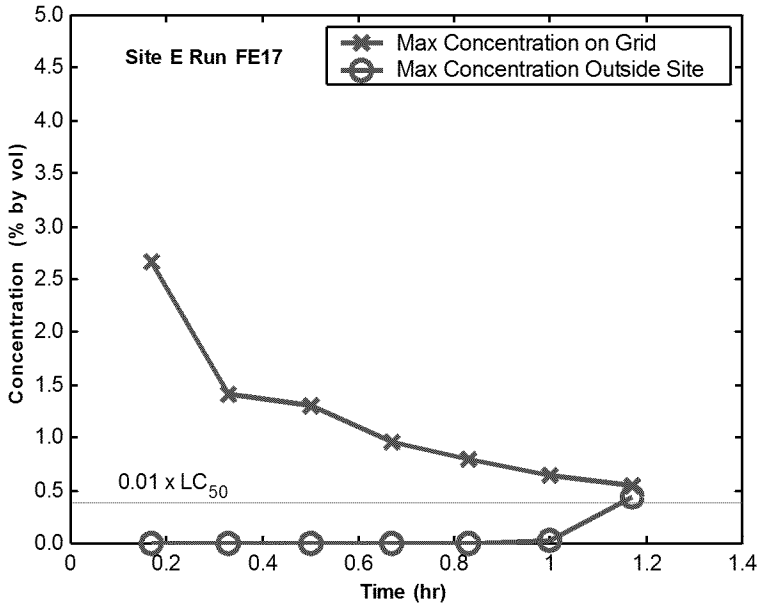

Figure A-91. Predicted change in dredged material plume concentration after release in Site E. Shown is the maximum concentration over the entire model grid and the maximum outside the site for a 5000 CY release with 40% clumps, 10% free water, and a 17 cm/s current. A water quality criteria of 0.38% dilution is also shown.

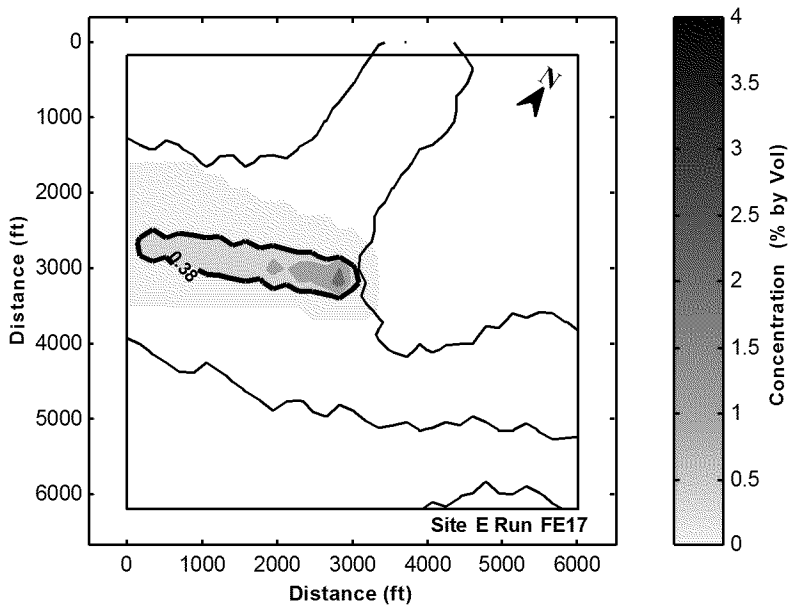

Figure A-92. Predicted depth-maximum plume concentration over the model grid after 120 min for a 5000 CY release in Site E with 40% clumps, 10% free water, and a 17 cm/s current. Bathymetric depth contour interval equals 2 ft.

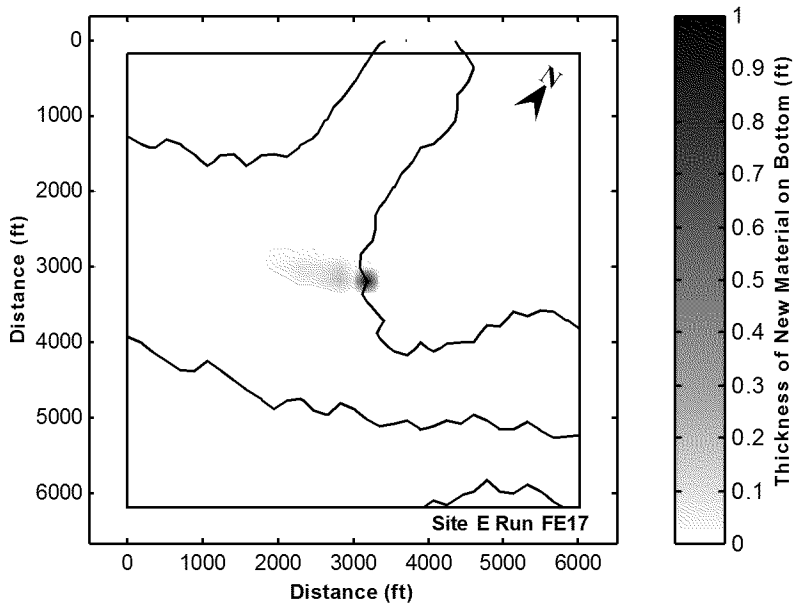

Figure A-93. Predicted total thickness of new material on the bottom for a 5000 CY release in Site E with 40% clumps, 10% free water, and a 17 cm/s current. Bathymetric depth contour interval equals 2 ft.

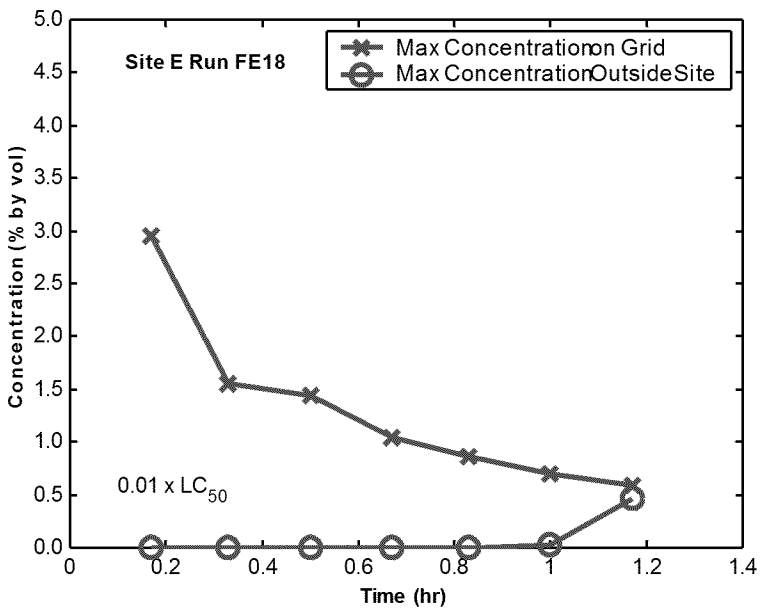

Figure A-94. Predicted change in dredged material plume concentration after release in Site E. Shown is the maximum concentration over the entire model grid and the maximum outside the site for a 5000 CY release with 60% clumps, 30% free water, and a 17 cm/s current. A water quality criteria of 0.38% dilution is also shown.

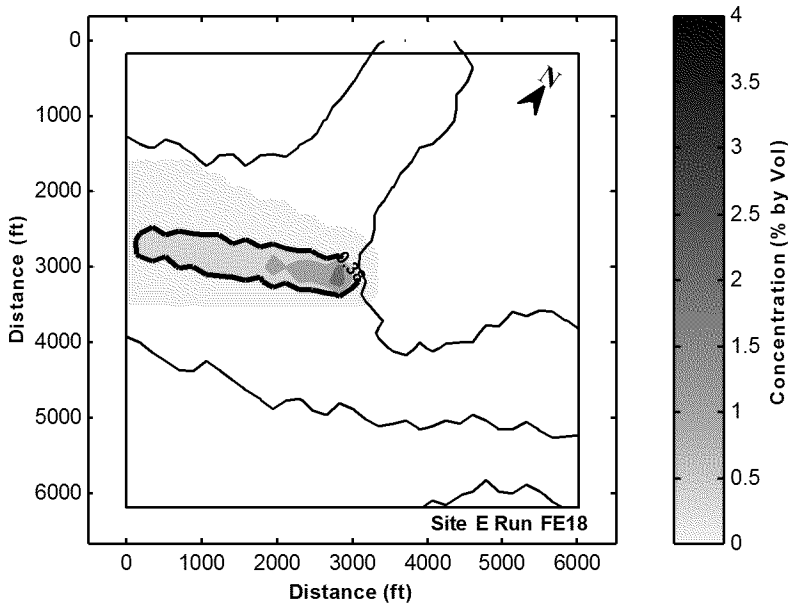

Figure A-95. Predicted depth-maximum plume concentration over the model grid after 120 min for a 5000 CY release in Site E with 60% clumps, 30% free water, and a 17 cm/s current. Bathymetric depth contour interval equals 2 ft.

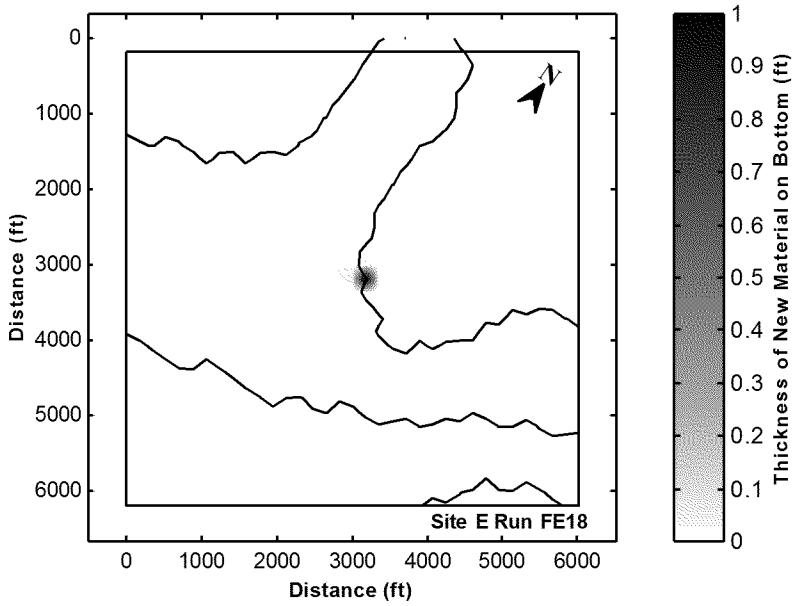

Figure A-96. Predicted total thickness of new material on the bottom for a 5000 CY release in Site E with 60% clumps, 30% free water, and a 17 cm/s current. Bathymetric depth contour interval equals 2 ft.